

Detection and Partitioning of Bacteriophage in Fluid/Solid Systems:
Application to the Ecology and Mobility of Viruses in the
Environment

Thesis by
Stanley Clement Baugh Grant

In Partial Fulfillment of the Requirements
for the Degree of
Doctor of Philosophy

California Institute of Technology
Pasadena, California

1992

(Defended September 3, 1991)

**Copyright © 1992 by Stanley Grant
All Rights Reserved**

If you want to understand the invisible, look carefully at the
visible.

-The *Talmud*

"Faith" is a fine invention
When Gentlemen can *see*-
But *Microscopes* are prudent
In an Emergency.
-Emily Dickinson

Acknowledgements

Caltech is a wondrous place, primarily because it is filled with wondrous people. I was fortunate to have one of the best of all possible advisors (in this best of all possible campuses), Mary Lidstrom. She helped me navigate the craggy world of microbiology and generously opened her lab to my work, inspite of the fact that there are no known viruses that oxidize methane. E. John List, my co-advisor, lent mathematical expertise, praise, and enthusiasm for my work. Norman Brooks sung of "dimensional analysis" and "solution by inspection". Jim Morgan (a.k.a. William of Ockham) made life interesting with his amazing collection of hats and profound advice. Frances Arnold provided guidance and served on my thesis committee. Keith Stolzenbach showed me that discussions about the fluid mechanics of particle transport could be fun.

Despite their backgrounds in biology, Christina Morris, Brenda Speer, Kerstin Laufer, Andrei Chistorserdov and Mila Chistorserdova were all great friends. They patiently suffered my crazy ideas and, by counseling prudence, probably spared me from scientific ruin. Thanks especially to Tina for all of her help. If only we could all be so wickedly good at tennis. Brenda was always eager to explain why my research was fundamentally flawed, and

usually she was right. Jeremy Semrau was personally responsible for breaking my nose. Worse yet, he's from Texas. Kerstin Laufer gave me food for thought, over tea of course.

Thanks be to...

...all of those machine runners. Jean Edens, Pat Koens, Dale Laird, Carol Garland, and John Paul Revel all helped me with the transmission electron microscope. Thanks especially to Jean "Hell's Bells" Edens who was so inspired by my work, she left town immediately after finishing my project. Peter Dervan's lab allowed me to use their wonderful phosphoimager. Paul Carpenter helped me with the scanning electron microscope, and probably caught one of my flu viruses in the process. Yigal Erel helped me with the plasma emission spectrometer. Joe Fontana and Rich Eastvedt helped me build beautiful devices that Jeremy, inevitably, broke. Tom Boyce introduced me to "Zen and the Art of Computer Maintenance".

...all of those females. Daryle Wachter-Brulla taught me sterile technique (watch out, world!). Laura Hernandez was a great SURF. Peggy Arps helped with a manuscript and chose to live in Alaska, which automatically makes her a good person. Natasha Kotronarou gave me a lot to live up to, and showed me who was boss by beating me out the door. Karin Perkins helped me titer phage and count plates, but, alas, turned out to be a lousy skier. Jeremy shaved (once).

...all of those liberal commie fiddle players. Delores Bing's boundless maternal instinct could coax beautiful music out of a turnip

(which isn't a bad model system for a Caltech student). Monica Kohler's musical virtuosity (*and passion!*) made our Caltech Centennial Recital a joy. Liz Wood played great but worried too much (usually about being left-handed). David Koerner explained why I worked too hard, and recommended a second career as a pianist.

...all of those pillars of support. Secretaries Elaine Granger, Evelina Cui, Fran Matzen, and Karen Hodges kept me straight. Librarians Rayma Harrison, Gunilla Hastrup and Susan Leising kept me well read. Lisa kept me.

I am grateful to both the Andrew W. Mellon Foundation and the National Institute of Health Bioprocess and Biochemical Technology Training Grant program for their financial support of this project.

While Caltech may be a great place, it just can't compete with my family. My mom and dad gave me the love, support (and money) needed to make what I've done possible (whatever that is). Susie and Kathleen gave me at least one of the above (whatever that was). Lisa, my better half, was my friend when nothing worked, a colleague when I needed advice, my playmate when I wanted to have fun, and the person to whom I dedicate this work.

Table of Contents

<i>Acknowledgements</i>	<i>iv</i>
<i>Abstract</i>	<i>xiii</i>
<i>List of Tables</i>	<i>xv</i>
<i>List of Figures</i>	<i>xvi</i>
Introduction and Literature Review.....	1
1.1. Introduction.....	1
1.2. Virus Detection.....	2
1.2.1. Plaque Forming Units.....	3
1.2.2. Nucleic Acid Hybridization.....	5
1.3. Virus Survival.....	7
1.4.1. Mechanical Filtration.....	8
1.4.2. Aggregation.....	10
1.4.3. Adsorption to Surfaces.....	10
1.4.3.1. Electrostatic Interactions.....	10
1.4.3.2. van der Waals Interactions.....	12
1.4.3.3. Hydrophobic Interactions.....	13
1.4.3.4. Specific Interactions.....	14
1.4.3.6. Equilibrium Models.....	19
1.5. Thesis Overview.....	20
1.6. Model System.....	22
1.6.1. Virus Selection.....	22
1.6.2 Adsorbent.....	23

2. Factors Affecting Detection of Bacteriophage DNA Using Hybridization Techniques	36
3. Estimating Virus Viability Using a Modified Nucleic Acid Hybridization Assay	49
3.1. Summary	49
3.2. Introduction.....	50
3.3. Materials and Methods	52
3.3.1. Preparation of Bacteriophage.....	52
3.3.2. DNA/DNA Hybridization	53
3.3.3. DNase Treatment	54
3.3.4. Viability Measurements	55
3.3.5. Transmission Electron Microscopy.....	55
3.3.6. Bacteriophage λ Inactivation.....	56
3.4. Results.....	56
3.4.1. Measurement of total DNA.....	56
3.4.2. Measurement of Virus Encapsulated DNA.....	59
3.4.3. Inactivation Experiment	63
3.5. Discussion	73
3.6. Conclusions.....	75
4. Kinetic Theory of Virus Adsorption and Inactivation in Batch Experiments.....	76
4.1. Summary	76
4.2. Introduction.....	77
4.2.1. Motivation	77
4.2.2. Background	78

4.3. Model Development.....	81
4.3.1. Problem Definition.....	81
4.3.2. Kinetic Expressions for Reaction Extents	84
4.3.2.1. Kinetics of Reversible Binding	84
4.3.2.2. Kinetics of Fluid and Surface Inactivation	84
4.3.2.3. Irreversible Adsorption	86
4.3.3. Dimensional Analysis	86
4.4. Solutions of the Kinetic Model.....	89
4.4.1. Closed Form Solutions for Limiting Cases.....	90
4.4.1.1. Pure Inactivation	90
4.4.1.2. Instantaneous Quasi-Equilibrium Adsorption.....	92
Case I.....	92
Case II.....	93
Case III.....	93
4.4.1.3 Irreversible Binding	95
4.4.2.1. Non-instantaneous Quasi-Equilibrium Adsorption.....	95
4.4.2.2 Slow Approach To QEA.....	97
4.4.2.3. Slow Approach to QEARI.....	99
4.4.2.4. Slow Approach to QEASS	99
4.4.2.5. Summary of Simulations	101
4.5. Discussion	102
4.5.1. New Experimental Approach.....	102

4.5.1.1. Reversible Adsorption & No Surface Stabilization or Sinks ($N_s N_i = 1$).....	104
4.5.1.2. QEASS or QEARI ($N_s N_i \neq 1$).....	104
4.5.2. Virus Populations	105
4.6. Conclusions.....	105
5. Experimental Investigations of Bacteriophage Lambda	
Adsorption to Ottawa Sand Over Long Time Scales	108
5.1 Summary	108
5.2. Introduction.....	110
5.2.1. Background	110
5.3. Materials and Methods	111
5.3.1. Virus Preparation.....	111
5.3.3. Transmission Electron Microscopy.....	112
5.3.4. Sand Treatment.....	112
5.3.5. Scanning Electron Microscopy.....	113
5.3.6. Adsorption Experiments.....	113
5.3.7. Elution Experiments.....	114
5.3.8. Isotherm Experiments.....	115
5.3.9. Aggregation Experiment.....	115
5.3.10. Computer Simulations.....	116
5.4. Results.....	117
5.4.1. Characterization of Ottawa Sand.....	117
5.4.2. Batch Adsorption Experiments.....	120
5.4.3. Elution Experiments.....	126
5.4.4. Isotherm Experiments.....	132

5.4.5. Virus Aggregation and Biological Contamination	135
5.5. Discussion	138
5.5.1 Summary of Results.....	138
5.5.2 Alternative Adsorption Mechanisms	140
5.5.2.1. Reversible Adsorption	140
5.5.3. Environmental Implications.....	143
5.5.3.1. Significance of Irreversible Adsorption.....	143
5.5.3.2. Environmental Transduction.....	145
5.5.3.3. Virus Mobility in Sandy Environments	145
5.5.3.4. Groundwater Transport Models	146
5.6. Conclusions.....	147
6. Effects of Solution pH and Electrolyte Composition on Long Time Scale Adsorption and Inactivation.....	149
6.1. Summary	149
6.2. Introduction.....	151
6.3. Methods and Materials.....	151
6.3.1. Adsorption Experiments.....	151
6.3.2. Plasma Emission Spectroscopy	152
6.3.3. Data Reduction.....	153
6.4. Results.....	153
6.4.1. Inactivation Data	154
6.4.1.1. NaCl as the Electrolyte.....	154

6.4.1.2. MgCl ₂ as the Electrolyte.....	161
6.4.1.3. Humic Acids as the Electrolyte.....	161
6.4.1.4. Normalization of Inactivation Data.....	164
6.4.2. Adsorption Experiments.....	164
6.4.2.1. NaCl at 10mM.....	166
6.4.2.2. NaCl at 100mM.....	168
6.4.2.3. MgCl ₂ at 10 & 100mM.....	168
6.4.2.4. Humic Acid at 0.1 & 1.0 mg/l	169
6.4.2.5. Comparison of Sand Data	170
6.5. Discussion	172
6.6. Conclusions.....	174
7. Conclusions and Future Research.....	176
7.1 Conclusions.....	176
7.2 Implications for Future Research	179
References	182
Appendix A.....	201
Appendix B.....	203
Appendix C.....	204
Appendix D.....	208
Appendix E.....	210

Abstract

Viruses are ubiquitous in natural environments where they can exist as natural inhabitants or as contaminants from the disposal of human and animal wastes. Studies of viruses in nature are hampered because currently available methods for detection are not ideally suited to environmental applications. In the first part of this thesis, a modified hybridization assay is presented which employs DNase protection and slot blot methods to measure quantitatively the concentration of soluble and bacteriophage-encapsulated DNA in fluid samples. The potential use of this assay for estimating virus viability was tested with a model system consisting of inactivating bacteriophage lambda particles. These experiments show that the new hybridization assay provides upper-limit estimates of bacteriophage viability when inactivation results in the release of DNA.

The mobility and ecology of viruses in natural environments is strongly influenced by the adsorption of virus particles to solid surfaces. In the second part of this thesis, a kinetic theory for virus adsorption and inactivation in batch experiments is presented. Based on the results of this theory, a new experimental approach is

proposed for studying the effects of solid surfaces on virus partitioning and survival over long time scales.

In the third part of the thesis, this new experimental approach was used to investigate the interactions between bacteriophage lambda particles and Ottawa sand over the course of days. Virus/surface interactions on these time scales were strongly dependent on solution pH and electrolyte composition. Sand stabilized the virus at high pH (10) and reduced fluid-phase virus infectivity at intermediate to low pH (5 and 7). The observed reduction in virus infectivity at pH 7 was attributed to virus adsorption to the sand surface, based on data from elution experiments. Viruses adsorbed to the sand at pH 7 desorbed when the sand was resuspended in nutrient broth, but not when the sand was resuspended in a virus-free pH 7 buffer. When model simulations were compared to elution data, virus adsorption did not follow the predictions of quasi-equilibrium adsorption models. On the basis of these results, several alternative kinetic mechanisms for virus adsorption are proposed.

List of Tables

<u>Table</u>	<u>Page</u>
3.1	Calculated inactivation rate constants.....68
5.1	Summary of contact times used in batch studies.....108
5.2	Elution by nutrient broth.....124
6.1	Adsorption and inactivation data (NaCl=10mM).....155
6.2	Adsorption and inactivation data (NaCl=10-mM).....155
6.3	Adsorption and inactivation data (MgCl ₂).....155
6.4	Adsorption and inactivation data (Humic acid).....156
6.5	Fluid inactivation constants.....162

List of Figures

Figure 1.1.	Procedure for PFU assay.	4
Figure 1.2	Procedure for Nucleic Acid Hybridization	6
Figure 1.3.	Size spectrum of aqueous particles	9
Figure 1.4.	Sphere-plate model	15
Figure 1.5.	Interaction energy profiles	17
Figure 1.6.	Structure of bacteriophage lambda	25
Figure 1.7.	TEM of lambda	27
Figure 1.8.	Color Picture of Ottawa sand.	29
Figure 1.9.	Low magnification SEM of sand.	31
Figure 1.10.	Intermediate magnification SEM of sand	33
Figure 1.11.	High magnification SEM of sand	35
Figure 2.1	Blots of λ particles and genomic DNA	38
Figure 2.2	Effect of EDTA, NaOH, & $MgSO_4$ on hybridization	40
Figure 2.3	$MgSO_4$ precipitate formation	42
Figure 2.4.	Effect of buffer composition on hybridization	44
Figure 2.5.	Effect of heating on hybridization	45
Figure 2.6.	Effect of rinsing	46
Figure 2.7	Spatial variations across slot blot	47
Figure 3.1.	Correlation of bacteriophage and radioactivity	58
Figure 3.2	DNase procedure	60
Figure 3.3.	Effect of DNase digestion on hybridization	62

Figure 3.4.	Autoradiogram of the inactivation experiment	65
Figure 3.5	Hybridization, TEM and PFU data	67
Figure 3.6.	TEM of inactivating bacteriophage	71
Figure 3.7	TEM counts of bacteriophage and debris	72
Figure 4.1	Virus/Surface Interactions	83
Figure 4.2	Semilog plots of QEA, QEARI, and QEASS	91
Figure 4.3	Solutions for QEA, QEARI, and QEASS	94
Figure 4.4	Slow approach to QEA	96
Figure 4.5	Slow approach to QEARI	98
Figure 4.6	Slow approach to QEASS	100
Figure 4.7	Proposed experimental protocol	103
Figure 5.1	SEM of Ottawa sand texture	119
Figure 5.2	Arithmetic plot of batch adsorption data	121
Figure 5.3	Semilog plot of batch adsorption data	122
Figure 5.4	Semilog plot comparing final slopes	123
Figure 5.5	Nutrient broth elution data	127
Figure 5.6	PIPES elution data	130
Figure 5.7	Langmuir isotherm plots	133
Figure 5.8.	TEM of bacteriophage monomers	137
Figure 5.9	Kinetic model for adsorption	141
Figure 5.10	Numerical simulations of adsorption experiment	144
Figure 6.1	Results of batch experiments (pH 5.0)	157
Figure 6.2	Results of batch experiments (pH 7.0)	158
Figure 6.3	Results of batch experiments (pH 10.0)	159
Figure 6.4	Comparison of inactivation data	160

Figure 6.5	Normalization of inactivation data	163
Figure 6.6	Normalization of adsorption data	165
Figure 6.7	Elements released after fluid exposure to sand	167
Figure 6.8	Comparison of adsorption data	171

Introduction and Literature Review

1.1. Introduction

Viruses are found in most, if not all, natural environments, where they exist as natural inhabitants (Proctor and Fuhrman, 1990; Bergh et al., 1989; Borsheim et al., 1990) or as contaminants introduced from waste treatment (Gerba and Lance, 1978; Kettratanakul et al., 1991). The fact that viruses are so ubiquitous has important implications for many fields of environmental science. Groundwater used for irrigation and municipal supply frequently contains pathogenic viruses, bacteria, and parasites released from nearby septic tanks or other sources of sewage effluent (Keswick and Gerba, 1980). In a 1986 EPA survey (USEPA, 1986), 46 states cited failing septic tanks as a major source of groundwater contamination, with 9 of those ranking septic tanks as the number one cause of aquifer contamination. This contamination has direct and measurable effects on human health. It is estimated that over half of the 62,273 cases of waterborne disease reported in the U.S. between 1946 and 1977 were caused by the ingestion of sewage contaminated groundwater (Keswick, 1984).

Recent evidence suggests that viruses, and especially bacteriophage, are present in marine pelagic environments at high

levels (Proctor and Fuhrman, 1990; Bergh et al., 1989; Borsheim et al., 1990). Bacteriophage propagate by infecting appropriate host bacteria and, therefore, may be a dominant factor in regulating natural host population densities (Proctor and Fuhrman, 1990). Since bacteria control the chemical nature of the earth's biosphere to a large extent (Atlas and Bartha, 1981), the regulation of their populations by bacteriophage is of fundamental importance.

Bacteriophage can also mediate the exchange of genetic material between bacteria through a process called transduction (Kokjohn, 1989). Transducing bacteriophage are a potentially important vector for the dispersal of recombinant DNA from genetically engineered microorganisms, and are of concern for regulating the environmental release of these organisms (Saye and Miller, 1989).

In this chapter, current literature on virus detection, survival and partitioning in the environment is reviewed, followed by a description of the model system used in this study and an outline of research objectives.

1.2. Virus Detection

Methods for detecting viruses in natural environments are needed for investigating the role of viruses in natural ecosystems and for protecting water resources from wastewater contamination. Most of the techniques that are currently available possess serious limitations when applied to the examination of environmental

samples. These techniques and their respective strengths and weaknesses are discussed below.

1.2.1. Plaque Forming Units

Concentrations of fluid-borne viruses can be estimated using an assay of virus viability in plaque forming units (PFU). Figure 1.1 illustrates this technique for the detection of bacteriophage. A dilution of the sample of interest is mixed with host cells, plated on nutrient agar, and incubated (Arber et al., 1983). During the incubation period, plaques (cleared zones) form on a lawn of bacteria at locations where successful bacteriophage infection occurred. By counting the total number of plaques on a given plate and multiplying by the appropriate dilution factor, the concentration of infective viruses particles in the original sample can be estimated. Variants of this assay also exist for other types of viruses (Olson, 1991).

Methods exist to elute viruses from soil by exposure to beef extract (Hurst et al., 1991), and to concentrate fluid-borne viruses by membrane filtration (Shields et al., 1986; Shields and Farrah, 1982). These techniques have been used in conjunction with PFU assays to detect viruses in a variety of environments (Gerba et al., 1978).

PFU assays are not completely efficient at detecting virus particles. Under ideal conditions, the assay only detects approximately one-half of the total fluid-borne virus particles (Arber et al., 1983). For environmental systems, PFU estimates of bacteriophage abundance are at least four log units below estimates obtained using transmission electron microscopy (TEM) (Proctor and

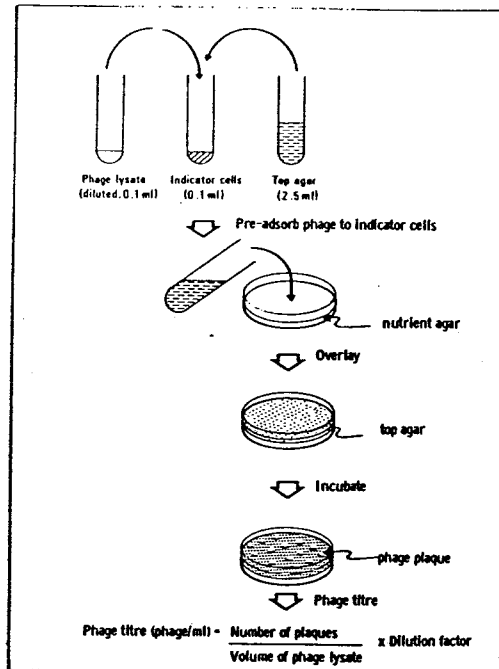


Figure 1.1. Procedure used for detecting viruses using an infectivity assay. Viruses are mixed with host cells, incubated, and added to top agar. The resulting mixture is spread over a petri dish containing nutrient agar and incubated. Growth of the host cells across the plate forms a lawn. Within the lawn, clear regions called plaques form which represent the location of successful virus infections. By counting the total number of plaques appearing on a given plate, the concentration of infective virus particles present in the original sample can be determined. (From Lin et al., 1984).

Fuhrman, 1989; Bergh et al., 1990; Borsheim et al., 1990). In the case of mammalian viruses, PFU measurements are usually a factor of 100 or more below the actual concentration of virus particles (Dubrou et al., 1991).

1.2.2. Nucleic Acid Hybridization

Another approach to detecting viruses in natural samples is to detect the nucleic acid corresponding to a specific virus using hybridization techniques. This approach involves isolating the total nucleic acid present in a sample, immobilizing the nucleic acid on a membrane, and hybridizing the membrane with a nucleic acid probe that contains a sequence unique to the virus of interest (Figure 1.2). The probe is linked to a reporter group, usually a radioisotope, so that the amount of probe that successfully hybridizes to the target DNA can be detected and quantified. This approach has been used successfully to detect nucleic acids from both mammalian viruses (Preston et al., 1990; Tougianidou et al., 1991; Margolin et al., 1991; De Leon and Gerba, 1991; Richardson et al., 1988; and Dubrou et al., 1991) and bacteriophage (Ogunseitan et al., 1990) in natural samples.

Hybridization techniques possess several limitations which significantly restrict their utility for environmental studies. Because a certain number of reporter groups are needed for a detectable signal, hybridization techniques are relatively insensitive, requiring at least 1000 genome copies/ml for a positive signal (Saylor and Layton, 1990). Polymerase chain reaction (PCR) has been used to amplify target nucleic acid sequences prior to hybridization (Olson, 1991).

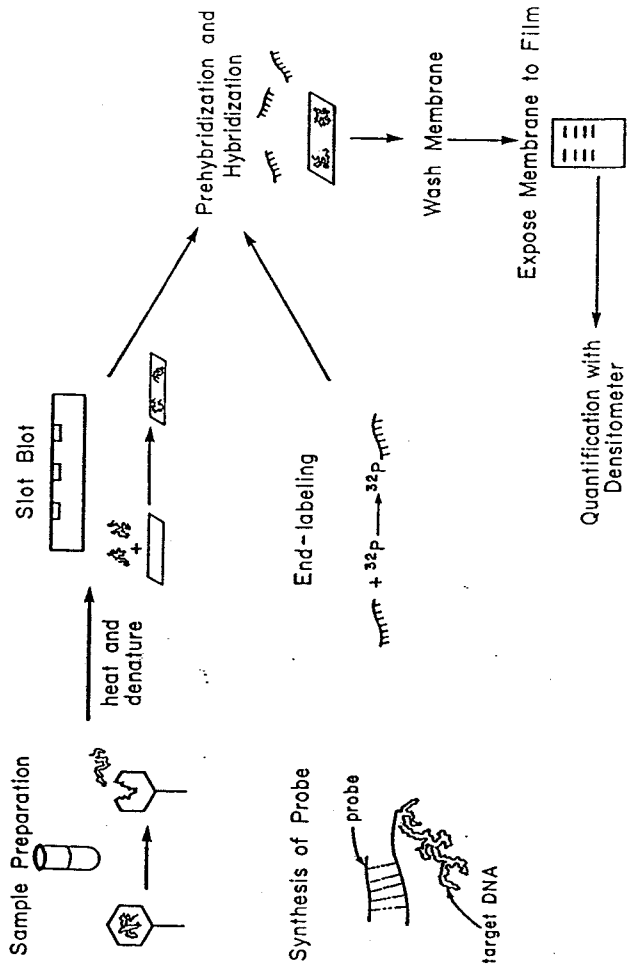


Figure 1.2. Procedure for nucleic acid hybridization. Samples containing virus particles are heated in alkali to release and denature nucleic acids. The sample is then passed through a filter (usually nylon) using a slot blot apparatus. The filter is hybridized with a probe linked to a reporter group (in the case shown here, the radioactive isotope of phosphorous, ^{32}P). During the hybridization step, the probe binds to complementary nucleic acids present on the filter. Excess probe is removed by washing. The radioactivity retained by the filter can be quantified by direct counting or by densitometry of exposed X-ray films. Since the amount of radioactivity present on the filter is proportional to the amount of bound probe, the resulting signal is a measure of the number of target virus particles present in the original sample.

This technique has been successfully applied to both the detection of viruses (De Leon and Gerba, 1991) and bacteria (Bej et al., 1990; Steffan and Atlas, 1988) in natural samples. Unfortunately, natural compounds, like humic and fulvic acids, can significantly interfere with the ability of PCR to amplify nucleic acids (Olson, personal communication), implying that this technique may not be useful for many environmental systems.

More significantly, hybridization methods cannot differentiate between nucleic acid encapsulated in viable virus particles and nucleic acid dissolved in solution (Olson, 1991). This ambiguity significantly limits the environmental utility of hybridization techniques for several reasons. In the case of disease-causing viruses, only the fraction of nucleic acid present in viable virus particles is of interest. For ecological studies, separate estimates of both virus-encapsulated and dissolved nucleic acids would be useful, since only the former can control population densities of host organisms while both reservoirs of nucleic acid can participate in gene transfer. Until techniques are developed for discriminating between these two reservoirs of nucleic acid, many questions about the ecology and mobility of indigenous and disease-causing viruses in environmental systems will remain unanswered.

1.3. Virus Survival

Because viruses cannot metabolize compounds for energy, over time they lose their ability to infect host cells through a process called inactivation. This inactivation often follows first-order kinetics,

$$\frac{dn_f}{dt} = -k_1 n_f \quad (1.1)$$

where k_1 is an empirically determined decay constant, and n_f is the fluid concentration of virus infectivity, measured in plaque forming units (PFU).

The rate at which viruses inactivate in natural systems depends on many physical and chemical factors. These include temperature (Yates et al., 1984), the elemental composition of contacting soil and soil pH (Hurst et al., 1980), the concentration of indigenous microorganisms (Matthess and Pekdeger, 1981), virus type and ambient hydraulic conditions (McDowell-Boyer et al., 1986), the degree of virus aggregation (Young and Sharp, 1976), and whether the viruses are attached to soil grains or suspended in the fluid phase (Gerba and Schaiberger, 1975). The kinetics of virus inactivation can deviate from the first order rate law given by (1.1) under specific circumstances. Non-first-order infectivity decline has been observed for aggregated viruses and when significant variations exist in sensitivities among the viral population (Yates et al., 1987).

1.4. Partitioning in Soil or Groundwater

1.4.1. Mechanical Filtration

Virus particles can become adsorbed¹ to solid surfaces present in soil or groundwater environments through a number of different

¹In this thesis the terms binding, adsorption, and partitioning are used interchangeably. Although these terms may have very specific meanings in other fields (for example, gas adsorption to specific chemical sites on surfaces where reactions take place), here the terms only mean that virus particles accumulate in some unclear way at the solid-liquid interface.

processes. One such process is called mechanical filtration in which viruses are trapped between grains where the pore sizes are small relative to the size of the virus particle. Mechanical filtration is important only when the virus particles are large relative to the distribution of pore sizes. As Figure 1.3 shows, mechanical filtration of viruses is probably not important for all but very fine grain and/or clayey soil. Mechanical filtration results in an exponential decrease in fluid concentrations of virus particles with distance in the direction of flow (Matthess et al., 1988),

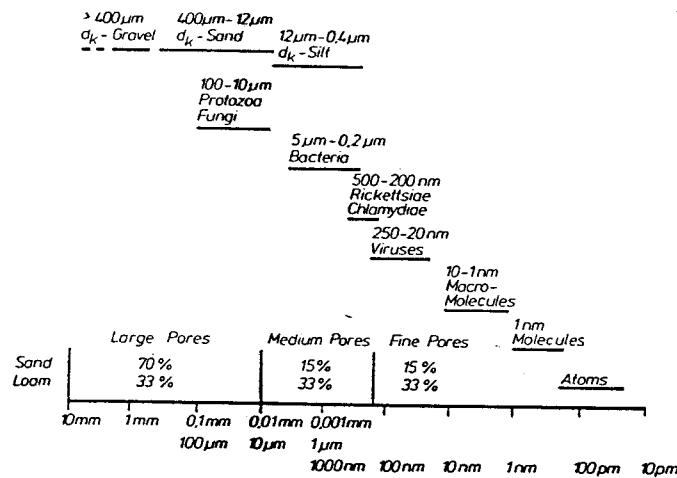


Figure 1.3. Relative sizes of bacteria, viruses, and molecules compared to hydraulic equivalent diameters of pore canals (from Matthess et al., 1988).

$$\frac{dn_f}{ds} = -k_s n_f$$

(1.2)

where s is path length and k_s is the filtration coefficient. k_s depends only on the size of the virus relative to the pore sizes (Fitzpatrick and Spielman, 1973).

1.4.2. Aggregation

Virus particles that are suspended in fluid can, under certain conditions, aggregate to form flocs. This aggregation can decrease observed inactivation rates (Young and Sharp, 1976), result in non-exponential inactivation (Gerba, 1984), and increase the effective size of the virus, potentially enhancing virus removal by mechanical filtration or gravitational sedimentation.

1.4.3. Adsorption to Surfaces

Virus adsorption to solid surfaces can be an important factor in the ecology and mobility of viruses in natural aquatic, soil, and groundwater systems. In groundwater or soil environments, irreversible virus adsorption to the pore matrix reduces virus mobility by "chemical" filtration, and increases the effective concentration of viruses at interfaces. In the case of bacteriophage, increasing the surface concentration of viruses increases the potential for gene transfer within and between bacterial colonies by transduction (Kokjohn, 1989). If adsorption occurs reversibly, viruses can still be dispersed through soil or groundwater, but at a rate slower than the average pore fluid velocity. Virus inactivation rates may also depend on whether the virus is suspended in the pore fluid or attached to a mineral surface (Gerba and Schaiberger, 1975).

1.4.3.1. Electrostatic Interactions

Viruses consist of a core of nucleic acid (the genome) surrounded by a protein coat (the capsid) and, in some cases, a lipid outer membrane (Brock, 1988). The protein coat contains weakly acidic and basic groups (e.g. carboxyl and amino groups) which can become ionized when suspended in an aqueous environment (Gerba, 1984). Ionization of surface residues results in a net surface charge that is pH dependent. The pH at which the virus has a zero net charge is called the isoelectric point (denoted pI). For pH conditions above and below the pI, viruses are respectively, negatively and positively charged. Oxide minerals can also develop surface charges that are pH dependent (Stumm and Morgan, 1981). At pH values typically found in natural environments, mineral surfaces will have a net negative charge (Bolt and Bruggenwert, 1978).

Charged surfaces in a liquid medium are surrounded by a layer of counter ions whose thickness depends inversely on the square root of the ionic strength of the liquid (Stumm and Morgan, 1981). The region occupied by both the surface charge and layer of counter ions is called the double layer. As virus/grain separations become small (on the order of 100 angstroms), the double layers associated with the virus and grain surfaces can overlap giving rise to a repulsive or attractive Coulombic force (Stumm and Morgan, 1981). Since the surface charge of the virus and solid are both dependent upon pH, the resulting force should also be pH dependent.

Published data confirm that electrostatic forces can influence virus attachment to solid surfaces. Attachment of viruses to

membrane filters is found to be favored at pH values where the virus and filter are oppositely charged (Mix, 1974; Sobsey and Jones, 1979). The adsorption of negatively charged poliovirus to over 34 different minerals and soils was found to be inversely correlated with the available negative surface charge on the adsorbent (Taylor et al., 1981; Moore et al., 1981). Correlations between adsorbent charge and the extent of virus attachment have also been observed for reovirus attachment to 30 soils, minerals and finely ground rocks suspended in synthetic wastewater (Moore et al., 1982) and bacteriophage T7 interaction with activated charcoal suspended in distilled water (Cookson, 1965).

Since double layer thickness depends inversely on the square root of the ionic strength of the suspending liquid, increasing ionic strength should decrease electrostatic virus/sorbent interactions. Decreasing the conductivity of water entering a packed column can result in mobilization and elution of pathogenic viruses previously attached to the soil (Landry et al., 1979, 1980; Dizar et al., 1984; Duboise et al., 1976; Gerba and Lance, 1978; Lance et al., 1976; Sobsey et al., 1980). Ionic strength has also been shown to influence the degree of virus attachment to membrane filters (Shields et al., 1986; Shields and Farrah, 1982) and to soil, minerals and crushed rocks (Murray and Parks, 1980; Moore et al., 1981).

1.4.3.2. van der Waals Interactions

Another force which may act to enhance virus attachment to soils is the van der Waals dispersive force. The van der Waals force

results from temporal fluctuations in the spatial distribution of electron clouds surrounding nuclear protons. These fluctuations result in instantaneous dipole-dipole interactions between neighboring atoms. It can be shown (Israelachvili, 1985) that the van der Waals force experienced between two macroscopic bodies is proportional to their size, and may be either repulsive or attractive. In the case of virus particles suspended in water interacting with a solid surface, the van der Waals force should be attractive and relatively strong (Murray and Parks, 1980). Its magnitude depends on the dielectric properties of both the virus capsid and sorbent. In the case of the sorbent, van der Waals forces should follow the trend:

Metals (strong) > Sulfides > Transition Metal Oxides >
SiO₂ > Organics (weak)

Murray and Parks (1980) found that poliovirus adsorption to various oxide mineral surfaces followed this trend and concluded that electrostatic and van der Waals forces were the dominant forces controlling adsorption.

1.4.3.3. Hydrophobic Interactions

Virus attachment to a solid surface may also occur by hydrophobic interactions. When a non-polar molecule (or macroscopic body made up of non-polar surface groups) is suspended in water, the water molecules arrange themselves into a highly ordered structure around the molecule called a clathrate cage

(Israelachvili, 1985). This ordering is entropically unfavorable, and can drive the molecule (or macroscopic body) out of solution onto a solid surface (Israelachvili, 1985; Norde, 1986). Hydrophobic interactions appear to be at least partially responsible for the adsorption of proteins such as human plasma albumin and bovine pancreas ribonuclease to negatively charged polystyrene surfaces (Norde and Lyklema, 1978), and the attachment of viruses to membrane filters (Shields et al., 1986; Farrah, 1982; Shields and Farrah, 1982).

1.4.3.4. Specific Interactions

Additional interactions which can influence virus attachment to solid surfaces include covalent interactions, hydrogen bonding, and electrostatic induction (Murray and Parks, 1980). Although such interactions have not yet been experimentally implicated in virus adsorption to mineral surfaces, they are known to be important for specific biological systems. For example, bacteriophage infection of a host cell occurs by an irreversible attachment (via hydrogen bonding) of the phage tail to specific receptors (or proteins) on the cell surface (Zarybnicky et al., 1980).

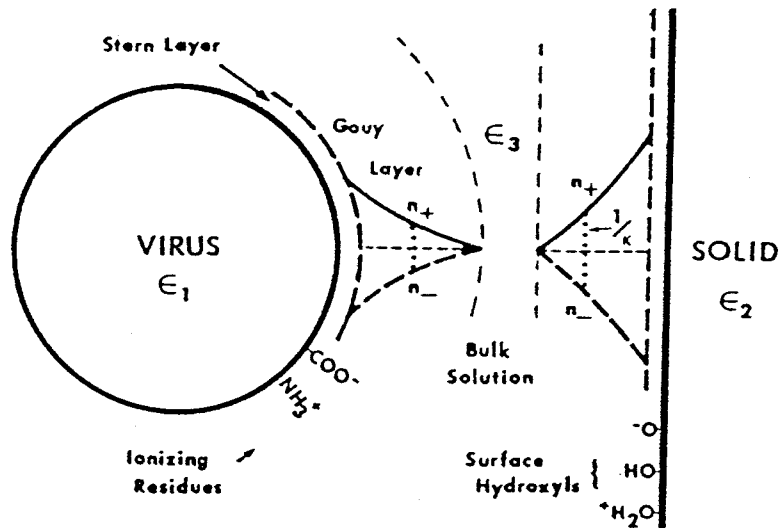


Figure 1.4. Sphere-plate model of virus interacting with a flat surface. From Murray and Parks (1980).

1.4.3.5. Theoretical Analysis of Attachment

Attachment of a virus to a solid surface can be idealized as the interaction of a rigid sphere with a flat plate (Figure 1.4). Because both the sphere and flat plate are charged, they each have a corresponding double layer which has a characteristic thickness $(1/K)$ where

$$K = \left[\frac{64\pi^2 e^2 c i^2}{\epsilon k T} \right]^{\frac{1}{2}}, \quad (1.3)$$

(e) is the charge on an electron ($1.602 \times 10^{-19} \text{C}$), (c) and (i) are the electrolyte concentration and valence, respectively, (ϵ) is the liquid dielectric constant, (k) is Boltzmann's constant

$(1.3805 \times 10^{-23} \text{J/K})$, and T is temperature (in Kelvin). The electrostatic force acting between the particle and wall (F_{el}) can be calculated from (Dabros and Adamczyk, 1978):

$$F_{el} = -\epsilon \zeta_1 \zeta_2 \tau g(H, \tau, Da) \quad (1.4)$$

where (ζ_1) , (ζ_2) are the electrokinetic potentials of the particle and plate surfaces, respectively. The nondimensional groups in (1.4) are defined as follows:

<u>Definition</u>	<u>Meaning</u>
$\tau = Ka$	dimensionless particle diameter
$H = (z/a - 1)$	sphere/plate separation
$Da = \frac{\frac{1}{2}(\zeta_1 - \zeta_2)^2}{\zeta_1 \zeta_2}$	sphere/plate charge asymmetry

where a is the sphere diameter and z is the sphere/plate separation.

The function $g(H, \tau, Da)$ can be written

$$g(H, \tau, Da) = \frac{\exp(-\tau H)}{1 \pm \exp(-\tau H)} \mp Da \frac{\exp(-2\tau H)}{1 - \exp(-2\tau H)} \quad (1.5)$$

The upper and lower signs in (1.5) correspond to, respectively, constant potential and constant surface charge double layer models.

The van der Waals force acting between the sphere and plate can be written,

$$F_{LV} = \frac{A_{123}}{6a} f(H, \bar{\lambda}) \quad (1.6)$$

where A_{123} is the Hamaker constant for the interaction of the sphere (1) with the planar surface (3) through medium (2). The retardation

parameter ($\bar{\lambda} = \frac{\lambda}{a}$) is a correction term which accounts for the finite travel time of electric fields between atoms undergoing dipole-dipole interactions. Retardation acts to reduce the strength of van der Waals forces (Israelachvalli, 1985). The function $f(H, \bar{\lambda})$ is given by,

$$f(H, \bar{\lambda}) = \frac{\bar{\lambda}(\bar{\lambda} + 2Hp)}{(\bar{\lambda} + Hp)^2 H^2} \quad (1.7)$$

where $p=11.12$ (Dabros and Adamczyk, 1978).

In natural systems, the electrostatic interactions between viruses and mineral surfaces (1.4) are repulsive (Gerba, 1984) while van der Waals interactions (1.6) are always attractive. Thus, depending on the relative strength of these two forces, particle

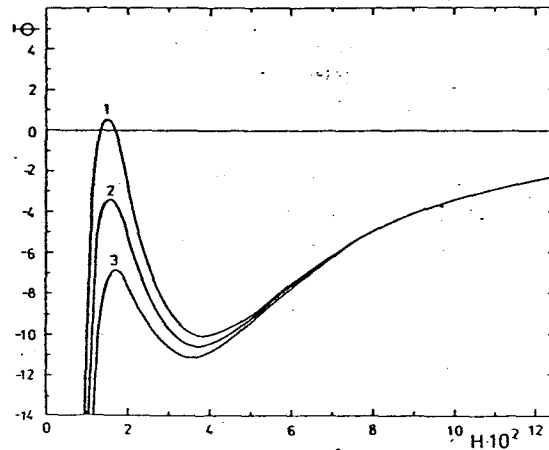


Figure 1.5. Interaction energy profiles calculated for selected values of Dl . For this calculation, $Ad=1.64$, $\bar{\lambda}=0.3$, $\tau=100$ (retarded interactions) and (1): $Dl=350$, (2) $Dl=330$, and (3) $Dl=310$. From Dabros and Adamczyk (1978).

attachment may occur strongly, weakly, or not at all. This balance between van der Waals and electrostatic interactions is usually evaluated in the context of an interaction potential. The interaction potential ($\bar{\phi}$) is defined as the work required to bring the particle from infinity to a separation distance(H):

$$\begin{aligned}\bar{\phi} &= \frac{\phi}{kT} = \frac{1}{kT_{\infty}} \int (F_{el} + F_{LV}) dH \\ &= \frac{1}{kT_{\infty}} \int (Dl \tau g(H, \tau, Da) + Adf(H, \bar{\lambda})) dH\end{aligned}\quad (1.8)$$

where the dimensionless parameters $Dl = \zeta_1 \zeta_2 \epsilon a / kT$ and $Ad = A_{123} / 6kT$ represent the normalized magnitude of the potentials generated by coulombic and van der Waals forces, respectively.

Figure 1.5 shows calculated interaction potentials as a function of separation distance H for various values of Dl , the double layer number. For $Dl > 0$, the charges on both sphere and surface are the same sign, and electrostatic forces act to repel the sphere from the planar surface. An increase in Dl increases electrostatic repulsion, resulting in a larger energy barrier to particle deposition. In Figure 1.5, a weak potential energy minimum is evident at relatively large separation distances ($H = .038$), probably due to a small double layer thickness (τ is large). Shallow energy minimums at large separation distances are called secondary minima. A primary minimum is evident at small separation distances ($H < .01$) in the figure.

Although the above model is useful for determining trends in adsorption behavior, it is probably not useful as a predictive tool for

determining whether or not adsorption will actually occur. Even in highly idealized experimental systems, the predictions of the sphere/plate model are not realized in practice (Elimelech and O'Melia, 1990; Elimelech, 1990). The model also fails to account for highly complicated interactions that can take place when a protein molecule adsorbs to a surface (Norde, 1986).

1.4.3.6. Equilibrium Models

Virus adsorption to natural materials is often interpreted in the context of Langmuir or Freundlich isotherms. Adsorption isotherms are obtained by adding virus particles to an aqueous dispersion of the solid material of interest. The suspension is mixed until virus adsorption reaches an apparent equilibrium (usually 1 hour or less) and fluid samples are taken and analyzed for PFU. By increasing the number of viruses in the system (or, alternatively, decreasing the weight of solids), apparent equilibrium distributions between the fluid (n_f =PFU/unit fluid volume) and adsorbed (n_s =PFU/unit solid weight) states can be obtained.

Adsorption isotherm data are usually interpreted in terms of Langmuir or Freundlich equilibrium adsorption models. A Langmuir model for virus adsorption can be derived by assuming,

- (i) viruses adsorb to discrete sites on the solid surface,
- (ii) lateral interactions between attached viruses are negligible,
- (iii) the maximum number of adsorbed viruses corresponds to monolayer coverage,

(iv) adsorption occurs by collision of a single virus and a discrete attachment site, and

(v) desorption rates depend only on the number of viruses attached to the surface (Hill, 1977).

If adsorption data can be fit by a Langmuir isotherm, it is often assumed that the adsorption process satisfies the above assumptions. Such conclusions are probably unwarranted in most cases, since adsorption data from systems that satisfy few of the above assumptions may still give rise to Langmuir-like behavior (Chapter 5). This observation has also been borne out in the field of protein adsorption. In a review paper on protein adsorption to surfaces, Norde (1986) notes:

...if an experimental isotherm does fit one of the corresponding equations, this is fortuitous since, in the case of protein adsorption, virtually none of the Langmuir premises is (sic) satisfied. Apart from the problem of reversibility, the adsorption does not take place on fixed sites, the molecule usually changes upon adsorption and lateral interaction may not be ignored. (p. 282)

Since the outer surface of most viruses consists of interlocking protein molecules, rules that apply for protein adsorption to surfaces may also apply to virus adsorption.

1.5. Thesis Overview

From the literature review above, two weaknesses can be identified in current approaches to studying the ecology and mobility of viruses in the environment. First, methods are needed for detecting viruses in environmental systems which do not rely upon conventional viability assays. The current alternative, the use of

hybridization assays, is not readily applicable to many environmental problems since it cannot discriminate between soluble and virus-encapsulated nucleic acids. Second, new methods for investigating virus partitioning to surfaces are needed to allow the adsorption process to be studied over time scales more relevant to many natural phenomena. Current reliance on “equilibrium” batch experiments confines investigations to relatively short time scales and does not provide a great deal of fundamental knowledge concerning the nature of virus adsorption to natural surfaces.

The research presented in this thesis makes significant progress in both of these areas. First, a quantitative nucleic acid hybridization assay was developed for bacteriophage lambda (λ) which measures reservoirs of both soluble and virus-encapsulated DNA in fluid samples. In Chapter 2, the results of preliminary experiments designed to determine the factors affecting DNA/DNA hybridization signals are presented, and this work was used to optimize the hybridization assay for further experiments. In Chapter 3, a modified hybridization assay is presented that distinguishes between soluble and virus-encapsulated DNA. The ability of the modified assay to provide upper-limit estimates of virus viability is evaluated in the context of conventional viability and transmission electron microscope measurements. These data indicate that valid upper-limit estimates of virus viability can be obtained from the new assay, provided that virus inactivation results in capsid rupture and release of nucleic acids.

The second part of this thesis focuses on developing a theoretical and experimental framework in which to investigate virus adsorption to natural surfaces. In Chapter 4, a new kinetic theory for studying virus adsorption and inactivation in batch experiments is presented. This theory suggests a new type of experimental approach which permits the investigation of adsorption processes occurring over relatively long time scales. Using this approach, bacteriophage λ adsorption to Ottawa sand was studied over the course of 4 days and the results are presented in Chapter 5. In Chapter 6, the effects of solution pH and electrolyte composition on long time scale lambda adsorption to sand are investigated. These data indicate that virus adsorption can be strongly time scale dependent, with important implications for both the mobility and dispersal of viruses in the environment. In the section that follows, a description of the model system used in the experimental portions of this thesis is presented.

1.6. Model System

1.6.1. Virus Selection

The virus used in this study was bacteriophage lambda (λ) (cI47) obtained from Dr. Peggy Leib, USC Medical School, Los Angeles, CA. A bacteriophage was selected for these studies for both practical and scientific reasons. Bacteriophage are relatively easy to detect and propagate, allowing a large number of experiments to be carried out in relatively short periods of time. Furthermore, bacteriophage are abundant in natural aquatic

environments (Borsheim et al., 1990), may be ecologically important predators of bacteria (Proctor and Fuhrman, 1990) and vectors for the exchange of genetic material between bacteria (Bergh et al., 1989). λ was chosen since it is one of the best characterized bacteriophage (Katsura, 1981; Katsura and Kobayashi, 1990), it is one of a class of viruses (the lambdoid phages) which appear to be ubiquitous in nature (Hershey and Dove, 1983; Anilionis and Riley, 1980; Riley and Anilionis, 1980) and it is similar in morphology and size to one of the most prevalent classes of viruses found in natural aquatic systems (Bergh et al., 1989). Since some studies have shown that virus adsorption to natural materials can be strain specific (Goyal and Gerba, 1979), the experiments in this study should be repeated using other types of viruses to test the generality of our results. The structure of bacteriophage λ is shown in Figure 1.6. An electron micrograph of λ particles is displayed in Figure 1.7.

1.6.2 Adsorbent

The adsorbent used in this study was Ottawa sand obtained from VWR Scientific. It is a well-sorted quartz sand with a mean diameter of 0.6-0.8mm and a surface area of 180 cm²/gm (Taylor et al., 1981). Ottawa sand was chosen for this study because it has been used in other virus adsorption studies (Taylor et al., 1981; Moore et al., 1981) and is mineralogically homogeneous.

The sand was treated for removal of surface coatings following procedures outlined in Chapter 5. Figure 1.8 shows the effect of treatment on the color of the sand. Figures 1.9-1.12 are a series of

electron micrographs that visually compare the surface of the treated and untreated sand at successively higher magnifications. An analysis of the elemental content of the sand surface was carried out using an energy dispersive spectrometer (EDS). Of the elements detectable with EDS, only silica was observed on the treated sand, while the untreated sand had detectable levels of iron. Scanning electron microscope (SEM) observations of the untreated surface reveals that the iron is in the form of iron oxide particles approximately $1\mu\text{m}$ in size. Techniques used for SEM and EDS investigations are described in Chapter 3.

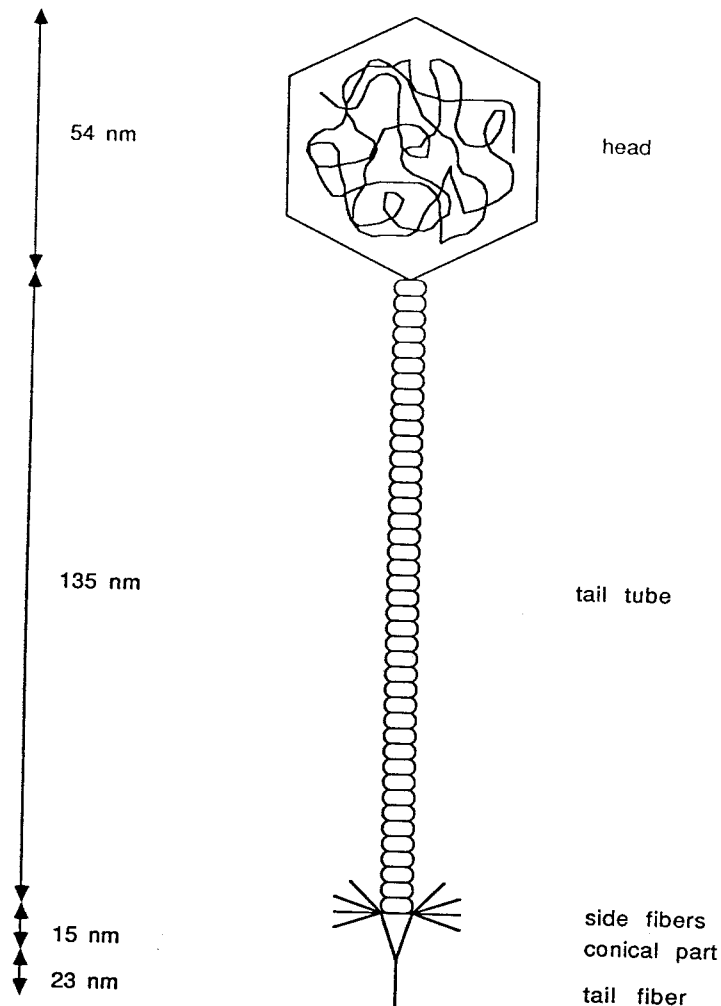


Figure 1.6. Structure of bacteriophage lambda (λ) used in this study. λ consists of an icosahedral head (54nm), a thin noncontractile tail (15x150nm) with fine cross-striation and a thin fiber (2x25nm) at the end. The phage contains a 40 kilobase double-stranded DNA molecule with a contour length of approximately 17.2 μ m. (Figure: Hernandez, 1989; Description: Fraenkel-Conrat, 1985).

Figure 1.7. Transmission electron micrograph (TEM) of bacteriophage lambda particles used in this study. Bar represents 100nm. See Chapter 3 for description of TEM methods.

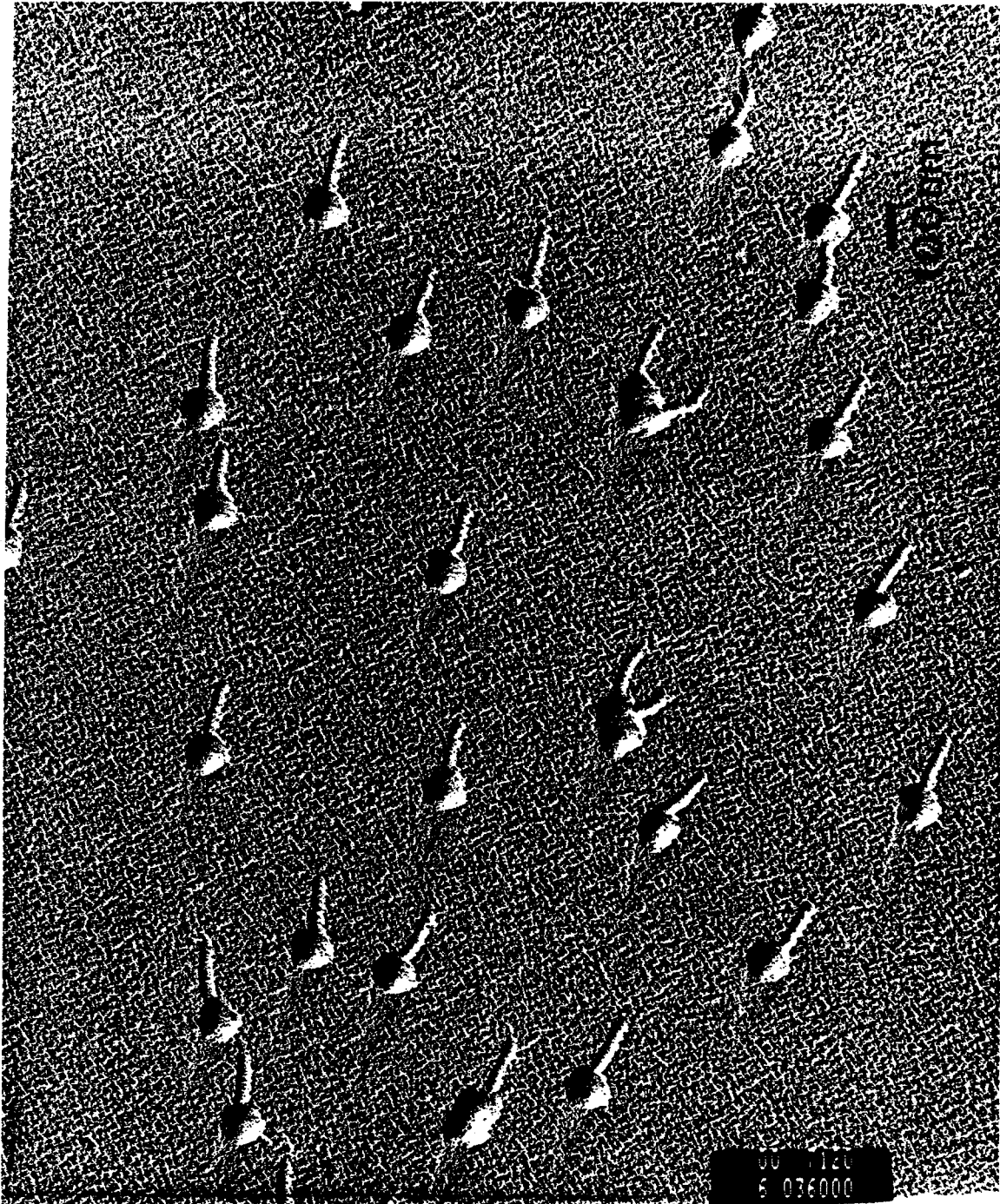


Figure 1.8. Effect of chemical treatment on the color of Ottawa sand.
Top: Treated Sand. Bottom: Untreated Sand.

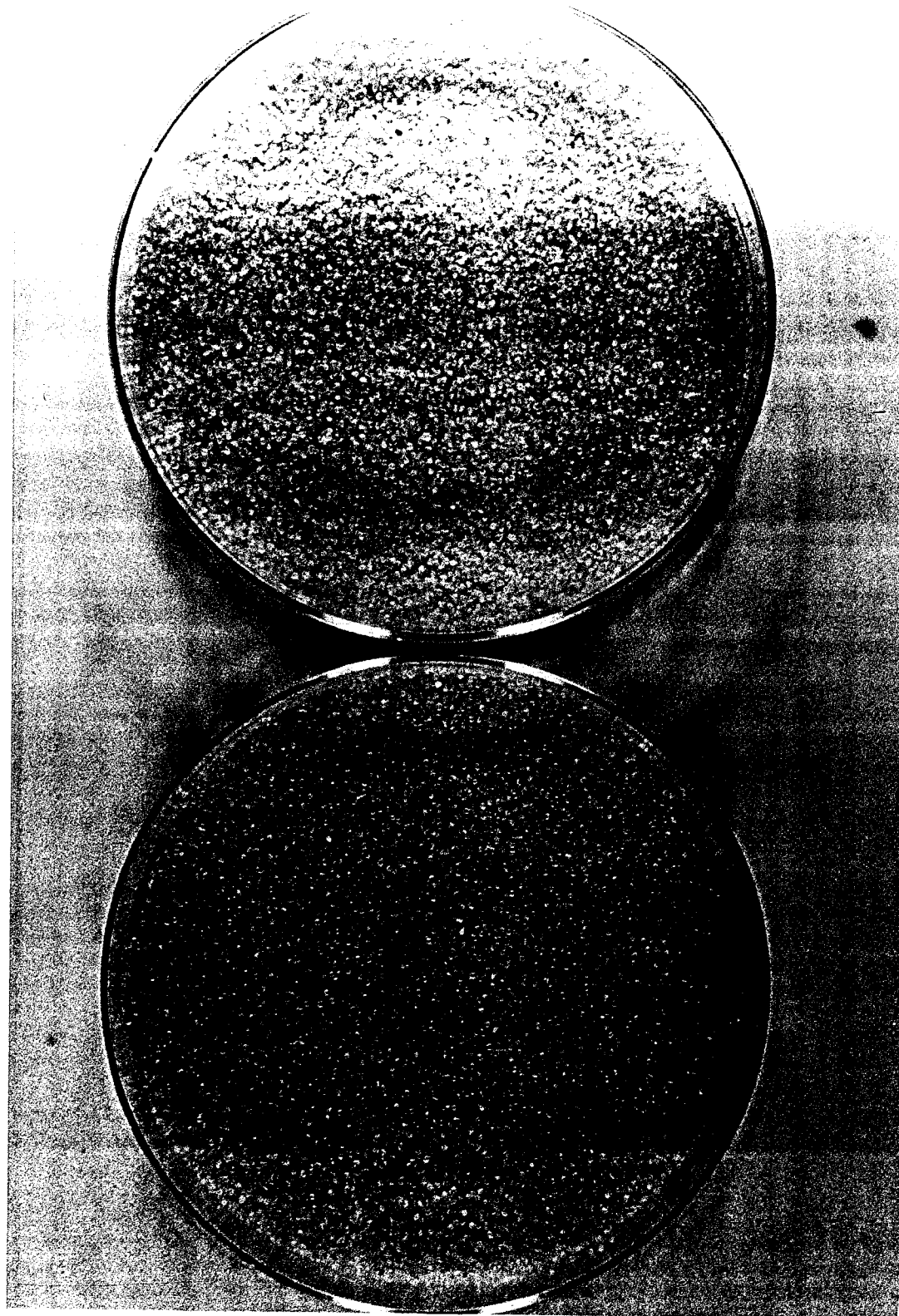


Figure 1.9. Low magnification (96x) scanning electron microscope (SEM) view of (A) treated and (B) untreated sand grains.

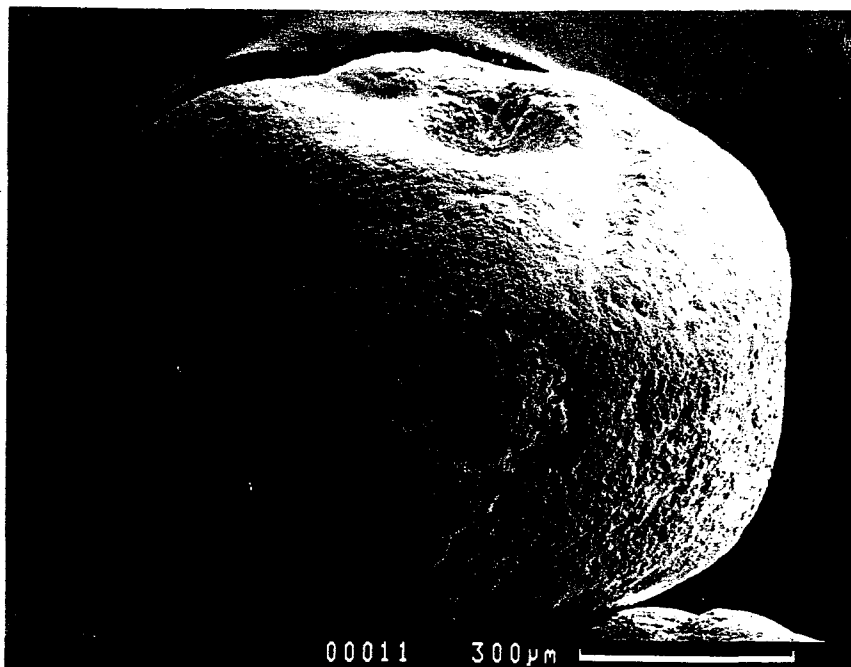
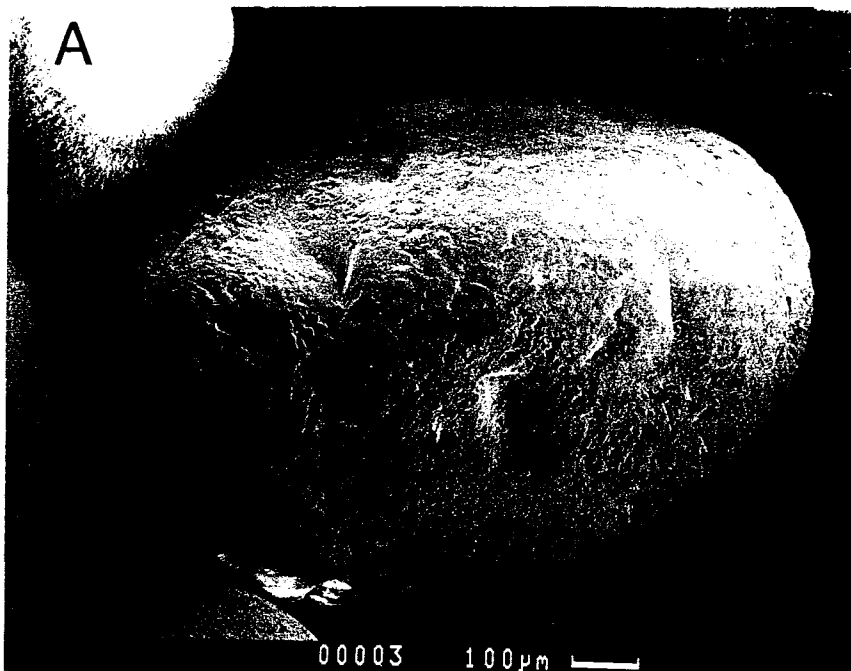


Figure 1.10. Intermediate magnification (1000x) SEM view of (A) treated and (B) untreated sand. Iron oxide particles are present in (B) as fine grained texture.

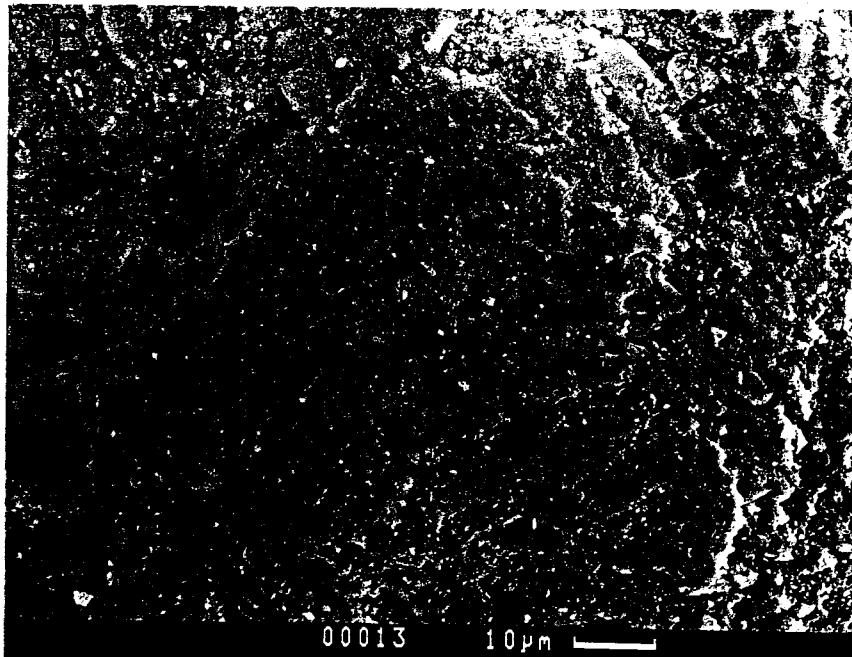
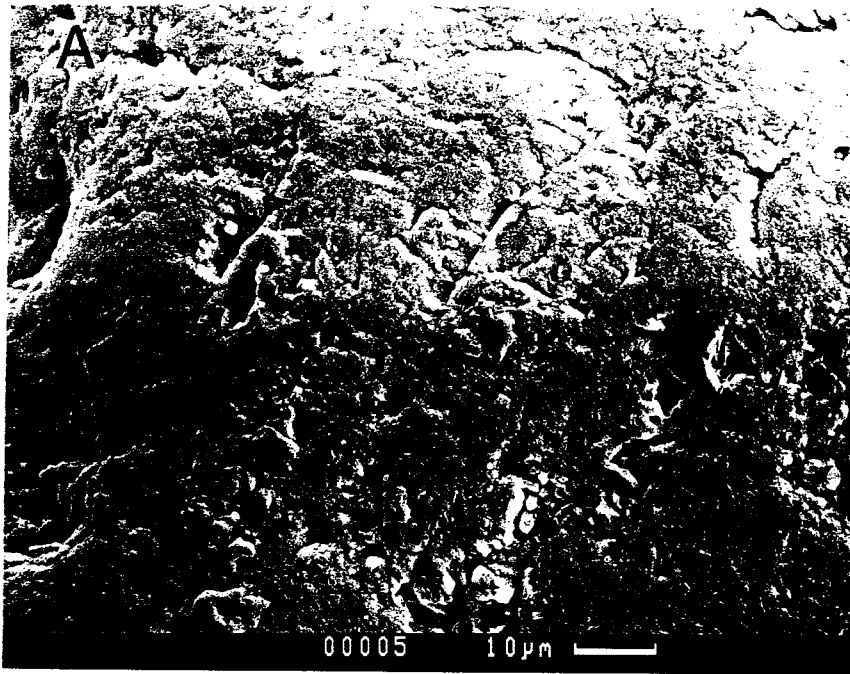
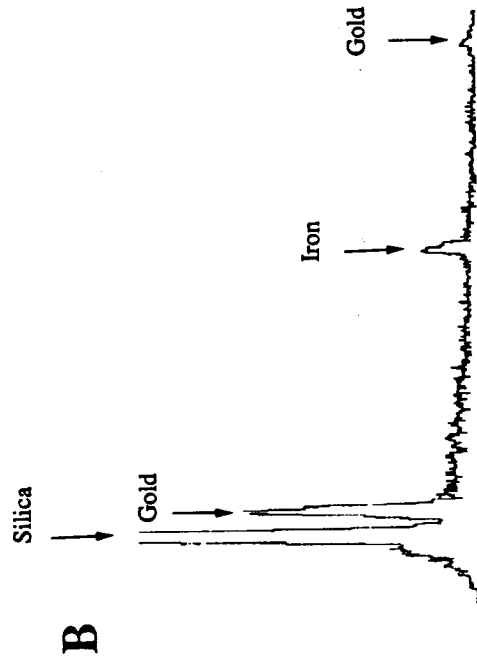
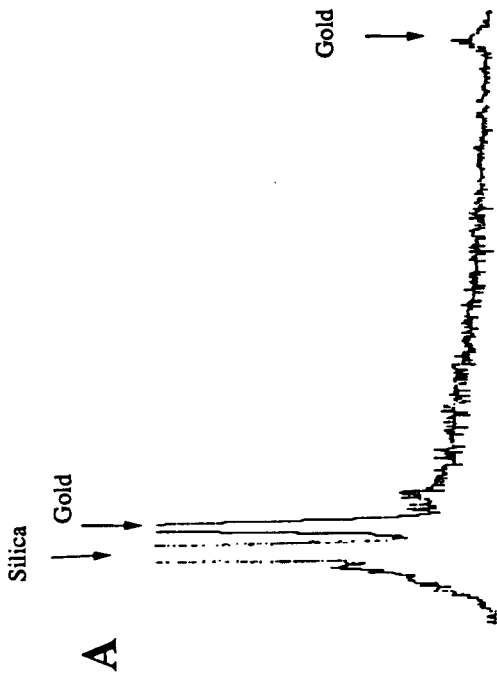
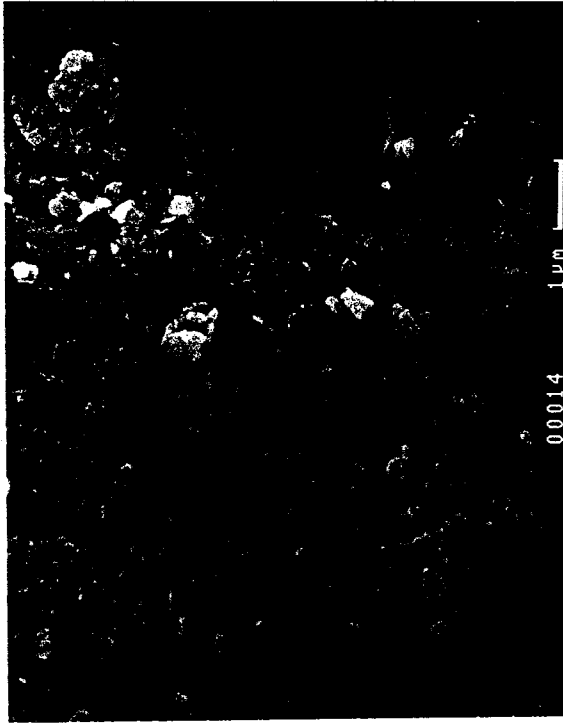


Figure 1.11. High magnification (10,000x) SEM view of (A) treated and (B) untreated sand. Energy dispersive spectra (EDS) of the two surfaces are shown adjacent to the micrographs. Energy Dispersive Spectrum of the sand surface show that iron is present on the untreated sand. The gold peak is from a coating that was applied to the sand prior to imaging with SEM (Chapter 5).



2. Factors Affecting Detection of Bacteriophage DNA Using Hybridization Techniques²

Recent transmission electron microscope (TEM) studies of aquatic samples indicate that bacteriophage are present at high concentrations in many aquatic environments (Proctor and Fuhrman, 1990; Bergh et al., 1989; Borsheim et al., 1990). The fact that bacteriophage are present in aquatic systems at high numbers suggests that they may be an important variable in regulating the population sizes of host organisms (Proctor and Fuhrman, 1990) and in mediating the exchange of genetic material between bacteria by transduction (Kokjohn, 1989). However, little is known about the ecology of these organisms or their host range, in large part because conventional infectivity assays are able to detect only a small fraction (<1/10,000) of the total population observed with TEM (Bergh et al., 1989). Nucleic acid hybridization assays may be an useful alternative for detecting and classifying natural populations of bacteriophage. Although such assays have been used to detect both disease-causing viruses and bacteriophage in natural samples (Preston et al., 1990; Tougianidou et al., 1991; Margolin et al., 1991; De Leon and Gerba, 1991; Richardson et al., 1988; Dubrou et al., 1991; and Ogunseitan et al., 1990), it is still not clear what factors

²To be submitted as a Note to *Applied and Environmental Microbiology*

influence the resulting signal intensities. Therefore, quantification of bacteriophage from natural samples has not been possible using this technique. In this report, bacteriophage λ is used as a model system to investigate physical and chemical factors affecting the intensity of hybridization signals obtained from slot blot procedures, in order to develop a quantitative hybridization assay.

Hybridization measurements of bacteriophage λ c147 DNA were carried out as follows. Samples containing the bacteriophage were heated to lyse phage and denature DNA, and filtered onto a nylon membrane (Zeta Probe, Biorad) using a slot blot apparatus (Schleicher and Schuell). The membrane was recovered from the slot blot and hybridized following manufacturer's recommendations. The probe used to detect DNA immobilized on the membrane was generated from a random primed DNA labeling kit (Boehringer Mannheim) using the entire λ genome as a template and ^{32}P -dCTP as the incorporated radioactive nucleotide. After the membrane was washed, it was exposed to X-ray film at -70°C with intensifying screens (Kodak). The radioactivity was quantified by scanning autoradiograms with a laser densitometer (LKB) and integrating the resulting peaks with an on line integrator (Hewlett Packard 3393A Integrator).

Standard protocols for DNA slot or dot blot hybridizations require that samples are adjusted to an alkaline pH and heated before the DNA is filtered onto a membrane (e.g. Biorad,

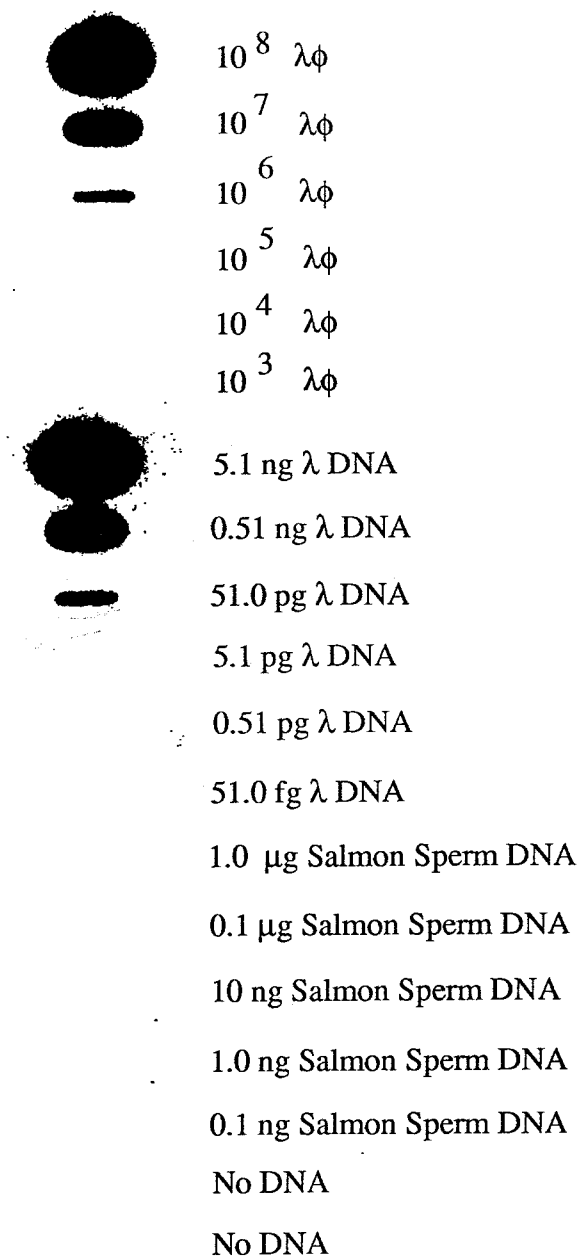


Figure 2.1. Hybridization signals from bacteriophage λ particles, λ genomic DNA, and salmon sperm DNA.

GeneScreenPlus). For the membrane used in this study, the manufacturer's recommendation is that samples should be adjusted to a final concentration of 0.4M NaOH, 10mM EDTA and then heated at 100°C. Figure 2.1 shows the hybridization signals obtained when bacteriophage particles, genomic DNA, and Salmon sperm DNA (Boehringer Mannheim) were diluted (>10,000 fold) into 0.4M NaOH, 10mM EDTA as recommended. Strong hybridization signals for both the purified genomic DNA and bacteriophage particles were obtained, with a lower limit of detection of approximately 10^5 genomes/slot under these conditions. It is known that 10^8 λ bacteriophage particles contain approximately 5.1ng λ DNA (Arber et. al., 1983). Thus, (in theory) the same hybridization signal should be obtained from either that number of virus particles or that amount of DNA. Comparing signal intensities from the bacteriophage particles and purified DNA in Figure 2.1, it appears that there is little difference between the hybridization intensities from the two sources of DNA. However, these results should be interpreted with caution since the number of virus particles in a fluid sample is usually underestimated by PFU measurements (Chapter 1 and 3). No hybridization to the Salmon sperm DNA was detected, suggesting that the random primed probe is specific for λ DNA.

The concentration of salts in environmental aquatic samples can be quite high. To determine if the addition of salts might have an effect on hybridization intensities, varying amounts of $MgSO_4$ and NaCl were added to samples prior to the alkaline heat treatment.

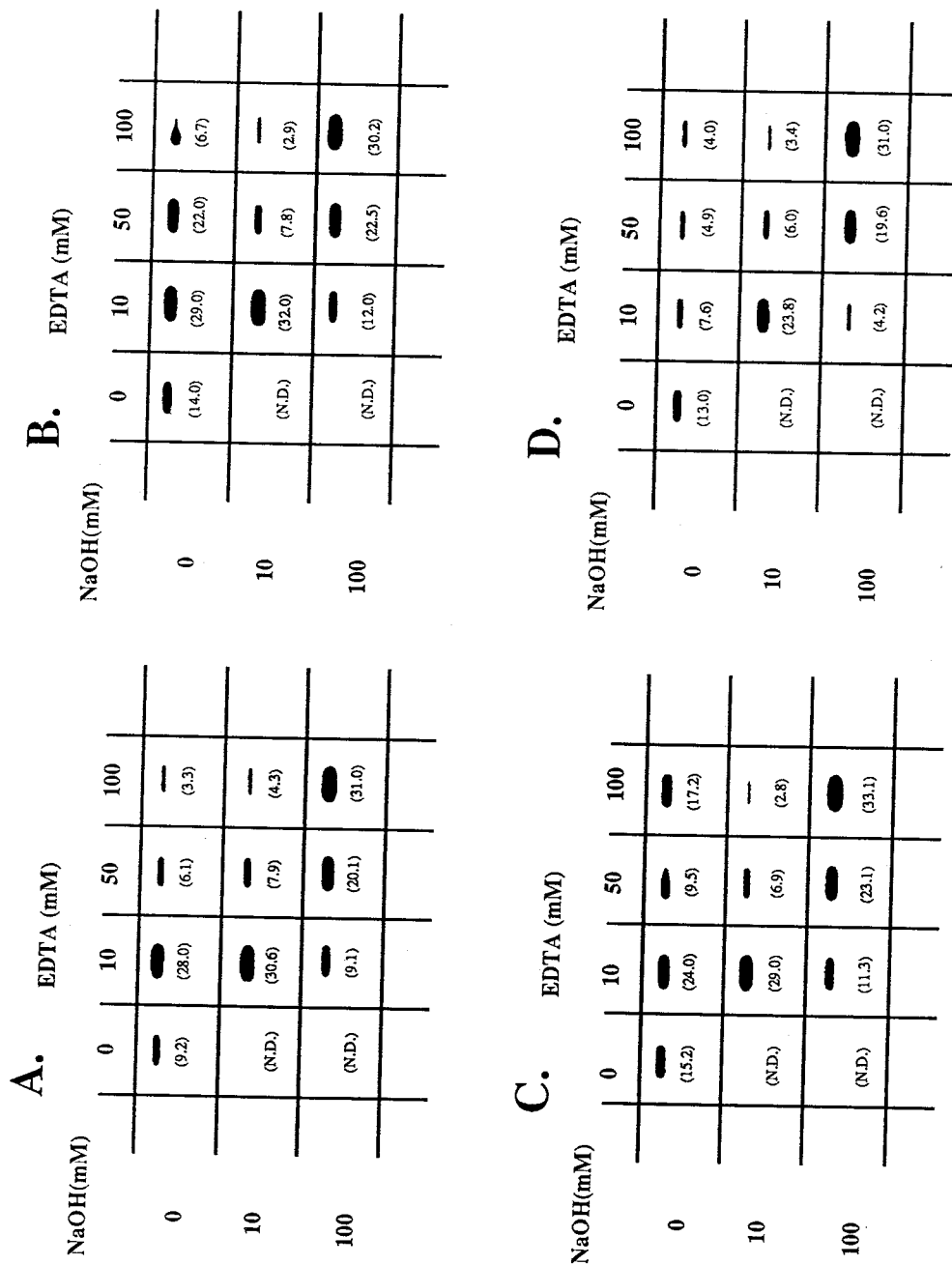


Figure 2.2. Effects of EDTA and NaOH on hybridization signals from $10^8 \lambda$ particles/slot. Tables correspond to different concentrations of NaCl: (A) 0mM, (B) 10mM, (C) 50mM, (D) 100mM. Black spots are reproductions of autoradiogram exposures. Numbers in parentheses are the areas under densitometer scans of each blot. MgSO_4 was 0.5mM in these experiments. N.D.: not detectable.

The hybridization signal was found to be relatively insensitive to NaCl, but quite sensitive to even small amounts of MgSO_4 (<0.5mM). Although this was not fully documented, the signal intensity appeared to change dramatically depending on the concentration and ratios of EDTA, NaOH and MgSO_4 . Figure 2.2 shows the result of an experiment in which MgSO_4 was held constant (0.5mM) and hybridization intensities were examined for a range of NaOH and EDTA concentrations (0-100mM). The resulting hybridization intensities were quite sensitive to both NaOH and EDTA concentrations. Optimum signals were obtained when the concentration of NaOH and EDTA were approximately equal. However, the intensity of hybridization signals did not appear to be affected significantly by NaCl, which varied in this experiment between 0-100mM.

Samples which contained relatively high concentrations of MgSO_4 drained more slowly when they were applied to the slot blot apparatus and showed decreased hybridization signals. This suggested formation of precipitates on the membrane, which might have caused the observed signal attenuation. To test this, solutions containing different concentrations of NaOH (40-1600mM) and EDTA (0-100mM) were prepared. MgSO_4 was added at concentrations of either 10mM or 100mM. The resulting solutions were heated at 100°C to mimic the pre-filtration sample treatment, allowed to cool, and visually inspected for the presence of precipitate. Figure 2.3 shows the results of experiments corresponding to the

A.		B.					
NaOH(mM)		EDTA (mM)					
0	10	50	100	0	10	50	100
40	+	+	-	40	+	+	-
100	+	+	-	100	+	+	+
200	+	+	-	200	+	+	+
400	+	+	+	400	+	+	+
800	+	+	+	800	+	+	+
1600	+	+	+	1600	+	+	+

Figure 2.3. Effects of NaOH and EDTA on precipitate formation in the presence of (A) 10mM and (B) 100mM MgSO₄. (+) indicates that precipitate was observed. (-) indicates that no precipitate was observed.

two MgSO_4 concentrations. Precipitate formation occurred in the majority of samples tested. Precipitate levels decreased with increasing concentrations of EDTA, suggesting that the precipitate was probably magnesium hydroxide.

Although the precipitate explains why samples drained more slowly and hybridization signals were attenuated for high MgSO_4 concentrations, it does not fully account for the signal variability seen in Figure 2.2. First, MgSO_4 concentrations were much lower in the latter experiments (0.5mM) and no precipitate was observed. Second, the occurrence of precipitate appears to be negatively correlated with increasing concentrations of EDTA, as expected (Figure 2.3). In the experiments shown in Figure 2.2, on the other hand, there is clearly an optimum EDTA concentration above and below which hybridization signals are significantly reduced.

Both addition of SDS and repeated cycles of heating and cooling can be used to enhance lysis of bacteriophage (Sambrook et al., 1989). Since release of DNA from phage heads is probably a prerequisite for detecting the DNA with a nucleic acid probe, it is possible that factors which result in more complete phage head lysis might also enhance hybridization signals. To test this idea experimentally, DNA was added to three different buffers which were then filtered onto a membrane after (a) heat treatment in alkali following the standard protocol, (b) addition of SDS and subsequent heat treatment in alkali, or (c) three cycles of heating (100°C) and cooling (on ice) in alkali.

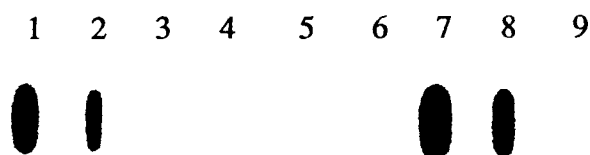


Figure 2.4. Hybridization signals from equivalent numbers of bacteriophage particles (1.5×10^8 PFU) suspended in NaOH buffer (0.4M NaOH and 10mM EDTA), Tris Buffer (10mM Tris HCl (pH 8.0), 10mM MgSO_4 , and 10mM CaCl_2), and MgSO_4 buffer (10mM MgSO_4). SDS was used at 1% (w/v). Slot numbers refer to: (1) NaOH buffer, (2) NaOH buffer, 3 heat and cool cycles, (3) NaOH buffer and SDS, (4) Tris buffer, (5) Tris buffer, 3 heat and cool cycles, (6) Tris buffer and SDS, (7) MgSO_4 buffer, (8) MgSO_4 buffer, 3 heat and cool cycles, (9) MgSO_4 buffer and SDS.

The results of this experiment are shown in Figure 2.4 and 2.5.

Hybridization of samples containing the Tris buffer resulted in no detectable signal. Samples in MgSO_4 buffer gave rise to

hybridization signals slightly higher than that observed for the NaOH buffer. When SDS was added to either of these buffers, however,

hybridization signals were reduced to undetectable levels. For both the NaOH and MgSO_4 buffers, repeated cycles of heating and

cooling prior to filtration reduced hybridization signals, possibly due to DNA shearing. However, the length of time samples were heated did not appear to significantly affect hybridization signals (Figure 2.5).

Only when the heating step was skipped altogether, was a significant decrease observed in the hybridization signal obtained from bacteriophage λ particles (Figure 2.5, blot 6).

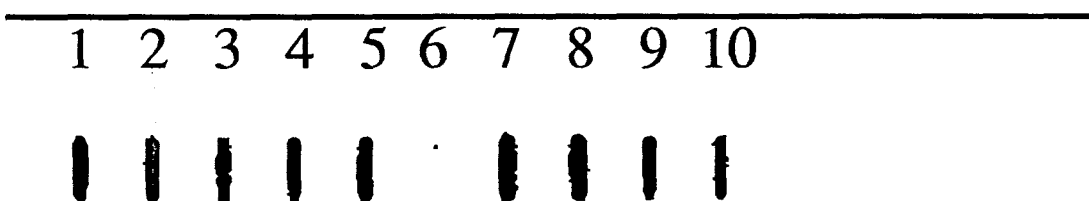


Figure 2.5. Effect of heating on hybridization signals from 3.8ng of genomic DNA (1-5) and 3.8×10^7 bacteriophage particles (6-10). Heating was performed for different times prior to applying samples to slot blots: 0 min (1,6), 5 min (2,7), 10 min (3,8), 30 min (4,9), 60 min (5,10).

Some protocols call for rinsing of slot blot wells after the sample has been drawn through a filter (e.g. Biorad). Figure 2.6 shows the effect of this rinsing step (using 0.5ml of ddH₂O) on hybridization signals. Rinsing the membranes after application of the sample reduced signal intensity by approximately 10 fold.

Another factor tested was the variability of hybridization signals from a given amount of DNA with respect to the position of the slot in the slot blot apparatus. This was examined by loading equal amounts of λ DNA into all reservoirs of the slot blot apparatus and filtering the samples onto a membrane. When the membrane was hybridized, washed and exposed to X-ray film, the resulting

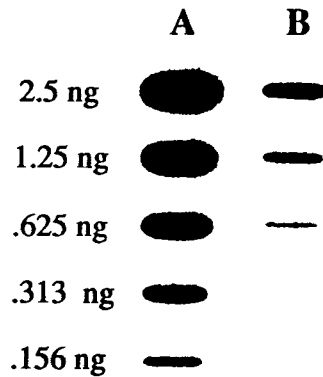


Figure 2.6. Comparison of hybridization signals from the same samples with (B) and without (A) a slot rinse after filtration. The amount of DNA loaded into each slot is indicated.

signals were within $\pm 10\%$ of 1×10^7 (arbitrary units). However, there was a systematic decrease in hybridization signals from samples located in the row nearest the suction port (row A in the figure). Hybridization intensities also decreased toward the bottom of the membrane, suggesting that spatial variability in gene probe signals can occur both along rows and down columns. The observed variations, although systematic, were still a relatively minor percentage of the overall signal. As long as the potential for spatially varying hybridization signals is recognized, the technique can be used to quantitatively compare DNA content in different fluid samples.

These results indicate that hybridization intensities obtained from slot blot methods can be extremely sensitive to the electrolyte composition of solutions containing DNA. Contrary to standard protocols (Biorad), optimum hybridization intensities were obtained

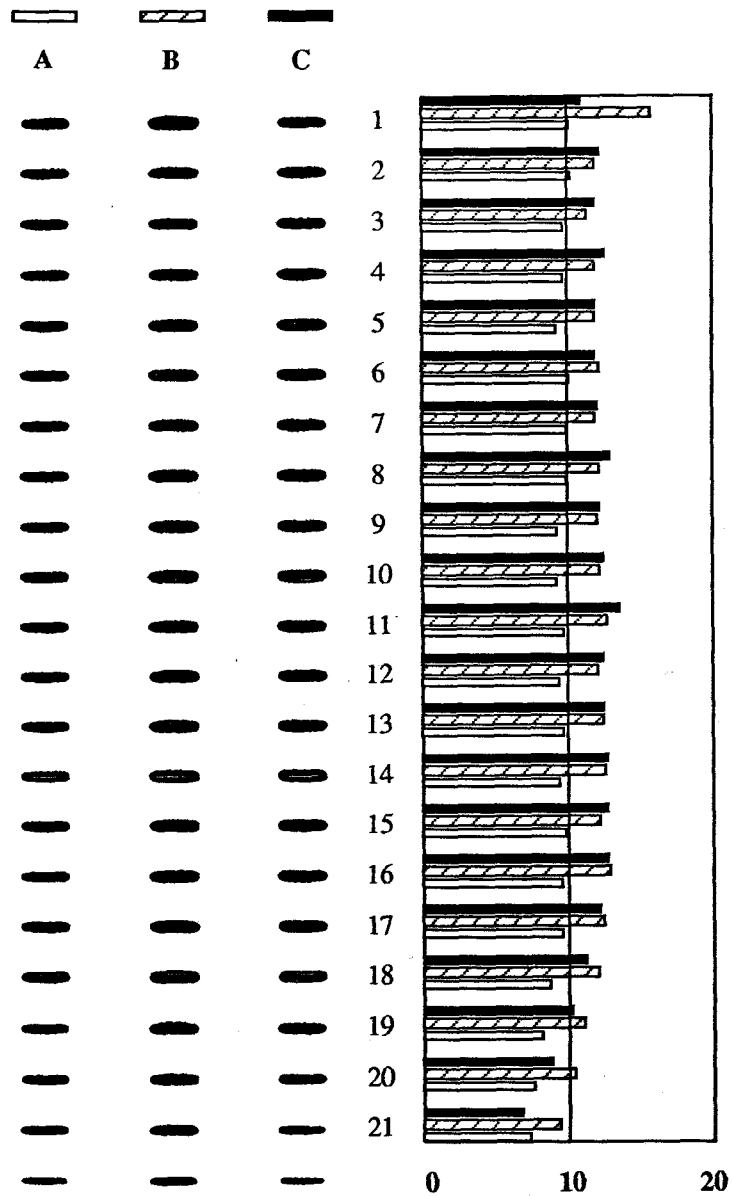


Figure 2.7. Spatial variations in hybridization signals obtained with the Schleicher and Schuell Minifold II slot blot apparatus. Column A is nearest the suction port. Bars represent densitometric scans of the blots ($\times 10^6$) corresponding to the three columns in a given row. $5 \times 10^6 \lambda$ particles were loaded into each slot.

for NaOH/EDTA ratios of approximately 1 when the MgSO_4 concentrations were $>0.5\text{mM}$. The addition of MgSO_4 resulted in drastic reductions in hybridization intensities in cases where NaOH concentrations were high relative to EDTA. The addition of NaCl did not appear to affect hybridization intensities, even at high concentrations, suggesting this effect was not related to ionic strength alone. At high MgSO_4 concentrations, precipitates can form in the presence of NaOH which may significantly reduce the ability of samples to be filtered with a slot blot apparatus, and may affect the resulting hybridization signal. Although hybridization intensities are found to be relatively insensitive to the length of time the sample is heated prior to filtration, repeated cycles of heating and cooling can result in loss of signal. When the solution chemistry of samples is fixed, hybridization signals are reproducible, with only small but systematic spatial variations across the membrane and are directly related to the amount of DNA in the sample (Chapter 3). These results suggest that hybridization techniques may be useful for quantitatively measuring bacteriophage DNA concentrations in natural samples, but hybridization intensities from samples collected under different salt conditions should be interpreted with caution.

3. Estimating Virus Viability Using a Modified Nucleic Acid Hybridization Assay³

3.1. Summary

Methods for detecting fluid-borne viruses are needed to investigate the role of viruses in aquatic ecosystems and to aid in the protection of water resources from wastewater contamination. One such method uses hybridization techniques to detect the nucleic acid corresponding to a specific virus. Interpretation of data from this approach can be difficult, however, since it is not clear whether the nucleic acid detected is dissolved in solution or associated with viable virus particles. Using bacteriophage λ as a model system, a modified hybridization assay has been developed which employs DNase protection and slot blot methods to quantitatively measure the concentration of soluble and virus-encapsulated nucleic acids in fluid samples. The possible use of this assay to obtain upper-limit estimates of virus viability was tested using a model system that consisted of inactivating bacteriophage lambda particles. DNase-protected DNA declined in parallel with estimates of virus viability in this system, indicating that inactivation was accompanied by capsid rupture. These data demonstrate that when virus inactivation results

³To be submitted to *Proceedings of the National Academy of Sciences, USA*. To be communicated by Professor James Bonner, Caltech.

in the release of nucleic acids, the modified hybridization assay can be used to obtain upper-limit estimates of virus viability. Since bacteriophage inactivate primarily by capsid rupture, the procedures described here should be applicable to most strains of these viruses.

3.2. Introduction

Viruses are found in a variety of natural environments, where they can exist as natural inhabitants (Proctor and Fuhrman, 1990; Bergh et al., 1989; Borsheim et al., 1990) or as contaminants introduced from waste treatment (Gerba and Lance, 1978; Ketratanadul et al., 1991). Recent evidence suggests that viruses, and especially bacteriophage, are present in natural aquatic environments at much higher levels than had been previously assumed (Proctor and Fuhrman, 1990; Bergh et al., 1989; Borsheim et al., 1990). These observations have raised the possibility that viruses may play an important role in natural environments both in controlling indigenous populations of host organisms (Proctor and Fuhrman, 1990; Borsheim et al., 1990) and in mediating genetic exchange between susceptible populations (Kokjohn, 1989). However, the ecology of viruses has not been well-studied, in part due to difficulties in detecting viruses using infectivity assays (Proctor and Fuhrman, 1990; Olson, 1991).

Nucleic acid hybridization techniques are a promising alternative to infectivity assays for virus detection. This approach involves extracting total DNA or RNA from a sample, immobilizing the nucleic acid on a membrane, and hybridizing the membrane with

a nucleic acid probe that has a nucleotide sequence unique to the virus of interest. Nucleic acid hybridizations have been used to identify poliovirus (Preston et al., 1990; Tougianidou et al., 1991; Margolin et al., 1991), rotavirus (De Leon and Gerba, 1991), and other human enteric viruses (Richardson et al., 1988) in fluid samples, hepatitis A virus and other enteroviruses in wastewater and surface water (Dubrou et al., 1991), and bacteriophage DNA in lake water (Ogunseitan et al., 1990) (for a review, see Sayler and Layton, 1990). Although these studies have demonstrated the presence of viral nucleic acids in samples, the hybridization techniques used do not discriminate between dissolved nucleic acid and nucleic acid associated with infective virus particles (Olson, 1991).

The fact that hybridization techniques cannot discriminate between these two reservoirs of nucleic acid seriously limits the method's potential for both environmental and ecological studies. For studies which aim to detect the presence of disease-causing viruses, only the fraction of nucleic acid encapsulated in viable viruses is of interest. In ecological studies, on the other hand, knowledge of the distribution of viral nucleic acid between dissolved and encapsulated states may be extremely important since only infective virus particles can affect host population viability, while both pools of nucleic acid are potentially available for environmental gene transfer. Since viable viruses encapsulate their nucleic acids in protein capsids, a method for distinguishing between protein encapsulated and soluble

nucleic acids would be useful for estimating the fraction of nucleic acid in a sample associated with viable viruses.

In this report, a modified hybridization assay is presented that utilizes bacteriophage λ as a model system. Bacteriophage λ was chosen since it is one of a class of viruses (the lambdoid phages) which appear to be ubiquitous in nature (Hershey and Dove, 1983; Anilionis and Riley, 1980; Riley and Anilionis, 1980), it is similar in morphology and size to many of the viruses found in natural aquatic systems (Bergh et al., 1989), and the processes responsible for its inactivation are well documented (Yamagishi and Ozeki, 1972; Yamagishi et al., 1973; Pollard and Solosko, 1971). The assay developed with this phage provides an upper-limit estimate of virus infectivity by determining the fraction of DNA in a fluid sample which is protected from DNase activity by protein encapsulation. The efficacy of this new technique for estimating nucleic acid reservoirs was tested on a suspension of inactivating bacteriophage λ . When hybridization data were compared with conventional viability and electron microscope measurements, the new method was found to provide reliable estimates of the distribution of nucleic acid between dissolved and encapsulated states.

3.3. Materials and Methods

3.3.1. Preparation of Bacteriophage

Bacteriophage λ cI47 was a gift from Dr. Peggy Leib, USC Medical School, Los Angeles, CA. Phage stocks were prepared by infecting host cell *E. coli* C600 at low multiplicity, isolating the phage

from cell debris by polyethylene glycol precipitation, purifying the phage by two sequential ultracentrifugations in CsCl gradients, and dialyzing the resulting phage suspensions against a standard salt buffer (SM) (Sambrook et al., 1989). Using these procedures, stock titers were routinely obtained with greater than 10^{12} plaque forming units (PFU)/ml.

3.3.2. DNA/DNA Hybridization

NaOH and EDTA were added to fluid samples at a final concentration of 10mM each and the samples were heated at 95°C for 10 min to rupture phage and denature DNA. Treated samples were loaded onto a slot blot apparatus (Minifold II, Schleicher and Schuell) and drawn through a nylon membrane (Zeta Probe, Biorad). Membrane prehybridization, hybridization, and washing steps were carried out in accordance with the manufacturer's recommendations. The probe used to detect DNA immobilized on the membrane was generated from a random primed DNA labeling kit (Boehringer Mannheim) using the entire λ genome as a DNA template and ^{32}P -dCTP as the incorporated radioactive nucleotide. Preparation of the probe followed manufacturer's recommendations. The average length of the probe was between 80-120 base pairs, based on information supplied by Boehringer Mannheim. After membrane hybridization and washing, portions of the membrane containing sample were removed, suspended in 20ml of scintillation cocktail (Safety Solve), and counted in a scintillation counter (Packard TriCarb 2000). Concentrations of λ DNA in the original sample

were calculated by comparing the counts per minute (CPM) from the hybridized sample with that obtained from dilutions of commercially prepared λ DNA (Boehringer Mannheim) present on the same membrane. Stock DNA used for standards was diluted (>500 fold) into exactly the same buffer used for samples. The concentration and purity of the stock DNA used for standards was determined from optical density (OD) measurements at wavelengths of 260 and 280nm using a spectrophotometer (Hewlett Packard Diode Array Spectrophotometer 8452A). Stock DNA had an $OD_{260/280}$ ratio of 1.84, indicating that it was not contaminated with either protein or RNA (Sambrook et al., 1989). OD_{260} measurements of the stock DNA, when converted to equivalent DNA concentrations, agreed with Boehringer Mannheim specifications. Concentrations were calculated by assuming that when $OD_{260}=1$, the solution had a DNA concentration of 50 μ g/ml (Miller, 1987).

3.3.3. DNase Treatment

Samples containing either bacteriophage λ particles and/or commercially prepared λ genomic DNA (Boehringer Mannheim) were adjusted to 10mM $MgSO_4$ and pH 6. DNase I (from bovine pancreas, Sigma) was added to a final concentration of 0.8U/ml. After a 10 min digestion period, NaOH and EDTA were added to the samples. The samples were then heated at 95 $^{\circ}$ C for 10 minutes, filtered onto a nylon membrane and hybridized as described in the previous section. The addition of NaOH and EDTA followed by

heating inactivates the DNase, lyses the phage particles, and denatures the DNA remaining after digestion by the enzyme.

3.3.4. Viability Measurements

Bacteriophage viability was determined by plaque forming unit (PFU) assays. Dilutions of each sample were mixed with host cells (*E. coli* C600), plated on nutrient agar and incubated following standard procedures (Arber et al., 1983). The resulting plaque counts were converted to PFU/ml and reported as equivalent DNA concentrations assuming $5.1\text{ng } \lambda \text{ DNA}/10^8 \text{ PFU}$ (Arber et al., 1983).

3.3.5. Transmission Electron Microscopy

Samples containing phage were added to an ultracentrifuge tube (Beckman 14x89mm polyallomer), a formvar coated grid was placed on the bottom of the tube, and the sample was centrifuged at 100,000g for 90 minutes at 5°C in a Sorvall RC-70 ultracentrifuge. Grids were subsequently shadowed in two perpendicular directions with platinum at a 5° angle from horizontal and imaged at 13,200X magnification with a Phillips EM420 transmission electron microscope (TEM) at 120kV. Intact bacteriophage particles and bacteriophage debris present on the grid were counted and reported as grid densities. Concentrations of intact bacteriophage in the original sample were calculated from grid densities from known parameters (cross sectional area of ultracentrifuge tube of 1.54cm^2) and by assuming (a) the phage were deposited uniformly across the bottom of the centrifuge tube, (b) the intact phage did not rupture during the centrifugation step and (c) the bacteriophage were cleared

from the suspension by the centrifugation step. Since these assumptions may not be satisfied completely in practice, the resulting estimates represent a lower limit of phage abundance. Fluid concentrations of intact bacteriophage calculated from grid densities were also converted to DNA concentrations for comparison with PFU and hybridization measurements.

3.3.6. Bacteriophage λ Inactivation

Bacteriophage λ inactivation was initiated by suspending phage particles in 40ml of 5mM NaHCO₃ (pH 10) equilibrated at room temperature to a final phage concentration of 1.45×10^9 PFU/ml. Samples of the inactivating suspension were collected over time and analyzed using DNA/DNA hybridization, PFU, and TEM techniques. The sample treatment for DNA/DNA hybridizations is illustrated in Figure 3.2. The samples were divided into DNase treated and untreated fractions, filtered through a slot blot apparatus, and hybridized as described above.

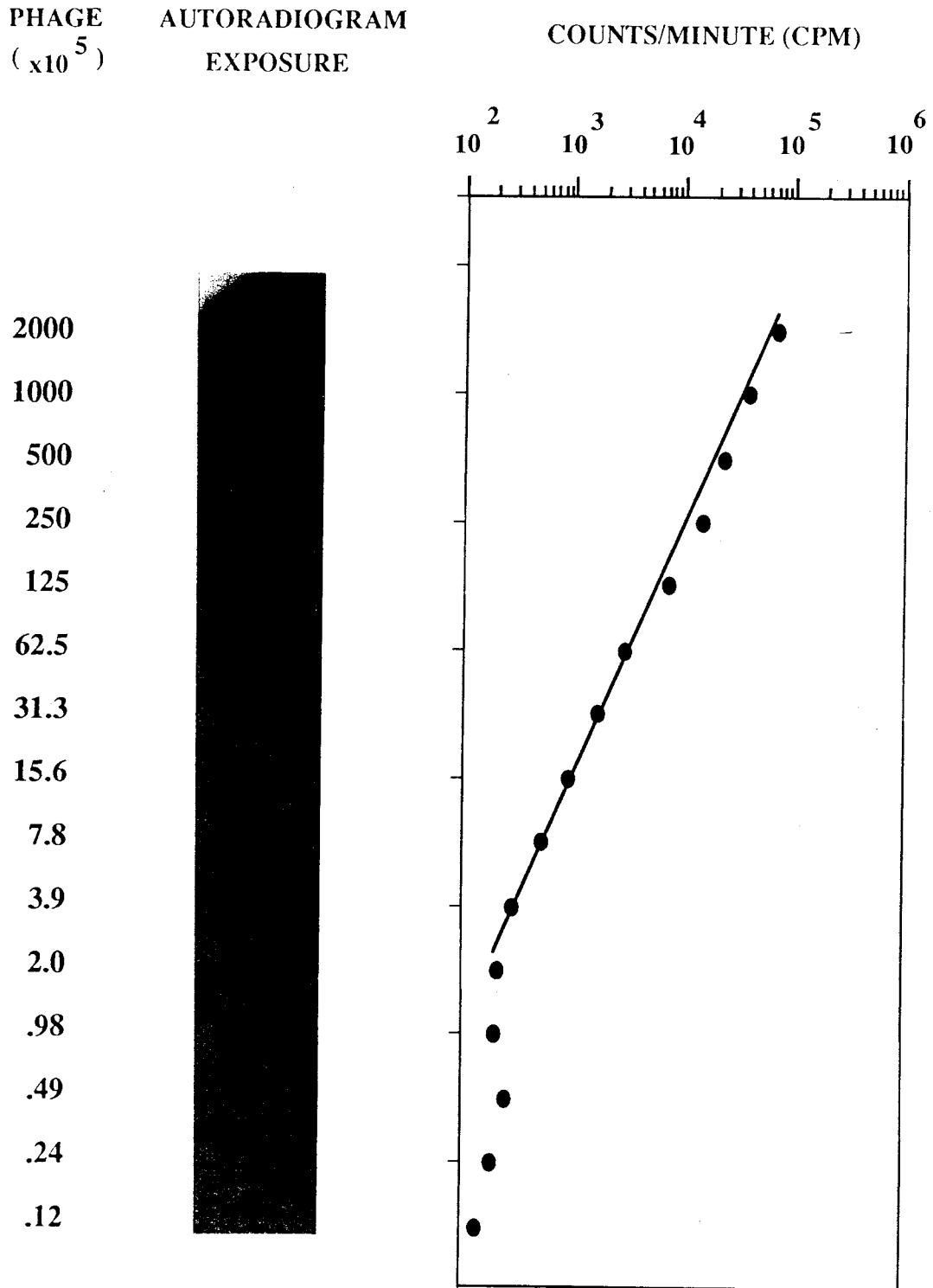
3.4. Results

3.4.1. Measurement of total DNA

To determine if a correlation existed between the concentration of total λ DNA in a fluid sample and the radioactivity obtained from a DNA/DNA hybridization of the sample with a λ -specific probe, dilutions of λ were prepared ranging from 2×10^4 to 4×10^8 phage/ml. When 0.5ml samples of these preparations were treated with NaOH/EDTA, heated, filtered onto a nylon membrane, and hybridized, the resulting radioactivity was found to be strongly

Figure 3.1. Correlation between the number of bacteriophage λ DNA molecules immobilized on a nylon membrane and the radioactive counts obtained from DNA/DNA hybridization of the membrane with a λ -specific radiolabelled probe. Autoradiogram exposures of the membrane are also shown for comparison. Estimates of the number of bacteriophage molecules present on the filter are based on PFU measurements of original fluid samples.

Figure 1



correlated to the amount of DNA immobilized on the nylon membranes (Figure 3.1). In over 30 different experiments, hybridization signals were found to be linearly correlated with DNA concentration above some threshold value (300 CPM in Figure 3.1). Depending on the specific activity of the probe and the hybridization conditions, DNA concentrations of 10^4 to 10^8 molecules/ml can be quantified by direct counting. Thus, under the appropriate conditions the intensity of hybridization signals can be used as a quantitative measure of nucleic acid concentration.

3.4.2. Measurement of Virus Encapsulated DNA

The technique described above detects total λ DNA in a fluid sample, regardless of whether the DNA is encapsulated in bacteriophage particles or in a soluble state. DNase treatment of samples prior to blotting was used to distinguish between soluble and bacteriophage encapsulated DNA using the procedure illustrated in Figure 3.2. Time course experiments were performed in which fluid suspensions of bacteriophage particles, soluble λ DNA, or a mixture of the two were treated with DNase. Hybridization signals from these solutions, both before and after addition of DNase, are shown for one such experiment in Figure 3.3. In each case, DNase quantitatively removed all soluble DNA in the samples, leaving only the fraction of DNA encapsulated in intact bacteriophage particles. The kinetics of this digestion were rapid, with complete digestion of soluble DNA occurring in less than 2 minutes after the addition of the DNase. After the soluble DNA was digested by DNase,

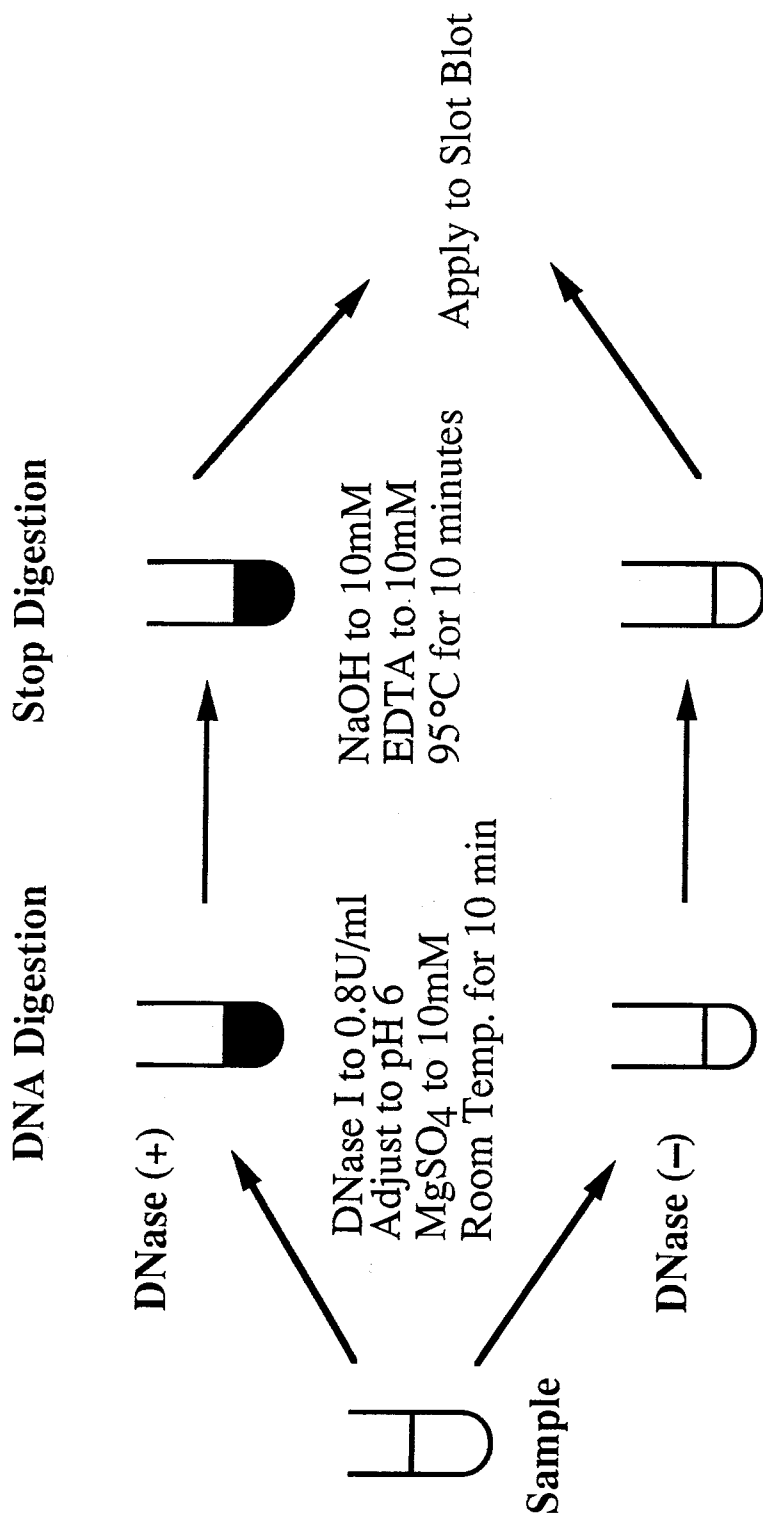


Figure 3.2. Procedure used to process samples for hybridization measurement of encapsulated and soluble DNA. DNase(-) samples were treated in an identical manner as DNase(+) samples, except DNase I was not added. Equal volumes of DNase buffer were added to both the DNase (+) and (-) fractions.

Figure 3.3. Effect of DNase digestion on detection of 5.4×10^8 PFU/ml λ bacteriophage particles (+), 90ng/ml λ genomic DNA (●), and a mixture of the two (▲). Control experiment (■) shows the mixture with no added DNase. CPM values are the average of samples from two separate membrane hybridizations. An autoradiogram exposure of one of these membranes is shown in the inset. We found that hybridization signals from equivalent amounts of DNA can vary spatially across a given membrane by as much as 5-10%. In this experiment, the hybridization signal from genomic DNA samples was relatively high on one of the membranes. Therefore, hybridization signals from samples containing genomic DNA (●) and bacteriophage particles (+) add up to a slightly higher signal than that from the mixture (▲) prior to addition of DNase I.




hybridization signals from all solutions remained constant for the duration of the experiment (210 minutes). No bacteriophage λ inactivation was detected during the digestion step as determined by PFU measurements of the suspension containing only bacteriophage particles (data not shown). These results demonstrate that the DNase treatment procedure shown in Figure 3.2 can be used to quantitatively measure the concentrations of both encapsulated and soluble bacteriophage DNA in a fluid system.

3.4.3. Inactivation Experiment

To determine whether encapsulated DNA concentrations can be used to estimate phage viability, an inactivation experiment was performed in which bacteriophage λ was suspended in an alkaline solution of low ionic strength. λ is unstable under conditions of alkaline pH and low ionic strength (Arber et al., 1983), and phage suspended in this solution immediately began to lose viability. Samples of the suspension were taken at the times noted and analyzed for PFU, encapsulated DNA and total DNA. The state of bacteriophage particles in the inactivating suspension was observed using a transmission electron microscope (TEM).

An autoradiogram exposure of blots from the inactivation experiment is shown in Figure 3.4. At the beginning of the experiment, hybridization signals from DNase treated and untreated samples were roughly equivalent. As the experiment

Figure 3.4. Autoradiogram exposures of blots from the inactivation experiment. Panel A and B are replicates. Panel C shows the radioactive signal from 36ng λ genomic DNA/slot with and without DNase pretreatment. The DNase (+) rows in panel C represent a DNase positive control for the experiment; the DNase (-) rows are the standards used to convert all other hybridization intensities to equivalent DNA concentrations. See Figure 3.5 for conditions of the inactivation experiment.

Time (Hours)	DNase I	A	B	DNase I	C	
0	+			-		
	-			+		
0.5	+					-
	-			+		
1	+					-
	-			+		
2	+					-
	-			+		
4	+					-
	-			+		
5	+					-
	-			+		
6.5	+					-
	-			+		
9	+					-
	-			+		
11	+					-
	-			+		
14	+					-
	-			+		
16.5	+					-
	-			+		
25	+					-
	-			+		

proceeded, hybridization signals from the DNase treated samples decreased while those from the untreated samples remained constant. DNA concentrations estimated from hybridization and PFU measurements are compared in Figure 3.5. Initially, hybridization measurements of encapsulated and total DNA concentrations were the same (145 ng DNA/ml), suggesting that all of the λ DNA was encapsulated. However, only the equivalent of 80 ng/ml was detected by PFU measurements. The remaining 65 ng/ml of encapsulated DNA was either associated with nonviable particles or with viable particles that were not detected by the PFU assay. This discrepancy between DNA concentrations determined from PFU and hybridization assays was reproduced in all three replicate experiments performed. The decrease in λ viability with time shows two populations of differing sensitivity, in agreement with previous studies of λ inactivation (Pollard and Solosko, 1971; Yamagishi and Ozeki, 1972; Sternberg and Weisberg, 1977). In our experiment, λ viability decreased exponentially for approximately 12 hours, after which time a more resistant population (approximately 4% of the initial amount) was present.

DNA concentrations estimated from PFU decreased in parallel with estimates based on hybridization signals from DNase treated samples. Inactivation rate constants calculated from PFU

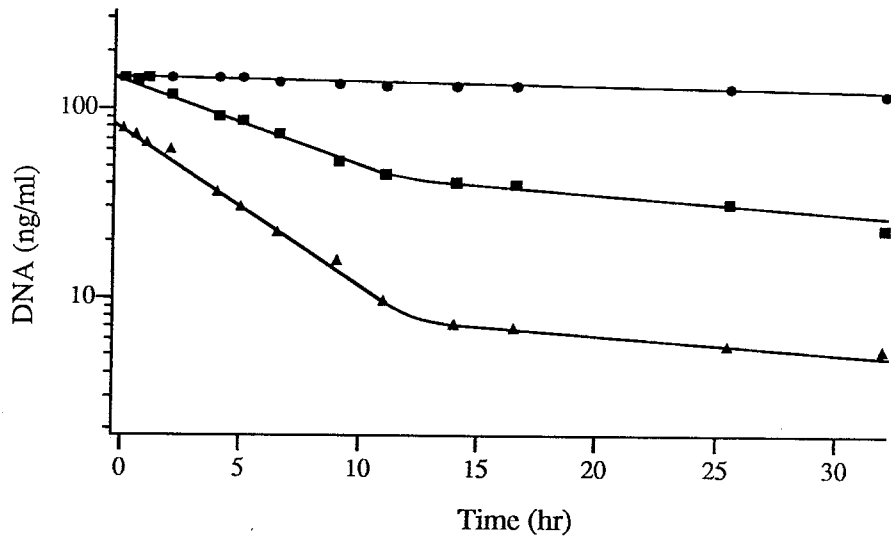


Figure 3.5. Comparison of DNA/DNA hybridization and viability measurements of samples from an inactivating suspension of bacteriophage λ . Horizontal axis represents elapsed time from beginning of the inactivation experiment. Inactivation was initiated by adding CsCl purified λ particles to 40ml of buffer (5mM NaHCO₃(pH 10) and MgSO₄ <0.1mM) for a final phage concentration of 1.45×10^9 PFU/ml. Concentrations of DNA corresponding to PFU (\blacktriangle), DNase-resistant DNA (\blacksquare), and total DNA (\bullet) are shown. Hybridization signals from DNase treated and untreated samples were counted with a scintillation counter and converted to DNA concentrations by comparison with DNA standards filtered onto the same membrane. For this experiment, samples were filtered onto a given membrane in duplicate, and a total of two membranes were prepared and hybridized to a λ -specific probe. The data shown here are the average of four measurements: two replicates from two separate membranes. This experiment was repeated three times with essentially identical results.

Table 3.1. Calculated inactivation rate constants.

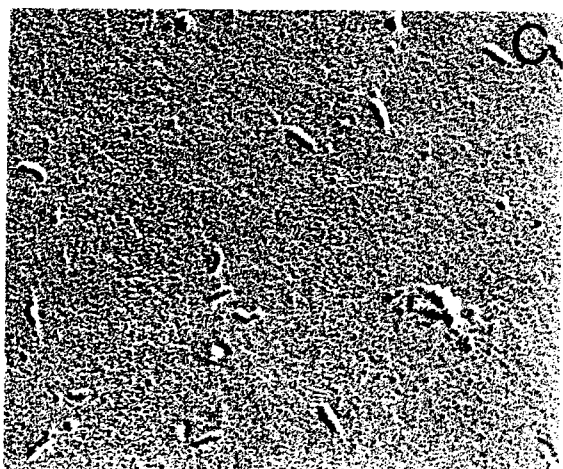
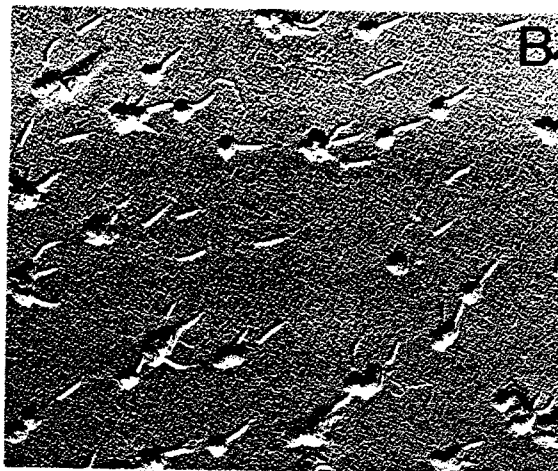
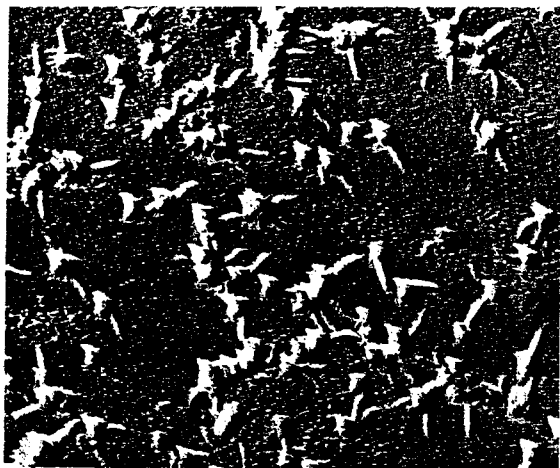
	First Order Rate Constants (1/time (hr))	
	Population #1	Population #2
	(0.0 to 11.0 hours)	(14.0 to 32.0 hours)
PFU	0.19	0.02
DNase (+)	0.11	0.02
DNase (-)	0.0	0.0

Rate constants based on data from PFU measurements and DNA/DNA hybridizations of samples with and without DNase pretreatment. Rate constants were calculated separately for the two virus populations observed in Figure 3.5.

and hybridization measurements are shown in Table 3.1. Rate constants calculated from hybridization measurements of DNase treated samples were similar to those calculated from PFU data. Hybridization signals from samples not treated with DNase remained constant over the course of the experiment, suggesting that λ DNA was stable in the inactivating suspension, even after it was no longer encapsulated. Southern blot analysis (Sambrook et al., 1989) of samples taken at various times during the experiment showed that the molecular weight range of λ DNA in the samples remained constant (data not shown). The fact that hybridization measurements of total λ DNA remained constant during the course of the inactivation experiment is confirmation that direct hybridization of samples with nucleic acid probes can be an unreliable method for detecting infective virus particles.

From earlier electron micrograph studies of bacteriophage λ inactivation, it has been proposed that the primary mechanism for inactivation is head capsid rupture and DNA release (Yamagishi and Ozeki, 1972; Sternberg and Weisberg, 1977). Figure 3.6 shows the appearance of bacteriophage on TEM grids at four successive times during the inactivation experiment. Initially (Figure 3.6A), intact bacteriophage were present at densities of approximately 6 phage/ μm^2 . At later times (Figures 3.6B-D), the density of intact bacteriophage decreased, accompanied by a relative increase in the amount of detached bacteriophage tails. Very few isolated bacteriophage heads were present on the grid, supporting the hypothesis that inactivation was primarily due to head capsid rupture. TEM estimates of intact bacteriophage and bacteriophage debris are shown in Figure 3.7. The density of intact bacteriophage decreased exponentially with time. When these densities were converted to DNA concentrations (right hand axis in Figure 3.7), they were approximately one-half the hybridization estimates of encapsulated DNA, but similar to DNA concentrations calculated from PFU data. The most reasonable interpretation of these data is that both the PFU and TEM methods underestimated the number of bacteriophage particles, and thus the DNA

Figure 3.6. Transmission electron micrographs of samples collected at various times during the inactivation experiment: A (2 hr), B (8 hr), C (13 hr), and D (25 hr). Scale bar represents 1 micron.



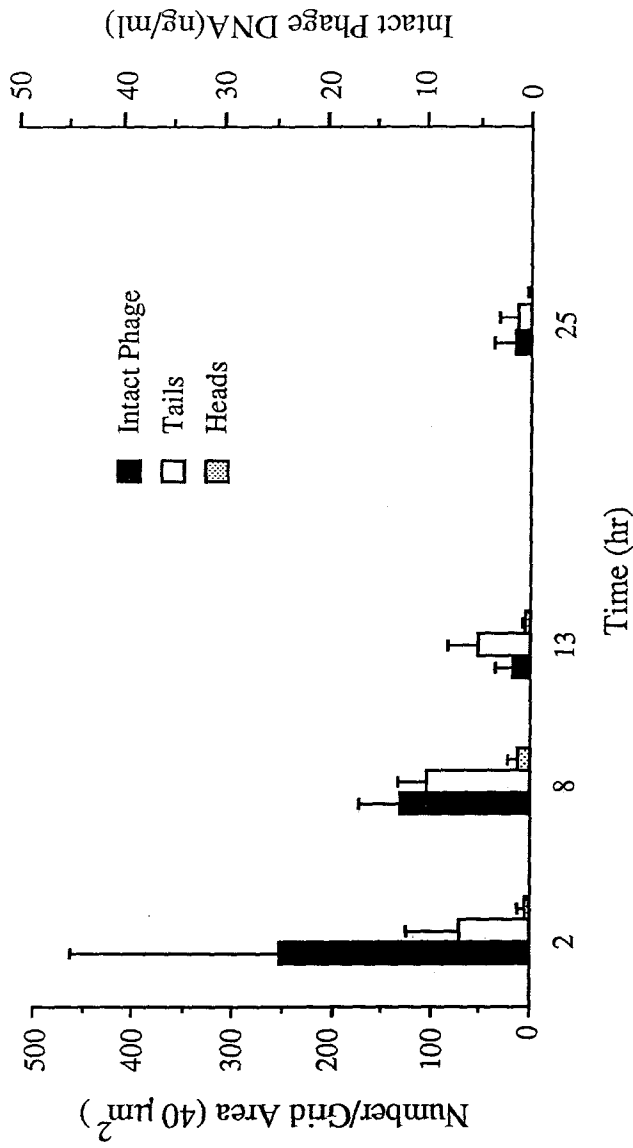


Figure 3.7. Transmission electron micrograph estimates of intact phage, isolated tails, and isolated heads at four separate times during the inactivation experiment. Grid densities shown are the average of counts from at least six different locations on the same grid. Error bars represent 1σ . DNA concentrations corresponding to intact phage counts (right hand axis) were calculated by converting observed grid densities into fluid concentrations and assuming $5.1 \text{ ng } \lambda \text{ DNA per } 10^8 \text{ phage}$.

concentration. It is known that PFU assays of bacteriophage λ underestimate, often by factors of two to three, the number of bacteriophage particles (Arber et al., 1983). In our hands, the TEM counts are also a low estimate of the number of bacteriophage since some of the grids, especially those corresponding to samples taken early in the inactivation experiment, contained large aggregates of bacteriophage particles. Only bacteriophage on the top layer of these aggregates could be counted, biasing grid density estimates to lower values.

3.5. Discussion

These results demonstrate that the modified hybridization assay can be used to quantitatively measure soluble and virus encapsulated nucleic acids. For strains of viruses, like bacteriophage λ , in which inactivation results in the release of nucleic acids, hybridization measurements of DNase treated samples can be used to obtain upper-limit estimates of viability. Linkage between inactivation and DNA release appears to be universal among strains of bacteriophage for which inactivation mechanisms are known (Pollard and Solosko, 1971; Yamagishi and Ozeki, 1972; Yamagishi et al., 1973; Sabatino and Maier, 1980) suggesting that the proposed assay could be a useful indicator of phage viability. As mentioned previously, bacteriophage are apparently ubiquitous in aquatic environments at high numbers, but little is known about the ecology of these viruses or their role in gene transfer (Kokjohn, 1989; Saye and Miller, 1989). The modified hybridization assay presented here

should provide a useful alternative to conventional PFU and TEM techniques for identifying and classifying natural populations of bacteriophage. Coliphage strains have been proposed as indicators of sewage contamination in water supplies (IAWRC, 1991). Thus, estimates of bacteriophage viability based on these hybridization techniques could be useful for screening water samples for fecal contamination and several direct applications could be envisioned.

The assay may also provide an alternative approach for detecting viable mammalian viruses in environmental systems. Several studies have found that poliovirus inactivation results in capsid rupture and the release of intact RNA (Breindl, 1971; Gebhard, 1960). However, poliovirus inactivation can occur for reasons other than capsid rupture, including damage to virus encapsulated RNA (Yeager and O'Brien, 1979; Ward, 1977). Even for viruses in which inactivation proceeds by more than one mechanism, DNase or RNase treatment of samples prior to hybridization can be used to obtain general upper-limit estimates of infectious virus concentrations.

In practice, nucleic acids may be protected from DNase or RNase digestion for reasons other than protein encapsulation. In the case of temperate bacteriophage, viral DNA can be incorporated into bacterial genomes (lysogeny). Adsorption of nucleic acids onto mineral surfaces, such as colloidal material present in the sample, can also result in increased resistance to DNase (Romanowski et al., 1991). However, since methods exist for separating suspended

viruses from those associated with either bacterial cells (Sambrook et al., 1989) or colloids (Gerba and Schaiberger, 1975; Hejkal et al., 1981), the hybridization procedures outlined above could be adapted to account for these two possibilities, further extending the information that could be obtained from natural samples.

3.6. Conclusions

A modified hybridization assay has been developed that can be used to measure reservoirs of bacteriophage DNA and determine the fraction of that DNA encapsulated in bacteriophage heads. Since bacteriophage inactivation occurs primarily by head capsid rupture, the encapsulated DNA detected by the hybridization assay can be used as an upper-limit estimate of DNA associated with viable bacteriophage. It may be possible to extend this assay for detecting viable plant and animal viruses, provided that these viruses are resistant to treatment with DNase or RNase and their inactivation results in the release of nucleic acids. This study shows that a simple DNase treatment of samples prior to hybridization can provide information concerning the potential infectivity of nucleic acids present in the sample. The proposed assay should prove to be a powerful alternative to current techniques for detecting and tracking viable viruses in environmental systems.

4. Kinetic Theory of Virus Adsorption and Inactivation in Batch Experiments⁴

4.1. Summary

The mobility and ecology of viruses in natural environments is strongly influenced by the binding of virus particles to solid surfaces in these systems. Historically, equilibrium Langmuir or Freundlich adsorption models have been used to characterize virus/surface interactions. The use of these equilibrium models to fit data from batch experiments, where viruses are the adsorbate, is not rigorously correct. Viruses inactivate continuously in these systems and thus a true state of equilibrium is never achieved. A kinetic model is presented which accounts for many of the complicated interactions that can occur when viruses encounter a natural surface. Closed form solutions were developed for certain limiting cases and compared to numerical simulations of the full model. Results of these simulations show that four classes of virus/surface interactions can be identified based on comparisons between data from experiments conducted with and without added solids. These results suggest a new experimental approach for investigating virus adsorption to natural surfaces which has many advantages over standard Langmuir or Freundlich analyses.

⁴To be submitted to *Water Resources Research* as the first in a series of three papers.

4.2. Introduction

4.2.1. Motivation

Experimental information about the nature of virus binding to solid surfaces in fluid systems is crucial to a broad spectrum of important environmental problems. Immobilization of viruses on mineral surfaces is the main mechanism impeding virus dispersal in soil or groundwater systems (Gerba, 1984). Thus, knowledge about the nature of that binding process is essential in developing models for the dispersal of mammalian viruses from sites where sewage effluent or sludge is released to the environment (Gerba & Lance, 1978; Ketratanadul et al., 1991), and for the dispersal of viruses used for pest control (Jaques, 1983). Viruses that infect bacteria, called bacteriophage, are apparently abundant at high levels in many aquatic systems (Bergh et al., 1989; Proctor & Fuhrman, 1990) and may represent a large reservoir of the total biocolloids present in these environments. Understanding factors affecting the partitioning of these viruses to solid surfaces in natural systems would be useful to a wide range of problems, including risk assessment for bacteriophage-mediated dispersal of engineered DNA sequences from recombinant microorganisms (Kokjohn, 1989; Saye & Miller, 1989), the role of biocolloids in contaminant transport, and the potential use of bacteriophage as models for inorganic colloids (Bales et al., 1989), environmental tracers (Herbold-Paschke et al., 1991), or as indicators for sewage contamination of water supplies (IAWPRC Study Group, 1991).

4.2.2. Background

The most common experimental approach for studying virus/surface interactions involves mixing a fluid suspension of viruses with a quantity of the solid material of interest. Concentrations of viruses present in the fluid fraction of this batch suspension are measured with time, usually using an assay of virus viability in plaque forming units (PFU). By varying either the amount of virus or solid added to this suspension, different apparent equilibrium distributions of viruses between the solid surface and fluid phase can be obtained. These steady state concentrations are used to construct isotherms which are typically fit with Langmuir or Freundlich equilibrium adsorption models (see Chapter 5). Although this approach has yielded an excellent data base on how virus binding to natural materials is controlled by the chemical composition of both fluid and solid materials (Gerba, 1984; Bitton, 1974), these studies do not necessarily provide useful information about the underlying mechanisms by which this binding is occurring.

It is widely assumed that virus binding occurs as a reversible process (Gerba, 1984; Vilker & Burge, 1980). This conclusion is based primarily on the observation that isotherm data from a vast number of experiments can be fit with either Langmuir or Freundlich isotherm models (Gerba, 1984). Both of these models assume that the distribution of adsorbate between adsorbed and unadsorbed states reaches an equilibrium, resulting from a dynamic balance between simple one-step adsorption and desorption. The two models

differ in the way they treat the change in adsorption free energy as available adsorbate surface sites begin to saturate (Morel, 1983).

It is not clear that such equilibrium models are appropriate for analyzing systems in which viruses are the adsorbate. Langmuir and Freundlich isotherm models assume that the adsorbate being studied is conservative, i.e. does not decay or grow with time. Unlike bacteria, viruses are not capable of metabolizing compounds for maintenance energy, and thus they lose their ability to infect host cells with time through a process called inactivation. Since most batch experiments involving viruses use infectivity assays to detect virus particles in the fluid fraction, the interpretation of data from these experiments is difficult in the context of either Langmuir or Freundlich models for the following reasons.

(i) If a loss of infectivity is observed in the fluid fraction after addition of solid materials, an ambiguity exists as to whether this loss is due to binding of the viruses to the solid fraction or virus inactivation.

(ii) Since virus inactivation is a continuous process, batch experiments involving viruses are fundamentally nonequilibrium systems making application of equilibrium models to these data inappropriate.

Even if it can be argued that inactivation can be neglected over the time scale of the adsorption experiment, this will only be true for a short period of time (minutes to hours). Confining experiments to these short time scales reduces the scope of questions that can be

asked, and makes impossible the investigation of binding mechanisms at time scales relevant to many natural processes.

Further, the assumptions that underlie both Langmuir and Freundlich models are often not satisfied, even in cases where the adsorbate being studied is conservative. It is now well established that the adsorption of polymers, dyes, proteins and detergents to various materials can give rise to Langmuir-type isotherm data, even when the adsorption is occurring irreversibly (Zawadzki et al., 1987). There is experimental evidence to suggest that this phenomenon is the result of two adsorption steps: an initial fast adsorption followed by a kinetically slower rearrangement of the adsorbate on the surface (Zawadzki et al., 1987). Inorganic colloids can also exhibit a similar type of adsorption behavior which has been termed aging. Kallay et al. (1987) found that the desorption of colloidal metal oxides from several materials was dependent on the history of the preparations. The longer time that was allowed for the colloids to adsorb or age, the less desorption was observed when the solid fraction was resuspended in colloid-free buffer. If relatively simple systems give rise to such complex adsorption behavior, it is difficult to believe the same would not be true for structurally complex adsorbates like viruses, especially when the adsorbent is a natural material.

These observations suggest the need for an improved method for examining virus/surface interactions. Rather than rely on equilibrium models of adsorption which are difficult to justify for

systems where the adsorbate is a virus, the possibility of using a kinetic model of virus binding and inactivation was investigated. When this model is nondimensionalized and limiting cases are examined, it is shown that different binding mechanisms give rise to characteristic solutions. These solutions suggest a new experimental approach for obtaining mechanistic information about virus partitioning to solid surfaces which circumvents many of the problems inherent in conventional batch "equilibrium" experiments.

4.3. Model Development

4.3.1. Problem Definition

The problem addressed here is that of a closed system (batch experiment) in which solid material is added to a fluid suspension of viruses. After the solid is added, the viruses present in the system can inactivate in the fluid, bind to the surface reversibly, bind to the surface irreversibly, and/or inactivate on the solid surface as represented by the reaction extents (ξ_j) in Figure 4.1. To facilitate solution of this problem, the following will be assumed:

- (i) the volume of fluid in the system remains constant,
- (ii) the mass of solid in the system remains constant,
- (iii) the experiment is conducted at concentrations such that viruses will not saturate the solid surface,
- (iv) the viruses do not aggregate with time, either on the surface or in the fluid phase, and
- (v) the concentration of viruses in the fluid phase is measured using a viability assay.

The concentration of viruses in the fluid and on the surface can be expressed as (Hill, 1977):

$$n_f = n_{fo} - \frac{\xi_1 + \xi_2}{V} \quad (4.1a)$$

$$n_{sr} = n_{sro} + \frac{\xi_2 - \xi_3 - \xi_4}{W} \quad (4.1b)$$

$$n_{sir} = n_{siro} + \frac{\xi_4 - \xi_5}{W} \quad (4.1c)$$

where

n_f = fluid concentration of viruses (PFU)(fluid volume)⁻¹,

n_{sr} = surface concentration of reversibly adsorbed viruses (PFU)(solid mass)⁻¹,

n_{sir} = surface concentration of irreversibly adsorbed viruses (PFU)(solid mass)⁻¹,

n_{fo} , n_{sro} , n_{siro} = initial concentrations of suspended, reversibly adsorbed, and irreversibly adsorbed viruses, respectively,

V = fluid volume of the system,

W = mass of suspended solids, and

ξ_i = extent of reaction i (PFU).

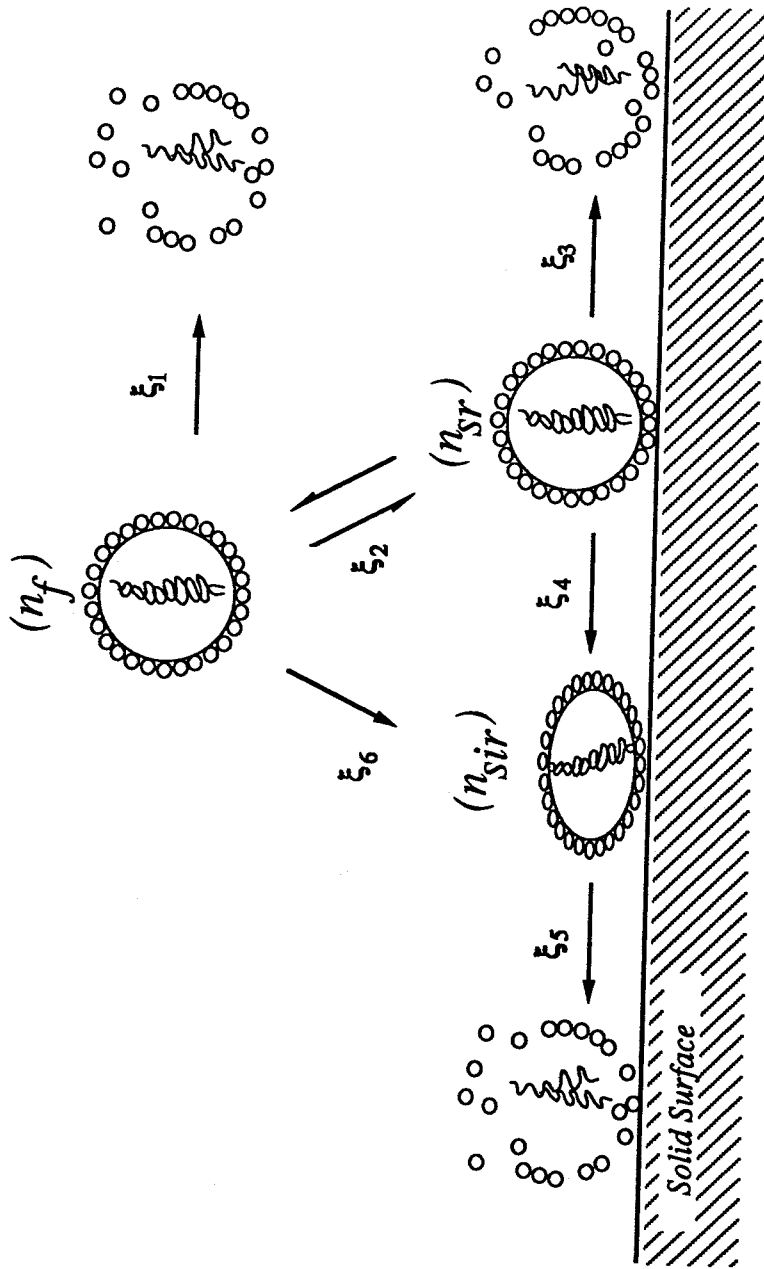


Figure 4.1. Processes occurring in the bulk fluid and at the solid-liquid interface. Viruses can: (i) inactivate in the fluid phase (reaction 1), (ii) adsorb to the solid surface reversibly (reaction 2), (iii) inactivate after they are adsorbed reversibly (reaction 3), (iv) undergo structural modifications that result in irreversible binding (reaction 4), (v) inactivate while in the structurally modified state (reaction 5), and (vi) adsorb irreversibly to the surface directly from solution (reaction 6). ξ_i is the extent of reaction for the i th reaction.

4.3.2. Kinetic Expressions for Reaction Extents

4.3.2.1. Kinetics of Reversible Binding

Cookson (1969) demonstrated that bacteriophage T4 binding to activated carbon in batch experiments followed first-order kinetics with respect to both the concentration of virus and activated carbon, or second-order overall. In the analysis presented here, the concentration of suspended solids is constant (assumption ii). Thus, the kinetics of binding in this system can be assumed to be pseudo first-order with respect to the fluid concentration of viruses. The resuspension or desorption of viruses from the surface back into the fluid phase is also assumed to be first-order with respect to the surface concentration of reversibly adsorbed viruses (n_{sr}) (Cookson & North, 1967). Therefore, the appropriate rate expression for reaction extent ξ_2 is:

$$\begin{aligned} \frac{1}{V} \frac{d\xi_2}{dt} &= k_2 n_f - k_{-2} n_{sr} \\ &= k_2 \left(n_{fo} - \frac{\xi_1 + \xi_2}{V} \right) - k_{-2} \left(n_{sro} + \frac{\xi_2 - \xi_3 - \xi_4}{W} \right). \end{aligned} \quad (4.2)$$

where

k_2 = first-order binding constant (time)⁻¹,

k_{-2} = resuspension constant (mass)(time)⁻¹(volume)⁻¹.

4.3.2.2. Kinetics of Fluid and Surface Inactivation

With time, viruses lose their ability to infect cells due to disruption of coat proteins surrounding the nucleic acid, degradation of nucleic acid, or some other process (Gerba, 1984). In fluid systems, this inactivation follows first-order kinetics with respect to

the fluid concentration of infective viruses, as measured by a viability assay (Gerba and Bitton, 1984). When natural materials are present in a fluid system, virus adsorption to these materials apparently decreases the rate at which the adsorbed viruses inactivate.

Reduced inactivation rates have been reported for viruses bound to soil (Hurst et al., 1980), to sediment (Liew and Gerba, 1980; Smith et al., 1978) to colloids (Bitton and Mitchell, 1974), and to clay minerals (Taylor et al., 1980; Babich and Stotzky, 1980). Several different mechanisms may be responsible for this enhanced survival. Surface stabilization of coat proteins, differences in the chemical and electrical nature of fluid near surfaces, and surface inactivation of antiviral chemicals or enzymes are all possible explanations (Bitton and Mitchell, 1974). In a few cases, virus inactivation has been shown to occur faster in the presence of solid surfaces (Gerba, 1984).

To model the fact that inactivation may proceed at different rates depending on whether a virus is suspended in fluid, bound to a solid surface reversibly, or bound to a solid surface irreversibly, separate rate expressions were used for inactivation occurring in these different states. In the model presented here, inactivation was assumed to follow first-order kinetics for both suspended and bound viruses,

$$\frac{1}{V} \frac{d\xi_1}{dt} = k_1 n_f = k_1 \left(n_{f0} - \frac{\xi_1 + \xi_2}{V} \right) \quad (4.3a)$$

$$\frac{1}{W} \frac{d\xi_3}{dt} = k_3 n_{sr} = k_3 \left(n_{sro} + \frac{\xi_2 - \xi_3 - \xi_4}{W} \right) \quad (4.3b)$$

$$\frac{1}{W} \frac{d\xi_5}{dt} = k_5 n_{sir} = k_5 \left(n_{siro} + \frac{\xi_4 - \xi_5}{W} \right) \quad (4.3c)$$

where

k_1 = fluid phase inactivation constant (time)⁻¹,

k_3, k_5 = surface phase inactivation constants (time)⁻¹.

4.3.2.3. Irreversible Adsorption

As discussed in the introduction, it is also possible that reversibly adsorbed viruses may become irreversibly bound to the surface with time (see Chapter 5). Assuming that this is a first-order process, the corresponding rate expression becomes:

$$\frac{1}{W} \frac{d\xi_4}{dt} = k_4 n_{sr} = k_4 \left(n_{sro} + \frac{\xi_2 - \xi_3 - \xi_4}{W} \right) \quad (4.4)$$

4.3.3. Dimensional Analysis

To formulate the model in such a way that limiting cases could be investigated, the following nondimensional groups were utilized:

<u>Group</u>	<u>Definition</u>
$n_f^* = \frac{n_f}{n_{fo}}$	Fluid PFU
$n_{sr}^* = \frac{n_{sr}W}{n_{fo}V}$	Reversibly Adsorbed PFU
$n_{sir}^* = \frac{n_{sir}W}{n_{fo}V}$	Irreversibly Adsorbed PFU
$n_{sro}^* = \frac{n_{sro}W}{n_{fo}V}$	Initial Reversibly Adsorbed PFU
$n_{siro}^* = \frac{n_{siro}W}{n_{fo}V}$	Initial Irreversibly Adsorbed PFU
$\tau = k_1 t$	Nondimensional Time
$R^{-1} = \left(\frac{k_2 W}{k_{-2} V} + 1 \right)^{-1}$	Fraction of Viruses in the Fluid ⁵
$N_i = \frac{k_3}{k_1}$	$\frac{\text{Fluid Inactivation Time Scale}}{n_{sr} \text{ Inactivation Time Scale}}$
$N_{sr} = \frac{k_5}{k_1}$	$\frac{\text{Fluid Inactivation Time Scale}}{n_{sir} \text{ Inactivation Time Scale}}$
$N_s = \left(\frac{k_4}{k_3} + 1 \right)$	$\frac{n_{sr} \text{ Inactivation Time Scale}}{\text{Structural Modification Time Scale}} + 1$
$N_b = \frac{k_2}{k_1}$	$\frac{\text{Fluid Inactivation Time Scale}}{\text{Reversible Binding Time Scale}}$
$N_{bir} = \frac{k_6}{k_1}$	$\frac{\text{Fluid Inactivation Time Scale}}{\text{Irreversible Binding Time Scale}}$

Based on these nondimensional groups, the fluid and surface concentration of viruses (4.1a) becomes,

⁵ Assuming that virus/surface interactions are limited to quasi-equilibrium reversible adsorption.

$$n_f^* = 1 - \xi_1^* - \xi_2^* \quad (4.5a)$$

$$n_{sr}^* = n_{sro}^* + \xi_2^* - \xi_3^* - \xi_4^* \quad (4.5b)$$

$$n_{sir}^* = n_{siro}^* + \xi_4^* - \xi_5^* \quad (4.5c)$$

$$\text{where } \xi_i^* = \frac{\xi_i}{Vn_{fo}}$$

The rate expressions for ξ_1^* , ξ_2^* , ξ_3^* , ξ_4^* and ξ_5^* (4.2-4.4) are a coupled set of linear ordinary differential equations. Rewriting this set using the nondimensional groups presented above:

$$\frac{d\xi_1^*}{d\tau} = 1 - \xi_1^* - \xi_2^* \quad (4.6a)$$

$$\frac{d\xi_2^*}{d\tau} = N_b \left[1 - \frac{n_{sro}^*}{R-1} - \xi_1^* - \xi_2^* \left(\frac{R}{R-1} \right) + \left(\frac{\xi_3^* + \xi_4^*}{R-1} \right) \right] \quad (4.6b)$$

$$\frac{d\xi_3^*}{d\tau} = N_i [n_{sro}^* + \xi_2^* - \xi_3^* - \xi_4^*] \quad (4.6c)$$

$$\frac{d\xi_4^*}{d\tau} = N_i (N_s - 1) [n_{sro}^* + \xi_2^* - \xi_3^* - \xi_4^*] \quad (4.6d)$$

$$\frac{d\xi_5^*}{d\tau} = N_{ir} [n_{siro}^* + \xi_4^* - \xi_5^*] \quad (4.6e)$$

This set can be simplified by noting that,

$$\frac{d\xi_3^*/d\tau}{d\xi_4^*/d\tau} = \frac{1}{(N_s - 1)} \quad (4.7)$$

Integrating this expression and solving for the fourth reaction extent:

$$\xi_4^* = (N_s - 1)\xi_3^* \quad (4.8)$$

Thus, equations (4.6b-e) can be reduced to the following set of three differential equations:

$$\frac{d\xi_2^*}{d\tau} = N_b \left[1 - \frac{n_{sro}^*}{R-1} - \xi_1^* - \xi_2^* \left(\frac{R}{R-1} \right) + \xi_3^* \left(\frac{N_s}{R-1} \right) \right] \quad (4.9a)$$

$$\frac{d\xi_3^*}{d\tau} = N_i \left[n_{sro}^* + \xi_2^* - N_s \xi_3^* \right] \quad (4.9b)$$

$$\frac{d\xi_5^*}{d\tau} = N_{ir} \left[n_{sro}^* + (N_s - 1)\xi_3^* - \xi_5^* \right]. \quad (4.9c)$$

4.4. Solutions of the Kinetic Model

After viruses contact a solid surface, a number of complicated interactions can occur. The interactions accounted for in the above analysis include,

- (i) reversible adsorption to the surface,
- (ii) irreversible adsorption preceded by a reversible step,
- (iii) surface stabilization and/or
- (iv) surface destabilization.

Two approaches were used to determine if the above virus/surface interactions might give rise to characteristic behavior in the time course of fluid phase PFU (n_f^*). First, closed form solutions for (n_f^*) were developed for several limiting cases, assuming that a quasi-equilibrium between virus adsorption and desorption is instantaneously achieved. Here quasi-equilibrium is defined as the

state where virus flux onto the surface (adsorption) is equal to virus flux off of the surface (desorption). This term does not imply that the system as a whole is at equilibrium. Second, numerical simulations were performed to determine the effect of a slow approach to quasi-equilibrium adsorption (QEA). In both cases, we assumed that the only viruses present in the system initially were those in the fluid phase.

It is also possible that viruses may adsorb irreversibly to the surface directly from solution (reaction pathway 6, in Figure 4.1). This last possibility is not included in the above analysis, but is discussed separately in section 4.4.1.3.

4.4.1. Closed Form Solutions for Limiting Cases

4.4.1.1. Pure Inactivation

If the viruses do not bind or interact with the solid material after it has been added and $\xi_1^* = 0$ when $\tau = 0$, then the problem reduces to one of pure inactivation and equation 6a reduces to:

$$\frac{d\xi_1^*}{d\tau} = 1 - \xi_1^*, \quad (4.10)$$

and the normalized fluid concentration of viable viruses becomes

$$n_f^* = e^{-\tau}. \quad (4.11)$$

As shown in Figure 4.2, if this expression is plotted against nondimensional time (τ) on a semi-log graph, the result is a straight line with slope $-1/(2.3)$.

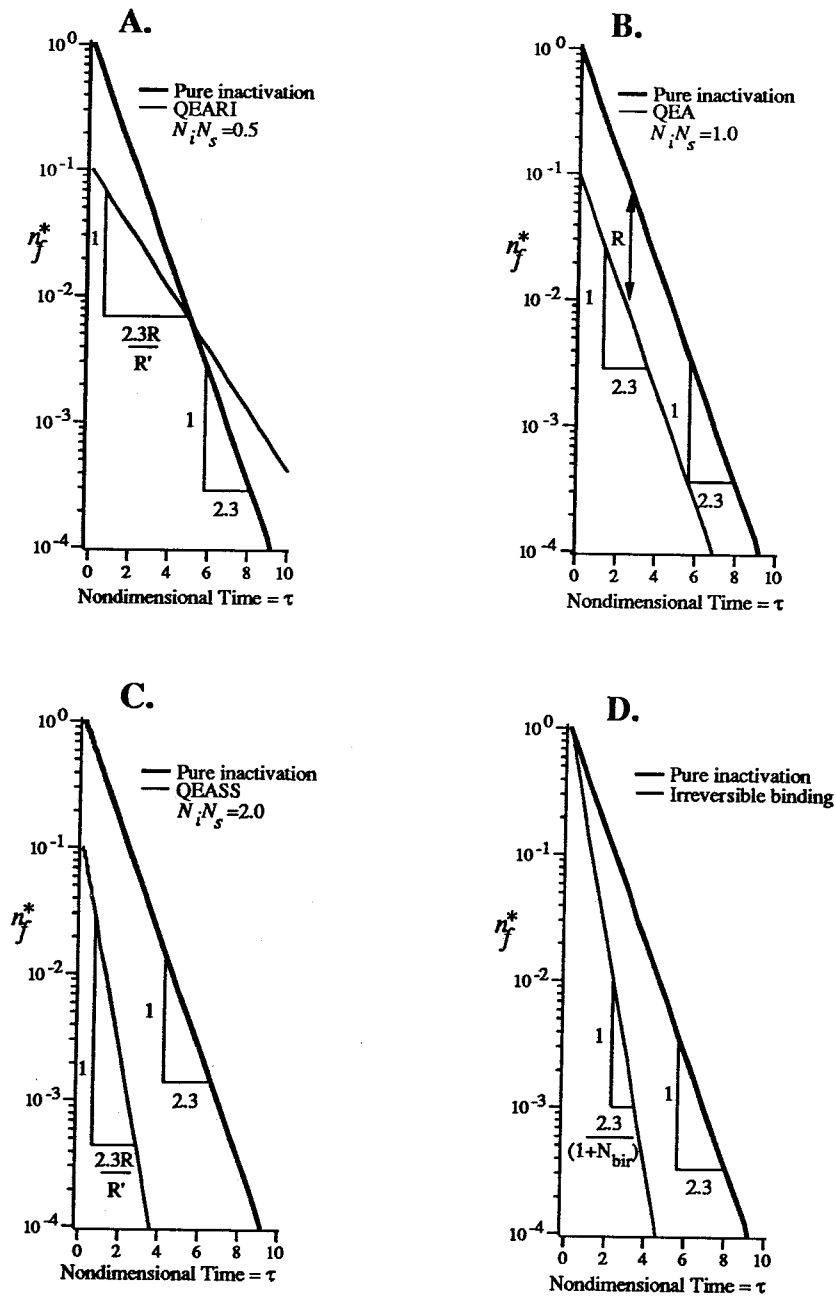


Figure 4.2. Semi-log plots of n_f^* against nondimensional time for the four limiting cases discussed in the text. The dark line corresponds to pure inactivation in each case. Lighter lines correspond to: (A) quasi-equilibrium adsorption with reduced inactivation (QEARI), (B) quasi-equilibrium adsorption (QEA), (C) quasi-equilibrium adsorption with a coupled surface sink (QEASS), and (D) irreversible adsorption directly from solution. Slopes of the lines are indicated. Graphs were generated using: $R=10.0$ and $N_b = N_{bir} = 1.0$. Values of N_i/N_s are indicated in each case.

4.4.1.2. Instantaneous Quasi-Equilibrium Adsorption

Here it is assumed that the viruses bind reversibly to the solid surface and that the flux of viruses on and off the surface reaches quasi-equilibrium instantaneously. As is detailed in appendix A, the resulting expression for fluid PFU is,

$$n_f^* = \frac{e^{-\left(\frac{R'}{R}\right)\tau}}{R} \quad (4.12)$$

where $R' = 1 + (R - 1)N_i N_s$.

This equation is compared with the curve for pure inactivation (4.11) in Figure 4.2A-C. Initially, (4.12) is lower than (4.11) by exactly the retardation factor, R (see the list of dimensionless parameters where R is defined in terms of its inverse). As time increases, the two curves either parallel, diverge, or converge, depending on the ratio R'/R . This ratio, in turn, reflects the underlying virus/surface interactions that are occurring in a given system. In particular, three cases can be identified.

Case I: Quasi-Equilibrium Adsorption & Reduced Inactivation (QEARI)

As mentioned previously, viruses may inactivate slower in the presence of solid materials. Mathematically, this condition means that $N_i < 1$. If virus adsorption only occurs reversibly (i.e. the irreversible binding coefficient $k_4 = 0$) then $N_s = 1$. Thus, in the case where solid-enhanced stability is accompanied by reversible adsorption, the modified retardation coefficient R'/R is less than one,

and the curves corresponding to equations (4.11) and (4.12) will converge with time. This case is shown in Figure 4.2A.

Case II: Quasi-Equilibrium Adsorption (QEA)

If virus stability is not influenced by the presence of the solid material (i.e. $k_1=k_3$) and reversibly adsorbed viruses do not become irreversibly adsorbed with time (i.e. $k_4=0$) then the inactivation and surface parameters (N_i and N_s) both equal to one. In this case, the modified retardation coefficient R' becomes identical with the retardation coefficient R and (4.12) reduces to

$$n_f^* = \frac{e^{-\tau}}{R} \quad (4.13)$$

which parallels the solution for pure inactivation for all time (Figure 4.2B).

Case III: Quasi-Equilibrium Adsorption & Surface Sink (QEASS)

The solid surface can also act like a "sink" for virus particles if virus inactivation is either accelerated in the presence of the surface (i.e. $k_3>k_1$) or reversibly adsorbed viruses become irreversibly adsorbed with time (i.e. $k_4>0$). In this case, either the inactivation parameter (N_i) or the surface parameter (N_s) are greater than one. Since this formulation assumes that both inactivation and irreversible binding occur as first-order surface sinks, it is not the individual value of N_i and N_s that is important, but their product. If $N_i N_s > 1$, then the curves given by (4.11) and (4.12) will diverge as shown in Figure 4.2C.

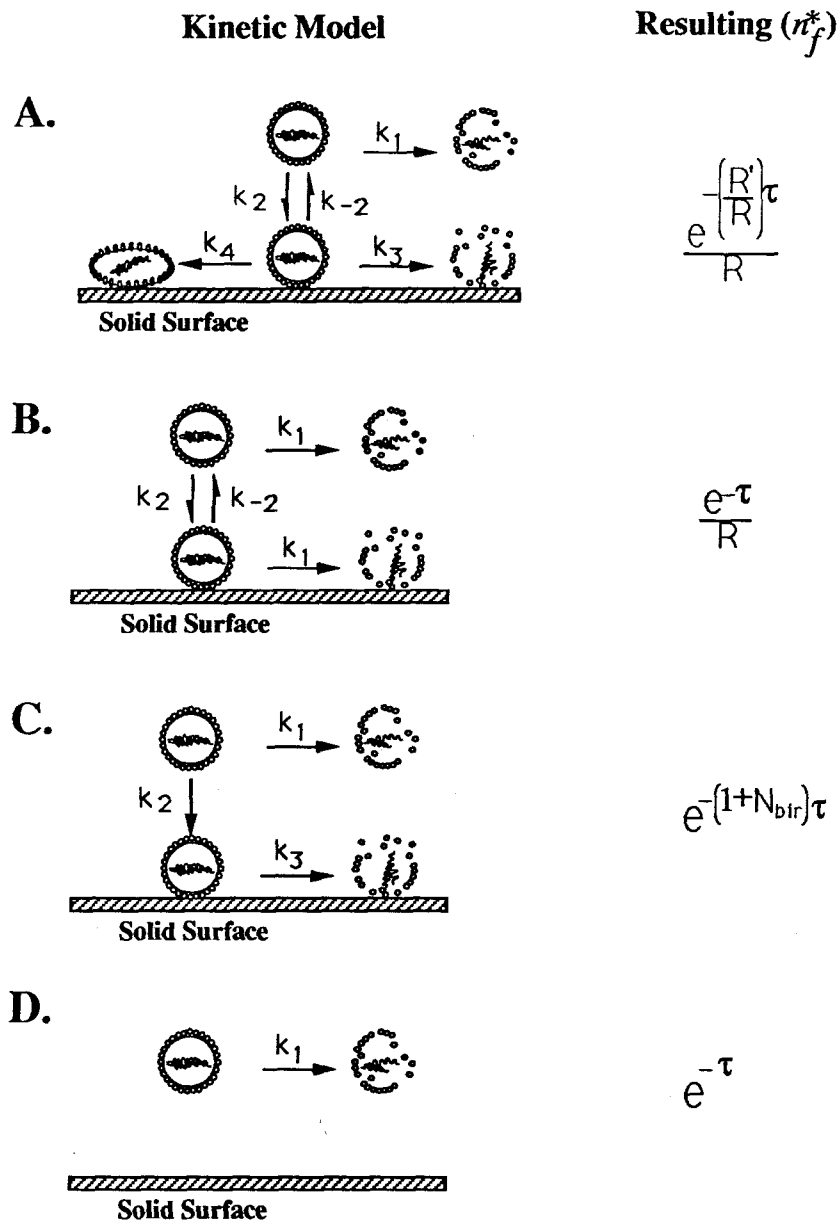


Figure 4.3. Closed-form solutions for several classes of virus/surface interactions in batch systems assuming instantaneous quasi-equilibrium adsorption. (A) Case where inactivation rates are altered by the solid material and/or conversion of reversibly adsorbed viruses to an irreversible state occurs (QEASS). $R'=1+(R-1)N_iN_s$, where R is the retardation coefficient, N_i is the ratio of surface and fluid inactivation constants, and N_s is 1 plus the ratio of kinetic constants for irreversible binding and fluid phase inactivation. (B) Interactions between virus and solid surface limited to reversible binding (QEA). (C) Irreversible binding of the virus to the surface. N_{bir} is the ratio of kinetic constants for irreversible binding and fluid inactivation. (D) No interactions between the virus particle and the surface.

4.4.1.3 Irreversible Binding

It is also possible that viruses may adsorb irreversibly directly from solution. Under these assumptions, the appropriate rate expressions are:

$$\frac{d\xi_1^*}{d\tau} = 1 - \xi_1^* - \xi_6^* \quad (4.14a)$$

$$\frac{d\xi_6^*}{d\tau} = N_{bir} [1 - \xi_1^* - \xi_6^*] \quad (4.14b)$$

$$\frac{d\xi_3^*}{d\tau} = N_i [\xi_6^* - \xi_3^*] \quad (4.14c)$$

Equations 4.14a,b and c are uncoupled, implying that if adsorption occurs irreversibly, the decline of fluid PFU does not depend on processes occurring after the viruses are adsorbed. Appendix B shows that the solution of 4.14a and b results in the following expression for fluid virus concentration:

$$n_f^* = e^{-(1+N_{bir})\tau} \quad (4.15)$$

This solution is compared to the result for pure inactivation in Figure 4.2D. The two curves have the same intercept, but the slope for the irreversible binding curve is $(1+N_{bir})$ steeper than that for pure inactivation.

The limiting cases presented here and corresponding expressions for n_f^* are shown in Figure 4.3.

4.4.2.1. Non-instantaneous Quasi-Equilibrium Adsorption

In reality, some time is required before QEA can be achieved between virus binding and resuspension. Closed form solutions could not be found for this problem, so numerical simulations of the coupled

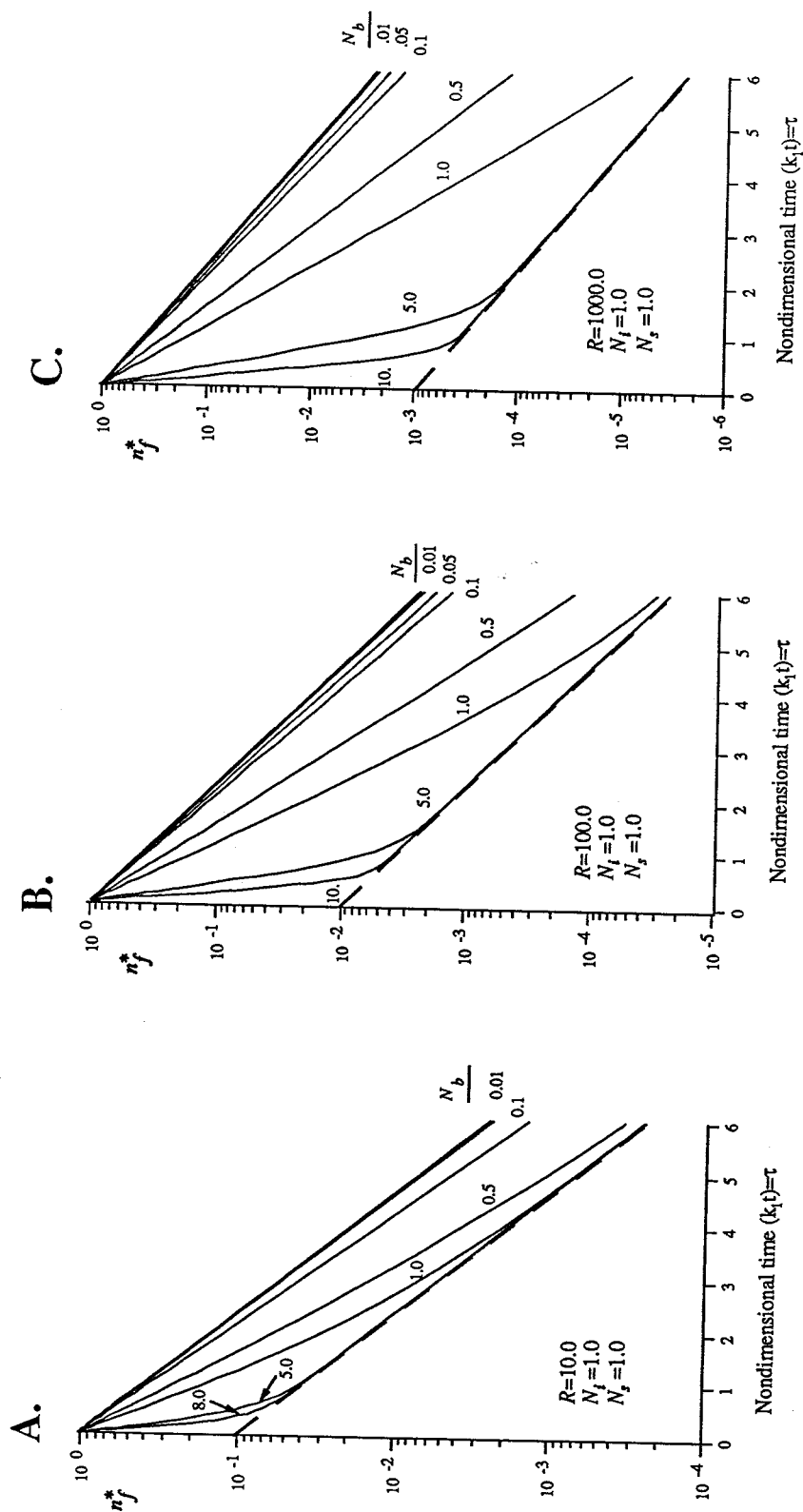


Figure 4.4. The effects of a slow approach to QEA on fluid PFU. In this case, inactivation rates are unaffected by the presence of solid material ($N_s=1$), and adsorption only occurs reversibly ($N_s=1$). The different panels correspond to different values of the retardation factor R : (A) 10.0, (B) 100.0, and (C) 1000.0. Solid and dashed dark lines correspond to the limiting cases of pure inactivation and QEA, respectively.

set of rate expressions (4.6a & 4.9a-c) were performed using a variable step Runge-Kutta algorithm (Press et al., 1986). The FORTRAN program used for these simulations can be found in appendix C.

4.4.2.2 Slow Approach To QEA

Here the effect of a slow approach to QEA is investigated, provided that virus inactivation takes place at the same rate in the fluid and on the surface and adsorption only occurs reversibly. Two nondimensional parameters, N_b and R , were varied to determine how much nondimensional time it would take for the full solution to approach the limiting cases described previously. Figure (4.4A-C) shows these results. For each R value tested, the resulting solution curves were bracketed above by the curve corresponding to pure inactivation and below by the curve corresponding to instantaneous QEA. The solution curves approach the instantaneous QEA curves at a rate which depends on N_b . When the rate of binding is large compared to the rate of fluid phase inactivation ($N_b > 5.0$), the resulting solution closely approximates the instantaneous QEA curve for all nondimensional times $\tau > 2$. When the inactivation rate is large relative to the binding rate ($N_b < 0.1$), the solution curves approach the pure inactivation curve. For intermediate N_b values, the solution curves approach the instantaneous QEA curve at a rate characteristic of N_b . This behavior was observed for all values of R tested, ranging between 10 to 1000.

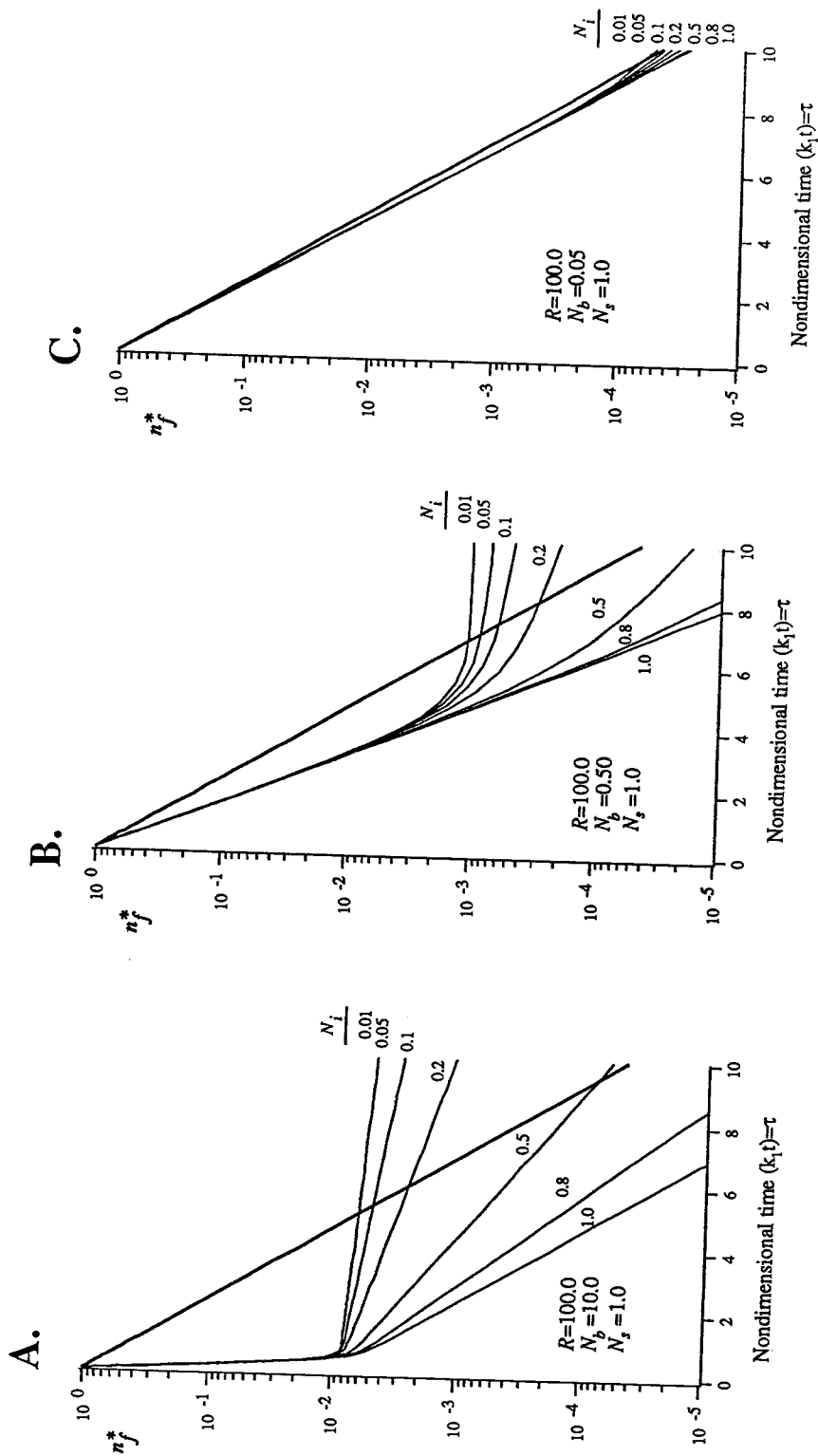


Figure 4.5. The effects of a slow approach to QEARI on fluid PFU. In these examples, surface sinks were assumed negligible ($N_s = 1$) and the retardation factor (R) was fixed at 100.0. Each panel corresponds to a different binding rate, Nb: (A) 10.0, (B) 0.50, and (C) 0.05.

4.4.2.3. Slow Approach to QEARI

Here it is assumed that the solid acts to stabilize the virus and QEA is not instantaneously achieved. To observe the effect of surface stabilization, the viruses must have a relatively large affinity for the surface. In this analysis, a large surface affinity is indicated by a large value of R , the retardation coefficient. For these simulations, a value of $R=100$ was selected, implying that under quasi-equilibrium adsorption 1/100 of the PFU in the system will be present in the fluid phase.

Figure 4.5A-C shows the results of numerical simulations using a range of values for the binding (N_b) and relative inactivation (N_i) parameters. In each simulation, the effect of decreasing the surface inactivation rate (N_i decreasing) was investigated at three fixed values of N_b , the rate of forward adsorption. As in the previous section, the rate of approach to QEARI is controlled primarily by N_b . The larger N_b , the faster QEA is achieved between virus binding and resuspension. As expected, the solution curves corresponding to $N_i < 1$ all eventually cross the curve corresponding to pure inactivation. The nondimensional time (τ) at which the crossover occurs is parameterized by N_i , with crossover occurring earlier for smaller values of this parameter.

4.4.2.4. Slow Approach to QEASS

Figure 4.6A-C shows the effect of noninstantaneous QEA on fluid PFU assuming the existence of a surface sink. In this case, the sink is assumed to involve the conversion of

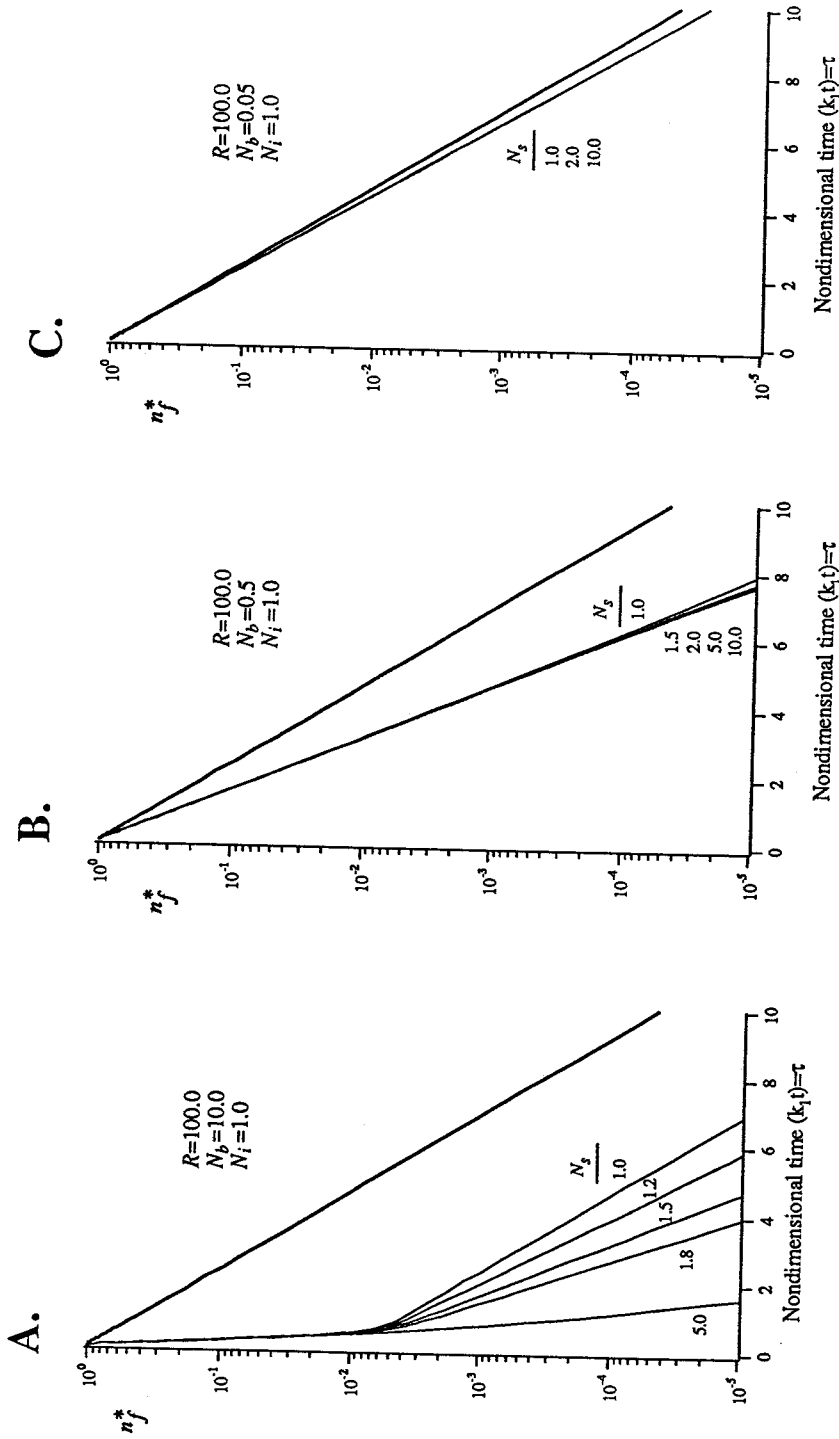


Figure 4.6. The effects of a slow approach to QEASS on fluid PFU. Inactivation was assumed negligible ($N_i = 1$) and the retardation factor (R) was fixed at 100.0. As in the previous figure, each panel corresponds to a different binding rate, N_b : (A) 10.0, (B) 0.50, and (C) 0.05.

reversibly adsorbed viruses to an irreversibly adsorbed state ($N_s > 1$) and values of R and N_b are the same as those tested in the last section. The resulting curves exhibit the same type of behavior observed in the previous simulations. After an initial period of time in which QEA is being established, the curves achieve a final slope (or rate) which is controlled by the nondimensional group N_s . When N_s is large (rate of conversion to irreversible adsorption is fast), the final rate of fluid PFU decline is faster than that corresponding to pure inactivation. This effect is less important the farther the system is away from QEA. As N_b decreases, the rate at which QEA is achieved decreases, and the surface sink becomes less important in determining the time course behavior of fluid PFU.

4.4.2.5. Summary of Simulations

These simulations suggest that processes occurring in this system affect fluid PFU concentrations in a stepwise manner. If the rate of virus adsorption is much faster than the rate of inactivation (N_b large), then initially fluid PFU decline will be dominated by virus adsorption to the solid surface. The rate of PFU decline decreases dramatically when the fraction of fluid-borne viruses reaches the quasi-equilibrium fluid fraction (R^{-1}), reflecting the onset of QEA. After this point, the PFU decline continues at a rate which is determined by whether the surface acts to sustain virus infectivity (surface stabilization), permanently removes viruses from the fluid phase, or has no influence beyond acting as a surface for QEA. The rate at which fluid PFU declines after QEA is established depends

quantitatively on the parameter R'/R , which is a modified retardation parameter.

4.5. Discussion

4.5.1. New Experimental Approach

The results presented above suggest a novel experimental approach for studying virus partitioning to surfaces in fluid systems. The idea is illustrated in Figure 4.7. Two batch suspensions of virus particles are prepared of equal concentrations. At the start of the experiment, the solid material of interest is added to one of these suspensions. Samples from the fluid fraction of both suspensions are taken with time and analyzed for virus viability. From the decline in PFU observed in the solid-free suspension, a first-order rate constant for virus inactivation is determined (k_1). Normalized viability (n_f^*) measurements from both batch mixtures are then plotted against nondimensional time (τ) using a semi-log scale. Comparisons between PFU decline in the solid-containing and solid-free batch reactions can be used to obtain qualitative information about the nature of the virus/surface interactions, as well as quantitative parameters that can be used in groundwater or soil transport models. Specific cases are outlined below.

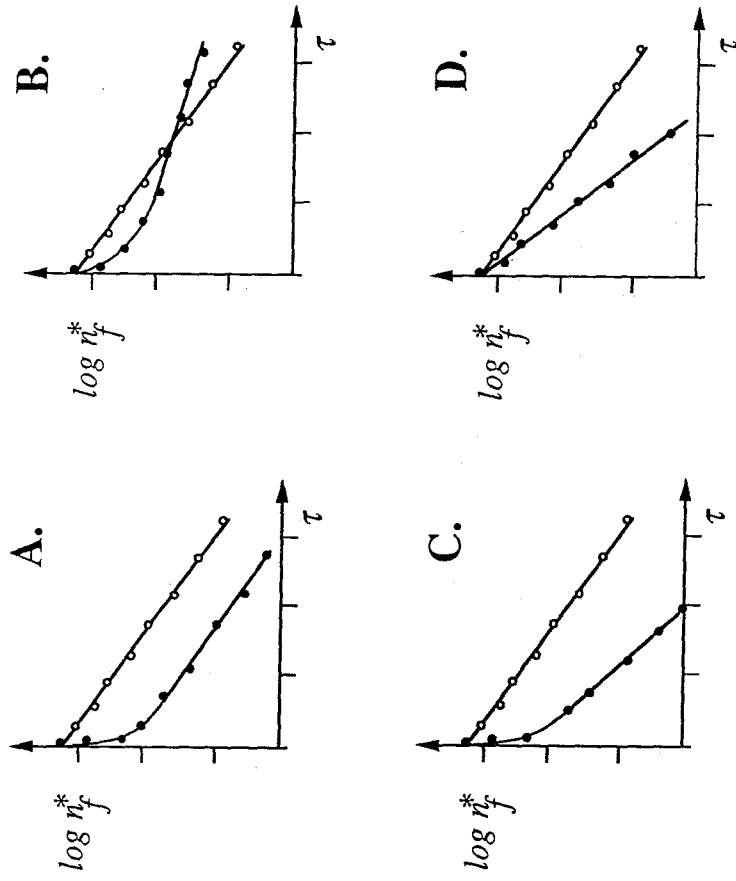


Figure 4.7. Proposed experimental approach for obtaining information about the nature of virus/surface partitioning and inactivation. Two batch suspensions of viruses are prepared, one with added solids (●) and the other solid-free (○). Samples of the fluid fraction from both preparations are taken at specific time intervals, analyzed for virus viability, and plotted as normalized PFU (n_i^*) against nondimensional time (τ) on a semi-log graph. Graph shows the expected response of such curves to different adsorption and inactivation mechanisms: (A) QEA, (B) QEARI, (C) QEASS, and (D) irreversible.

4.5.1.1. Reversible Adsorption & No Surface Stabilization or Sinks ($N_s N_i = 1$)

As shown in Figure 4.7A, once QEA is established, viability measurements from the two batch suspensions will decline in parallel. Since the multiplicative factor separating the two data sets in the second region is R , the retardation factor can be obtained directly from the plotted data. The initial rate of PFU decline in the solid-containing experiment can be used to obtain direct estimates of the first-order binding rate constant *vis a vis* N_b (see Figure 4.2D). Interpretation of data which exhibits this behavior requires some caution, since it is the product of N_s and N_i that determines the final slope of PFU data, not the individual values. The kind of system for which this might pose a problem is one in which reversibly adsorbed viruses are irreversibly adsorbing with time ($N_s > 1$) and simultaneously inactivating more slowly than viruses in the solid-free batch experiment ($N_i < 1$). However, since it is unlikely that these two processes would exactly balance, the type of behavior shown in Figure 4.7A can be used as partial evidence for QEA.

4.5.1.2. QEASS or QEARI ($N_s N_i \neq 1$)

As in the last section, values of N_b and R can be estimated from the initial slope and break in slope, respectively, of PFU data from the solid-containing experiment. If a surface sink dominates the system (QEASS), then the PFU data from solid-containing and solid-free reactions will diverge with time (Figure 4.7C). If the solid material significantly decreases the rate at which viruses inactivate,

then the two data sets will converge with time (Figure 4.7B). In both cases, measurement of the final slope can be used to estimate R'/R and thus the product $N_i N_s$. To determine specific values for N_i and N_s individually, more information is needed. For example, if elution experiments can be used to demonstrate that adsorbed viruses do not become irreversibly adsorbed with time (Murray and Parks, 1980; Chapter 5), then $N_s=1$ and the observed effect must be due to N_i alone.

4.5.2. Virus Populations

Some types of viruses exhibit inactivation which can be characterized by two or more virus sub-populations having different degrees of sensitivity toward inactivation. This phenomenon is well documented for some bacteriophages (Pollard & Solosko, 1971) and appears to be a consequence of the manner in which nucleic acid is packaged in the protein coats (Yamagishi et al., 1973; Yamagishi & Ozeki, 1972) and not a function of external properties of the virus that might affect binding characteristics. Since the differential equations describing this kinetic system are linear, solutions involving the simultaneous inactivation and binding of several virus populations can be found by merely adding the solutions corresponding to each of the individual populations alone. In practice, such multiple populations can be identified by breaks in slope of viability measurements when they are plotted as described in the last section.

4.6. Conclusions

A kinetic theory of virus partitioning to solid surfaces has been developed which accounts for many of the complicated interactions that can take place between viruses and solid surfaces in a batch reaction. Examination of limiting cases indicate that four classes of virus/surface interactions can be identified based on comparisons between data from experiments conducted with and without added solids. These cases include quasi-equilibrium adsorption (QEA), quasi-equilibrium adsorption coupled with a first-order surface sink (QEASS), quasi-equilibrium adsorption coupled with reduced inactivation in the presence of the added solids (QEARI), and direct irreversible binding. A new experimental approach for studying virus/surface interactions is proposed which offers several advantages over standard equilibrium Langmuir or Freundlich analyses of batch experiments. These include:

(i) Few assumptions are made about the nature of the virus/surface interaction allowing the operative binding mechanism in a particular system to be hypothesized in an *a posteriori* manner.

(ii) Nondimensional parameters relevant to groundwater or soil transport of viruses through the solid material being studied can be directly determined from the experimental data.

(iii) When experimental data are plotted on semi-log scale in (n_f^*, τ) space, the data are automatically normalized with respect to inactivation. Thus, adsorption data collected under widely varying conditions of solution pH or electrolyte composition and for different types of adsorbent can be compared directly to determine how

binding rates and mechanisms are influenced by chemical and physical factors.

(iv) Since inactivation is included in the analysis, experiments can be conducted over long time scales, allowing binding processes to be studied over time scales relevant to environmental transport.

5. Experimental Investigations of Bacteriophage Lambda Adsorption to Ottawa Sand Over Long Time Scales⁶

5.1 Summary

Existing kinetic models for virus adsorption to natural surfaces are based on limited experimental data collected over time scales which are short compared to many natural processes. Experiments were performed to elucidate the mechanisms involved in virus adsorption to natural surfaces over the time scale of days using bacteriophage lambda and Ottawa sand as a model system. Results indicate that Ottawa sand has significant adsorptive capacity for bacteriophage lambda when the adsorption is allowed to occur over the time scale of days. Surface adsorbed viruses did not desorb when diluted into clean buffer, suggesting that the adsorption of lambda onto the sand surface was at least partially irreversible. Quasi-equilibrium adsorption models could not be reconciled with both adsorption and elution data, and it is not presently clear what mechanism is responsible for lambda adsorption under these conditions. Several alternative mechanisms are proposed, but no direct evidence for any of these models is presented in this report.

⁶To be submitted to *Water Resources Research* as the second in a series of three papers.

These results have important implications both for the ecology of natural virus populations and the dispersal of viruses in the environment.

5.2. Introduction

5.2.1. Background

Virus adsorption to natural surfaces is an important factor in the mobility and ecology of viruses in the environment. Previous studies of

Table 5.1. Summary of contact times used in batch studies of virus adsorption.

Reference	Virus	Adsorbent	Contact Time (hours)
Taylor <i>et al.</i> (1981)	polio virus	Ottawa Sand, Clay, Soil, & Muck	1.0
Gerba <i>et al.</i> (1978a)	polio virus	Soil	0.5
Gerba <i>et al.</i> (1978b)	27 different enteroviruses	9 soil types	0.5
Vilker & Burge (1979)	bacteriophage ϕ x-174	silt loam soil	3.0
Moore <i>et al.</i> (1981)	polio virus	34 soils and minerals	1.0
Cookson & North (1967)	bacteriophage T4	Activated Carbon	12.0
Murray & Parks (1980)	polio virus	Metal Oxides	2.0
Moore <i>et al.</i> (1982)	reovirus	30 soils, minerals and ground rocks	24.0
Vilker <i>et al.</i> (1983)	polio virus	Montmorillonite Clay	0.5
Sobsey <i>et al.</i> (1980)	polio virus & reovirus	8 soil types	1.5
Goyal & Gerba (1979)	echovirus, polio virus, coxsackievirus, bacteriophages: MS-2, ϕ x174, T2, T4, & f2	9 soil types	0.5
Preston & Farrah (1988)	bacteriophage: MS-2, T2 & f2	Powdered filters	0.75
Gerba <i>et al.</i> (1975)	polio virus	Activated carbon	3.0
Drewry & Eliassen (1968)	bacteriophages: T1, T2, & f2	5 soil types	24.0
Carlson <i>et al.</i> (1968)	poliovirus & bacteriophage T2	3 clays	0.5
Lo & Sproul (1977)	polio virus	6 silicate minerals	0.5
Stag <i>et al.</i> (1977)	bacteriophage MS-2	Bentonite	1.0
LaBelle & Gerba (1979)	polio virus, coxsackievirus, echovirus	Estuarine sediment	0.5
Bitton <i>et al.</i> (1976)	polio virus	Magnetite	0.25
Taylor <i>et al.</i> (1980)	reovirus and bacteriophage R17	Clay mineral allophane	0.25
Gerba <i>et al.</i> (1981)	polio virus, echovirus, coxsackievirus, Simian rotavirus, bacteriophages: MS-2, ϕ x174, T2, T4, & f2	soils	0.5

virus adsorption to interfaces have focused on understanding the chemical and physical factors affecting virus adsorption (for reviews, see Bitton, 1975, Gerba, 1984) and the forces responsible for the partitioning process (Murray and Parks, 1980). However, few experimental data are available to adequately validate commonly assumed kinetic models for virus adsorption over time scales relevant to most natural processes (Table 5.1). Using several different experimental approaches, including the one proposed in the previous chapter, we studied bacteriophage lambda (λ) partitioning to the surface of Ottawa sand. The results presented here suggest a picture of virus adsorption to surfaces which is considerably more complex than widely accepted models.

5.3. Materials and Methods

5.3.1. Virus Preparation.

Stocks of bacteriophage λ were prepared by infecting host cell *E. coli* C600 at low multiplicity, isolating the bacteriophage from cell debris by polyethylene glycol precipitation, purifying the phage by two sequential ultracentrifugations in CsCl gradients, and dialyzing the resulting suspensions against a standard salt buffer SM (10mM NaCl, 1mM MgSO₄, 50mM Tris-HCl (pH 7.5), and 2% gelatin) following procedures outlined in Sambrook, et al. (1989).

Bacteriophage stocks were routinely obtained with fluid concentrations greater than 10^{12} plaque forming units (PFU)/ml.

5.3.2. Viability Measurements.

Bacteriophage viability was determined by plaque forming unit (PFU) assays. Samples diluted in SM buffer were mixed with host cells (*E. coli* C600), plated on nutrient agar and incubated following standard procedures (Arber et al., 1983).

5.3.3. Transmission Electron Microscopy.

To check for the presence of bacteriophage aggregates and biological contamination in the batch experiments described below, particulates in the bacteriophage suspensions were viewed with an electron microscope. Fluid suspensions of bacteriophage particles were added to an ultracentrifuge tube (Beckman 14x89mm polyallomer), a formvar coated grid was placed on the bottom of the tube, and the sample was centrifuged at 100,000g for 90 minutes at 5°C in a Sorvall RC-70 ultracentrifuge. Grids were removed from the ultracentrifuge tube with forceps, rinsed twice in double distilled (dd)H₂O, dried with filter paper, and immediately floated phage side down in 1% aqueous uranyl acetate solution (pH 4.0) buffered with malic acid. Uranyl acetate is a negative stain for bacteriophage particles and a positive stain for bacteriophage DNA (Yamagishi et al., 1973). Particles deposited on the grid were imaged using a Phillips EM420 transmission electron microscope (TEM) at 120kV.

5.3.4. Sand Treatment.

Ottawa sand was treated to remove organic and iron oxide surface coatings following protocols described in Black (1965). Organic coatings were removed by mixing the sand in a 10% (v/v) solution of hydrogen peroxide for 1 hour at 100°C. Iron oxide

coatings were removed by suspending 10-100 g of sand in 40ml of 0.3M sodium citrate solution. 5.0 ml of 1N sodium bicarbonate and 1g of solid sodium dithionite were added and the mixture was heated to 80°C. After a 15 minute incubation, the treated sand was recovered and rinsed at least five times in ddH₂O.

5.3.5. Scanning Electron Microscopy.

A scanning electron microscope (SEM) was used to determine the mineralogical composition and texture of the Ottawa sand surface. Sand which had been exposed to virus suspensions was rinsed briefly with ddH₂O, dried by capillary action, immobilized on an aluminum stub with carbon paint, and coated with greater than 300 angstroms of either gold or a gold/paladium mixture using an argon sputter coating device (Polaron). Sand that had not been previously exposed to fluid was treated in an identical manner without the prerinsing step. The surface of the coated sand was imaged with a CAM Scan Series II SEM. The distribution of elements on the sand surface was determined by an online Noran TN5500 energy dispersive spectrometer (EDS).

5.3.6. Adsorption Experiments.

Two 5.0×10^7 PFU/ml suspensions of bacteriophage λ were prepared by diluting the phage stock 20,000 fold into 50.0 ml screw cap tubes (Sarstedt) each containing a 40.0 ml solution of PIPES buffer (5mM piperazine-N,N'-bis[2-ethanesulfonic acid] (pH 7.0) and 10mM MgCl₂). At the start of the experiment, 25.0g of treated sand was added to one of the tubes. Samples (0.04ml) of the fluid fraction

from both suspensions were taken at specified time intervals and serially diluted in duplicate into SM buffer for a final 12,500 fold dilution. Between sampling periods, the batch reactions were mixed gently at room temperature. Because of the size and mass of the Ottawa sand, it was not necessary to use centrifugation techniques to separate the solid and liquid fractions during sampling. The sand-containing solution was simply mixed by inversion, the sand was allowed to settle to the bottom of the tube, and fluid samples were withdrawn from the overlying fluid. Portions (0.1ml) of the diluted samples were titered for phage in duplicate using the techniques described above.

5.3.7. Elution Experiments.

Three fluid suspensions of bacteriophage λ were prepared in 20ml of PIPES buffer, all at a final concentration of 3.4×10^7 PFU/ml. To two of these suspensions, 30g of sand was added and viruses were allowed to adsorb to the sand at room temperature with gentle shaking. After either 1 hour or 4 days, the fluid and sand fractions were separated by inverting the batch reaction, allowing the sand to settle, and decanting the overlying fluid. Fluid from the incubation step was titered so that apparent concentrations of viruses adsorbed to the sand (n_s^{app}) could be calculated using the equation⁷ :

$$n_s^{app} = \frac{V(n_f^{s-} - n_f^{s+})}{W} \quad (5.1)$$

⁷ This formulation assumes that bacteriophage inactivate at the same rate regardless of whether they are in contact with sand or not. As described later, this assumption appears to be valid under the specific conditions used in these experiments.

where V is the fluid volume (20 ml), W is the mass of sand in the batch reaction, n_f^{s+} and n_f^{s-} are the PFU/ml in batch mixtures with and without added sand, respectively.

After the fluid and sand fractions were separated, some fluid remained with the sand. A pipette tip was inserted into the sand and as much fluid as possible was withdrawn by applying suction. After the sand and fluid fractions were separated, two 10g aliquots of the sand were resuspended into 10ml of virus-free Nutrient Broth (Difco) and virus-free PIPES buffer, respectively. Nutrient broth contains beef extract which is relatively efficient at eluting viruses from sand and soil surfaces (Hurst et al., 1991). Fluid samples (0.04ml) from these mixtures were taken at specified time intervals, serially diluted in SM buffer, and titered.

5.3.8. Isotherm Experiments.

Twelve 3.4×10^7 PFU/ml suspensions of bacteriophage λ were prepared by diluting phage stock into 50 ml screw cap tubes containing 20 ml of the PIPES buffer. To eleven of these tubes, Ottawa sand was added at concentrations ranging from 0.25-300% (w/v basis). The resulting suspensions were mixed gently for either 1 hour or 4 days at room temperature. After the incubation period, fluid samples (0.04ml) from each of the tubes were serially diluted into SM buffer and titered. Surface concentrations of adsorbed bacteriophage in each of the batch reactions containing sand were estimated using (5.1).

5.3.9. Aggregation Experiment.

Two batch reactions (with and without sand, respectively) were prepared as described above for the adsorption experiments. Fluid samples (1.0 ml) were taken from these batch mixtures at times varying from 15 minutes to 14 days after addition of bacteriophage. Particulates in the samples were centrifuged onto a grid and imaged as described in the section on TEM methods.

5.3.10. Computer Simulations.

Adsorption Simulations. Numerical simulations were performed to predict the time evolution of n_f , n_{sr} , and n_{sir} in the adsorption experiments using the quasi-equilibrium adsorption (QEA) and quasi-equilibrium adsorption surface sink (QEASS) models described in Chapter 4. Parameters and initial conditions were determined directly from the observed data following the procedures described in the last chapter.

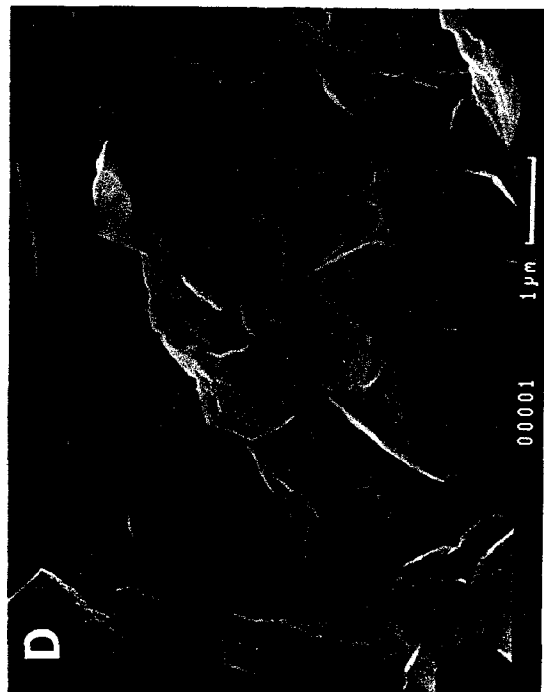
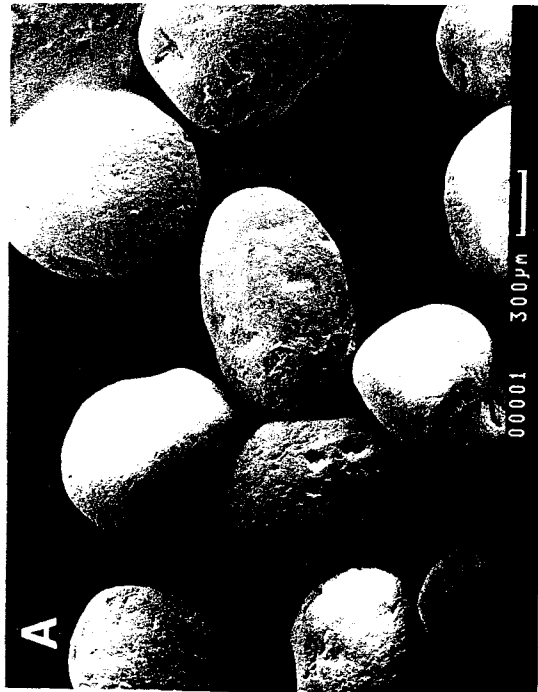
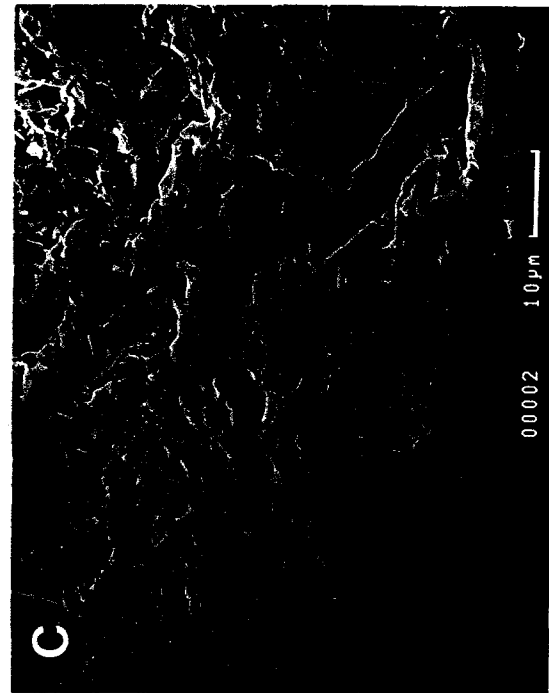
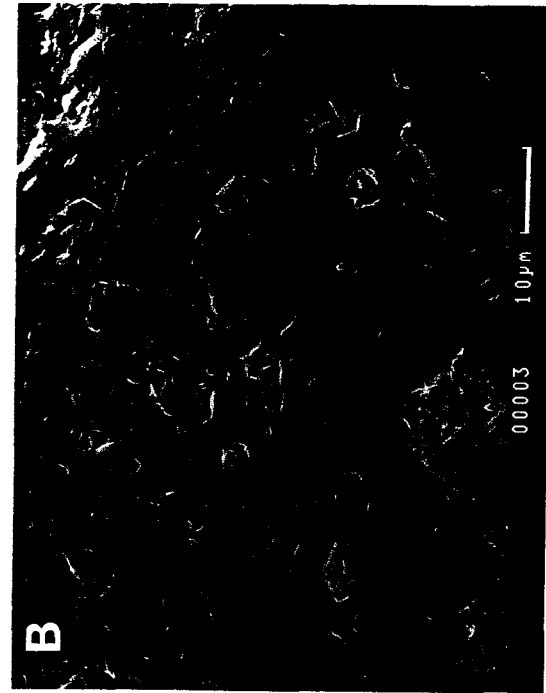
Elution Simulations. The time evolution of n_f , n_{sr} , and n_{sir} after sand resuspension were predicted using the QEA and QEASS models. Initial conditions for the elution experiments were determined as described in appendix 5.A1. Simulations were carried out by solving the appropriate set of differential equations using a variable step Runge-Kutta algorithm implemented on an IBM/AT personal computer. The FORTRAN code used for both adsorption and elution simulations is included in appendix E.

5.4. Results

5.4.1. Characterization of Ottawa Sand

The surface of the Ottawa sand was examined with a scanning electron microscope (SEM) and energy dispersive spectrometer (EDS). From EDS measurements, the surface of the treated sand is primarily silica (>90%). This silica appears to consist of a microcrystalline matrix of quartz crystals <1 μ m in length. Untreated sand was coated with iron oxide particles that are visible with SEM and detectable with EDS (Chapter 1). Examination of the treated sand surface with SEM revealed the presence of two types of surface textures shown in Figure 5.1. Most sand grains are smooth with surface irregularities <5 μ m (Fig 5.1B). Some grains have a surface coating like the one shown in Fig 5.1C. When this coating was examined at higher magnification (Fig 5.1D), it appeared to consist of quartz crystals <20 μ m in length. EDS measurements of the coating reveal that it is elementally identical to sand surfaces without the coating. This surface coat is probably microcrystalline quartz that precipitated from contacting pore fluids at some time before the sand was quarried. The sand surface shown in Fig 5.1C & D was exposed to suspensions of bacteriophage λ prior to imaging. In Fig 5.1D a particle (approximately 200nm in length) is present in the lower right that may be a virus.

Figure 5.1. Scanning electron micrographs of the Ottawa sand used in this study. (A) Low magnification of intact sand grains. (B) Typical surface structure (C) Example of surface coating. (D) Surface coating in (C) at higher magnification. Light grey minerals correspond to surface coat. The small particle in the lower right (arrow) of (D) may be a virus particle.



5.4.2. Batch Adsorption Experiments

To determine the influence of long time scales on the nature of virus adsorption to natural surfaces, sand-containing and sand-free fluid suspensions of bacteriophage λ were sampled over the course of 4 days and analyzed for PFU. These data are displayed arithmetically in Figure 5.2 and semi-logarithmically in Figures 5.3 and 5.4. Nondimensional times corresponding to each sample were calculated by assuming a first-order inactivation coefficient⁸ of $k_1=0.25/\text{day}$.

Most kinetic studies of virus adsorption to surfaces plot PFU data from adsorption experiments arithmetically as is done in Figure 5.2 (e.g. Cookson and North, 1967). In some cases, the adsorption data is corrected for inactivation by assuming that inactivation proceeds at the same rate in the presence and absence of sand (Vilker and Burge, 1980). Since virus adsorption can remove many log units of virus infectivity from solution (see Chapter 6), plotting adsorption data arithmetically can give the impression that the adsorption process rapidly achieves quasi-equilibrium, even if this is not actually the case. For the adsorption experiment conducted in this study, when the data is plotted arithmetically (either as the concentration of fluid PFU against time (Figure 5.2A) or the fraction of viruses removed from solution against time (Figure 5.2B))

⁸ Calculated from the decline in infectivity observed in the sand-free batch experiment. Based on the data presented in Figure 5.2, it may not be obvious whether inactivation in this system follows a first- or zero-order rate law. In experiments where inactivation was observed for longer periods of time, the first-order character of lambda inactivation is more obvious.

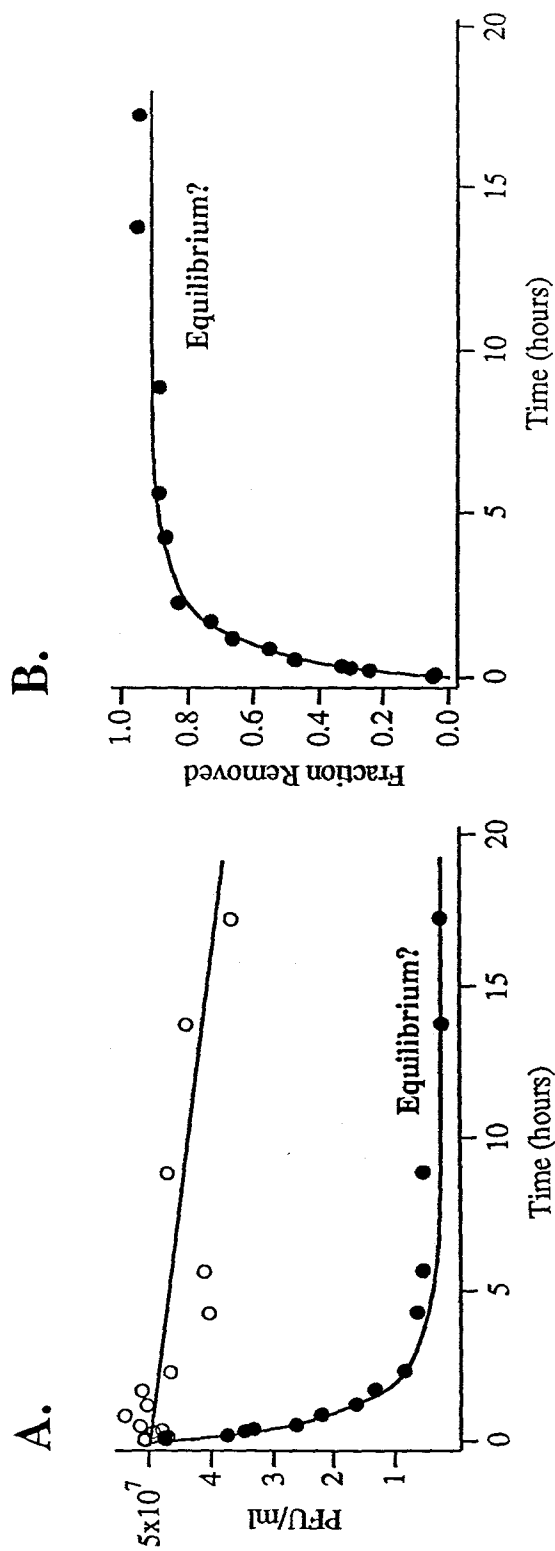


Figure 5.2. Batch adsorption and inactivation data plotted arithmetically against time. These two types of plots are frequently used to show that virus adsorption reaches quasi-equilibrium in relatively short periods of time: (A) Decline in PFU/ml of samples taken from the fluid fraction of sand-containing (●) and sand-free (○) batch experiments. Data from the experiment with sand are not corrected for inactivation. (B) Fraction of viruses removed from the fluid by adsorption and inactivation.

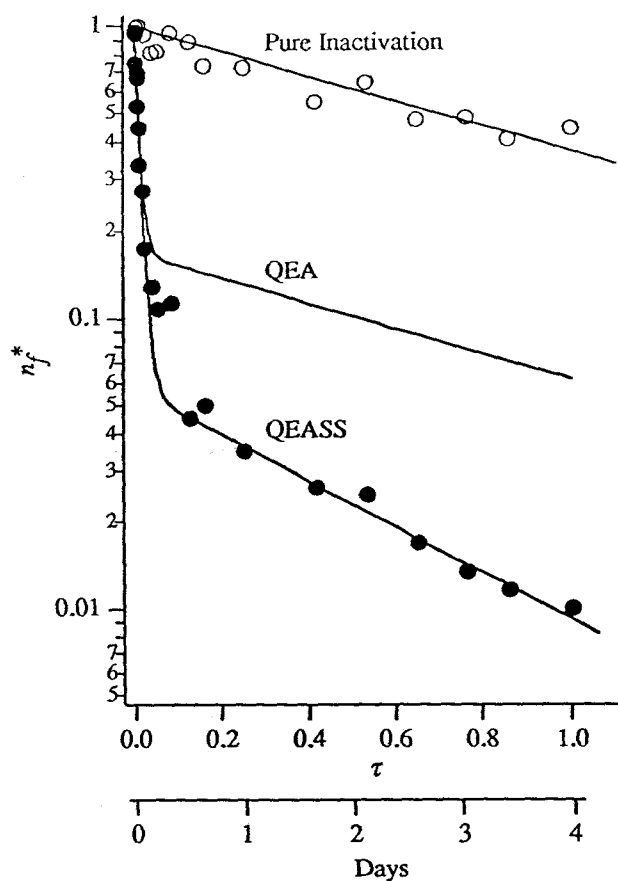


Figure 5.3. Plot of PFU normalized relative to initial conditions (n_f^*) against nondimensional time ($\tau=k_1 t$) for the same adsorption experiment shown in Figure 5.2, extended to 4 days. Symbols are data points (O, sand-free; ●, sand-containing). Lines labeled QEA and QEASS are model simulations of virus adsorption and inactivation. Both models assume that adsorption occurs reversibly. Line designated QEA is the prediction assuming that quasi-equilibrium adsorption is achieved after 1hour. QEASS is the prediction assuming that quasi-equilibrium adsorption is achieved after 13 hours and that a first-order process takes adsorbed viruses and removes them permanently from the fluid (surface sink). The final slopes of the quasi-equilibrium model (QEA) and surface sink model (QEASS) are, respectively, equal to and steeper than the slope associated with pure inactivation. Model parameters for the simulations are as follows. QEA: $N_i=1.0$, $N_b=80.0$, $R=6.0$, and $N_s=1.0$. QEASS: the same except $R=18.0$ and $N_s=1.87$. Model development and parameter descriptions are given in Chapter 4.

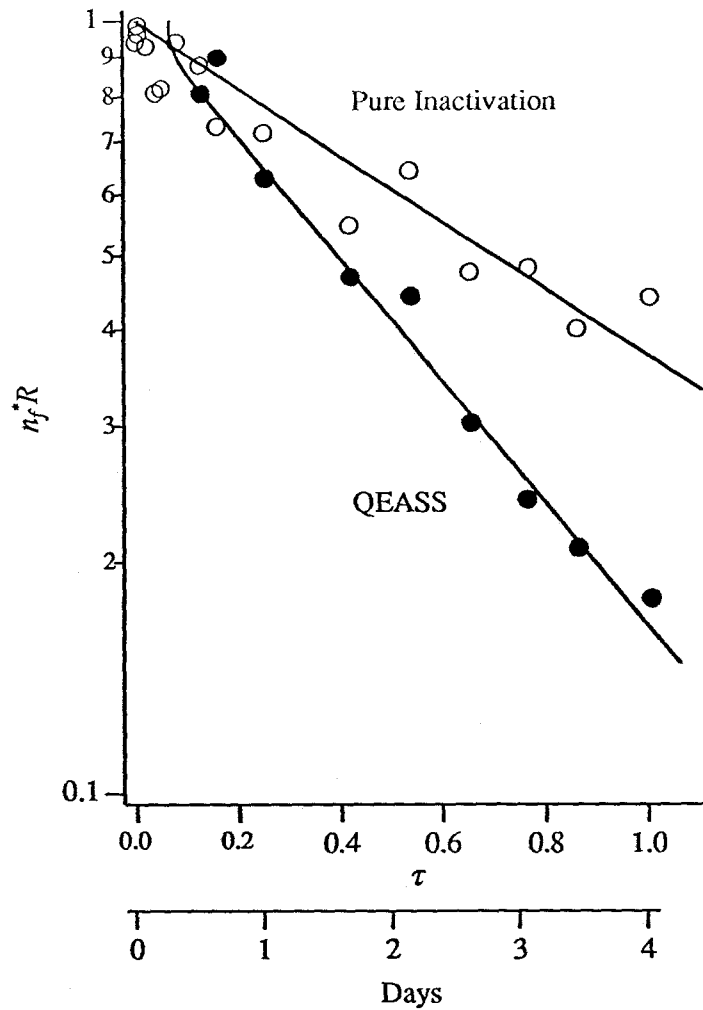


Figure 5.4. Comparison of final slopes for data corresponding to the sand-containing and sand-free batch experiments. PFU data from sand-containing experiment are corrected for quasi-equilibrium adsorption by premultiplying (n_f^*) by R . Loss of viruses in the presence of sand is faster than can be explained by the rate of inactivation observed in the sand-free suspension.

infectivity concentrations appear to reach steady-state within approximately 5 hours.

Figure 5.3 shows the same data set (extended to four days) plotted on a semi-log graph. When the data is presented in this way, measurements of fluid infectivity are seen to decrease at a rate which is time dependent. Initially (0-13 hours), virus decline is rapid and first-order with respect to fluid infectivity with a rate constant of 20/day. After 13 hours, the fluid measurements of infectivity declined more slowly, but at a rate which is faster than that observed in the sand-free experiment (first order rates of 0.47/day and 0.25/day, respectively). Fluid infectivity loss rates in this second region (i.e. after 13 hours) are compared directly in Figure 5.4. Based on the results of elution experiments (next section), the observed difference between measurements of fluid infectivity in the sand-containing and sand-free batch experiments appears to be caused by virus adsorption to the sand surface and not accelerated inactivation.

If it is assumed that virus adsorption is the main mechanism responsible for removing viruses from the fluid phase in the batch experiment with added sand, then the data presented in Figure 3.5 can be interpreted in at least two different ways. One possible interpretation is that adsorption is occurring reversibly (i.e. there is a flux of fluid-borne viruses adsorbing onto the surface and a flux of adsorbed viruses desorbing into solution) coupled with a first-order surface sink that permanently removes viruses from the fluid phase (QEASS model in Chapter 4). Invoking this model, the change in

slope (i.e. rate) of the infectivity data from the sand-containing batch experiment at 13 hours reflects the onset of quasi-equilibrium adsorption (QEA) in which the flux of viruses onto and off of the surface is equal. The decrease in fluid infectivity after QEA is assumed to be the sum of normal inactivation (i.e. inactivation observed in the absence of sand) and a first-order surface sink that removes viruses permanently from the fluid phase by irreversible adsorption, by structural modification of adsorbed viruses, or by accelerated inactivation. Such a surface sink would slowly draw the QEA toward the surface-adsorbed state with time and thus can be used to explain the difference in rate at which fluid infectivity declined in the sand-free and sand-containing experiments after 13 hours. Nondimensional parameters for the QEASS model were estimated from the data in Figure 5.3 and the resulting simulation (designated QEASS in the figures) is in quantitative agreement with the observed data over the entire 4 days of the experiment.

An equally plausible explanation for these data is that virus adsorption is really occurring irreversibly, but that different sub-populations of λ viruses have different affinities (and thus adsorption rates) for the surface. According to this model, the change in the rate of fluid infectivity decline at 13 hours occurs because one sub-population (the one with the greatest affinity for the sand surface) has been completely scavenged from solution. The remaining sub-population has less affinity, and thus binds more slowly. Sub-populations of λ exist that exhibit different degrees of sensitivity

toward inactivation (Chapter 3 and 6), but these differences are thought to result from the way DNA is packaged in the phage heads (Sternberg and Weisberg, 1977) and not from an external property of the virus that might affect binding.

5.4.3. Elution Experiments.

5.4.3.1. Sand-Accelerated Virus Inactivation

To better elucidate the processes occurring in the adsorption experiment, two elution experiments were performed in which phage were adsorbed to the sand for 1 hour in one trial and 4 days in another. In the first of these experiments, the effect of sand on virus inactivation was investigated. After each of the two incubation times, sand was isolated from the adsorption buffer and resuspended in nutrient broth. Nutrient broth is a standard buffer for stripping viruses from the surfaces of sand or soil (Hurst et al., 1991). Thus, by comparing the levels of viruses eluted after the two incubation times, information about the effect of sand on virus stability can be obtained.

The number of viruses eluted by the nutrient broth will be significantly different, depending on whether the dominant virus/sand interaction is (i) sand-accelerated inactivation and not adsorption (Case A), (ii) a combination of reversible adsorption and sand accelerated inactivation (Case B), or (iii) solely adsorption processes (i.e. the sand does not accelerate inactivation) (Case C). Table 5.2 shows predicted levels of viruses eluted from the sand after each of the incubation times, given the three different cases above. Since the

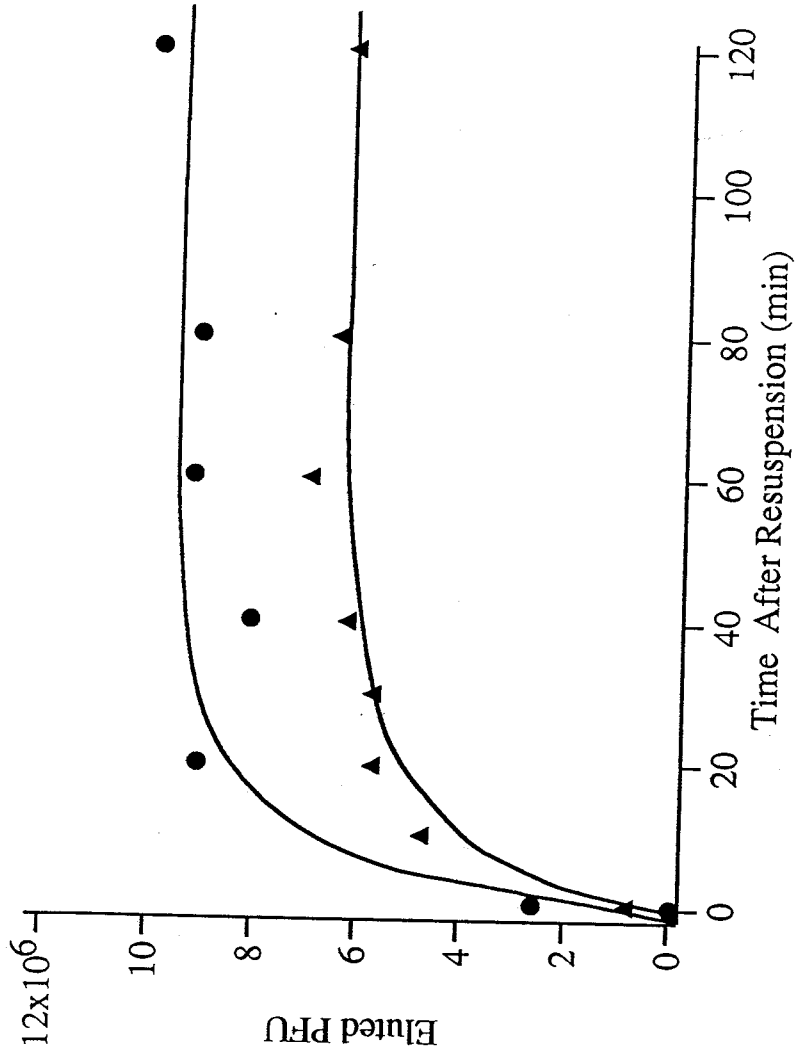


Figure 5.5. PFU eluted from sand using nutrient broth as the elutant. Sand was incubated with phage λ for 1 hour (●) and 4 days (▲) prior to resuspension in elutant.

nutrient broth is not 100% efficient at eluting viruses (Hurst et al., 1991), the relevant comparison is the fractional decrease in viruses eluted after the two incubation times.

Table 5.2. Predicted and observed levels of viruses eluted by nutrient broth.

Incubation Time	Eluted Viruses (PFU/ml)			
	Case A	Case B	Case C	Observed
1 Hour	0	1.9×10^7	1.9×10^7	9×10^6
4 Days	0	4.8×10^6	1.2×10^7	6×10^6

Predicted elution levels for the three cases were determined as follows. *Case A*: Since this case assumes that virus adsorption does not occur in the incubation step, no viruses should be eluted. *Case B*: To predict elution levels for this case, numerical simulations of the incubation step were performed with the QEASS model using parameters determined by fitting the adsorption data in Figure 5.3 ($N_i=1$, $N_b=80$, $R=18$, and $N_s=1.87$). The concentration of reversibly adsorbed viruses (n_{sr}) was estimated from the model at the end of both incubation times, and used to calculate elution levels ($n_{sr}W/V$). *Case C*: The QEASS model was also used in this case, but the surface sink was assumed to be something other than inactivation. The level of viruses eluted after the appropriate incubation time was calculated from $(n_{sr} + n_{ss})W/V$, where n_{ss} is the surface concentration of viruses in the surface sink state (i.e. irreversibly adsorbed).

For Case A, it is assumed that virus adsorption does not occur, and thus no viruses should be eluted when the sand is resuspended in nutrient broth. For cases B and C, resuspension of the sand in

nutrient broth should result in the release of surface adsorbed viruses. However, the number of viruses eluted after the four day incubation should depend on which of the two cases is operative in this system. If the predicted elution levels in Table 5.2 are normalized by the 1 hour level, the predicted decrease in elution levels after the 4 day incubation are 75% and 37%, respectively, for cases B and C. Figure 5.5 shows the time course of fluid PFU after the sand from each of the incubation periods was resuspended. Significant levels of viruses were removed from the sand surface, indicating that Case A does not apply to this system. The maximum number of viruses eluted after the four day incubation was approximately 33% lower than that observed after an incubation time of 1 hour. This is almost exactly the level expected (37%) assuming that the sand does not influence inactivation (Case C).

5.4.3.2. Adsorption Reversibility

The above data are strong evidence that adsorption processes must account for at least some of the behavior observed in Figure 5.3. Another set of elution experiments were conducted to obtain more information about the adsorption process, and specifically to determine if λ adsorption to Ottawa sand occurs reversibly under these conditions. As in the previous elution study, viruses were incubated with sand for 1 hour in one experiment and 4 days in another. The sand was isolated from the adsorption buffer and resuspended in virus-free buffer that was chemically identical to the buffer used in the incubation step. If virus adsorption occurs

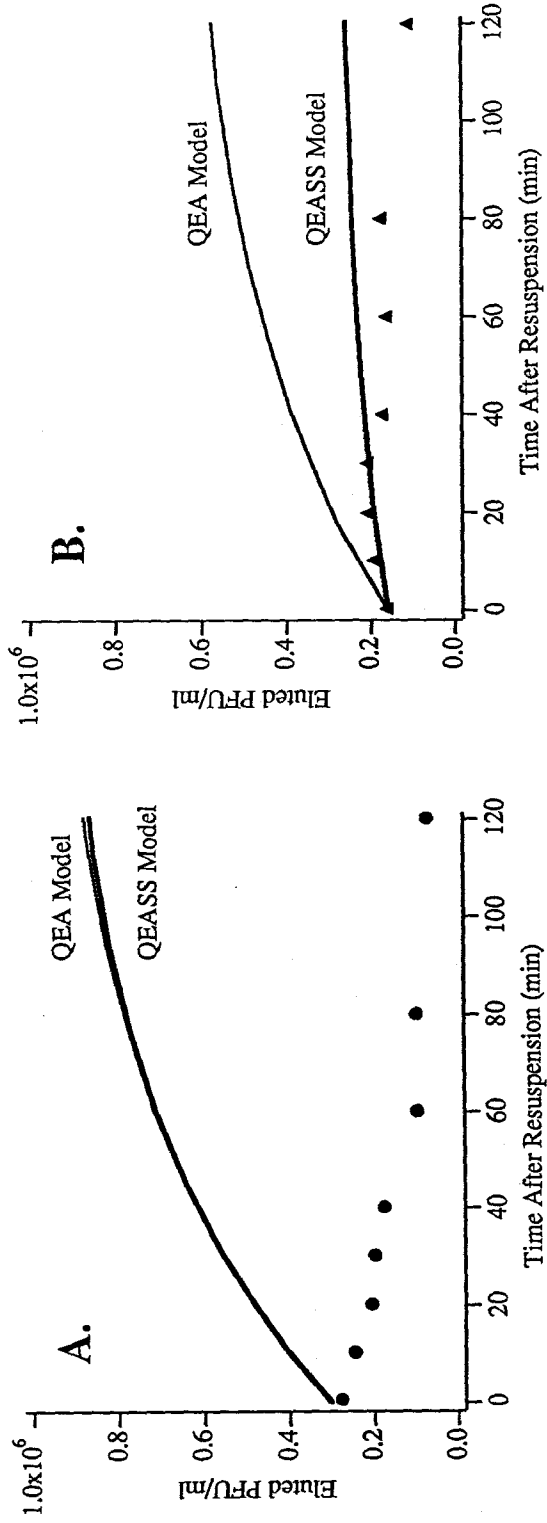


Figure 5.6. PFU eluted from sand using the PIPES buffer as an elutant (●,▲) and predicted from models (lines). Elution profiles correspond to 1 hour (A) and 4 days (B) of incubation. Parameter values used for QEA and QEASS simulations are as follows. QEA: $N_i=1.0$, $N_b=80.0$, $R=18.0$, and $N_s=1.0$. QEASS: the same except $N_s=1.87$. Initial conditions for the simulations were determined as described in Appendix D.

reversibly, then virus desorption should occur when surface adsorbed viruses are diluted into clean buffer. Further, if the QEASS model is an accurate model of the adsorption mechanisms operating in this system, then parameters developed by fitting the model to the adsorption data (Figure 5.3) should apply equally well to the elution data, provided the initial conditions of the elution experiment are well constrained (see Appendix D).

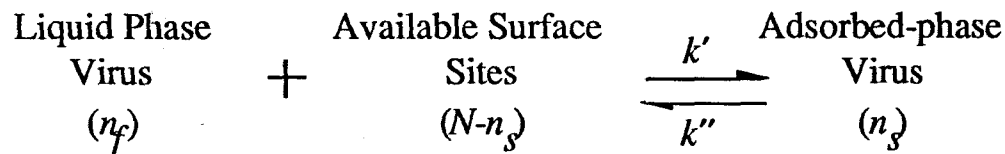
Results of this experiment and predictions from numerical simulations of the QEA and QEASS models are shown in Figure 5.6. Viruses did not desorb from sand incubated for either the 1 hour or 4 day times. Despite an enormous desorption pressure [calculated initial flux rates⁹ off the surface of approximately 10^7 bacteriophage/(g of sand)/day], resuspended sand from the 1 hour incubation actually *adsorbed* viruses that were carried over with the sand in the retained fluid. This behavior cannot be explained in the context of either the QEA or QEASS models since both predict a net flux of viruses off the sand surface (Fig 5.6A). The QEASS model is a better predictor of observed virus desorption for the sand incubated for 4 days prior to resuspension (Figure 5.6B). However, even in this case, the QEASS model predicts a net flux of viruses off of the sand surface while the data show that the flux is going in the opposite direction. These data reveal two important characteristics about

⁹ Initial flux rates off the surface were calculated from $\left(\frac{dn_s}{dt}\right)_o = \frac{V}{W}(k_2 n_{fo} - k_{-2} n_{so})$ where n_{fo} and n_{so} were estimated as described in Appendix D.

the nature of virus adsorption in this system. First, virus adsorption appears to be irreversible, at least when surface adsorbed viruses are diluted into clean buffer. Second, parameter values can be chosen for the QEASS model that cause it to "fit" either the adsorption data or the elution data, but not both. Thus, the QEASS model probably has little or no physical significance for this system, despite the fact that it can be made to "fit" the adsorption data.

5.4.4. Isotherm Experiments

Further evidence that virus adsorption in this system is not occurring as a simple one step adsorption and desorption process was obtained by comparing adsorption isotherms corresponding to incubation times of 1 hour and 2 days (Figures 5.7A,B). Adsorption isotherm data are often analyzed in the context of a reversible or Langmuir kinetic mechanism of the form (Vilker & Burge, 1980):



where N is the maximum number of adsorption sites. If the distribution of viruses between the surface and fluid is assumed to be in quasi-equilibrium, the following expression can be derived,

$$n_s = \frac{NK_L n_f}{(1 + K_L n_f)} \quad (5.2)$$

where the equilibrium constant K_L is the ratio of kinetic coefficients k'/k'' . This equation predicts that as n_f increases and available surface sites become occupied, resulting plots of n_s versus n_f will

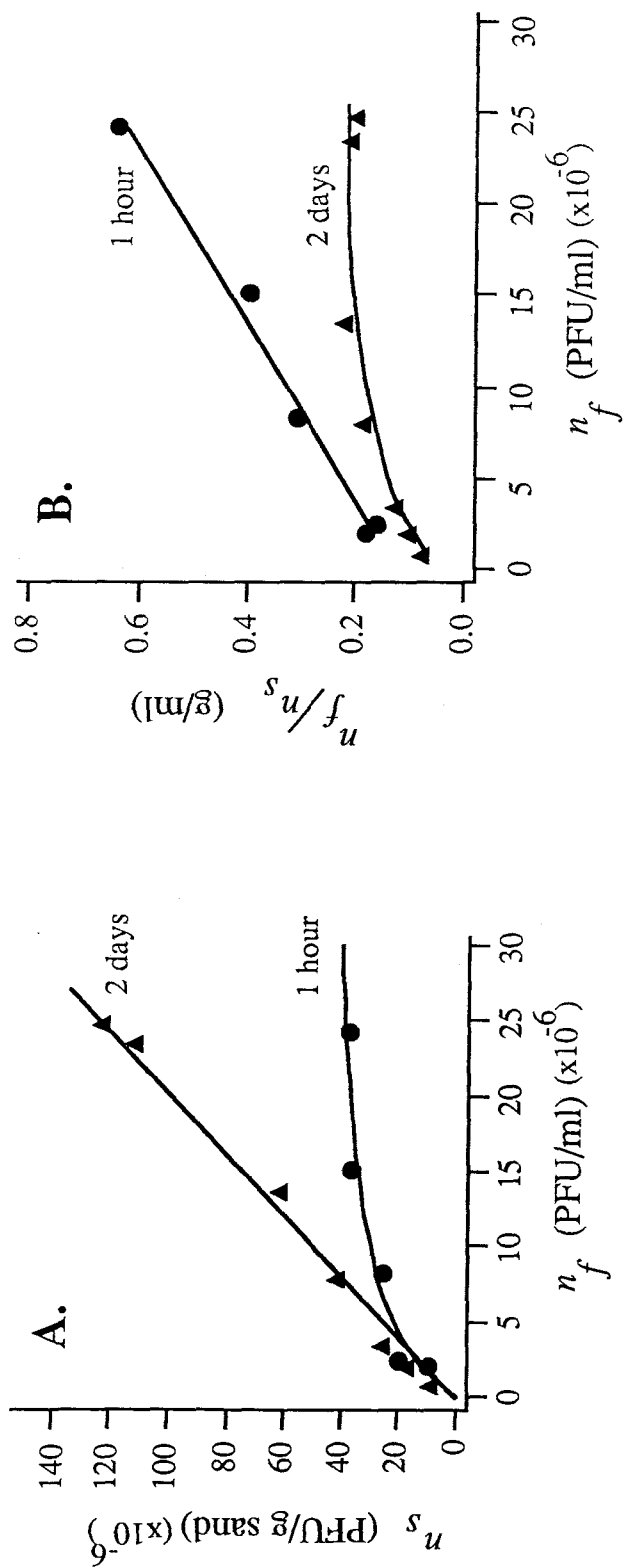


Figure 5.7. Batch adsorption isotherms corresponding to a 1 hour (●) and 2 day (▲) incubation period. (A) Distribution of viruses between fluid (n_f) and surface phases (n_s). Surface concentrations (n_s) were calculated from Equation (5.1). (B). Same data as in (A) plotted in linearized form.

exhibit a saturation profile. There are many examples in the literature in which virus adsorption isotherm data can be fit with (5.2). Such fits are obtained by using the linearized form of (5.2),

$$\frac{n_f}{n_s} = \frac{1}{NK_L} + \frac{n_f}{N}. \quad (5.3)$$

Estimates of the maximum number of surface sites (N) and equilibrium constant (K_L) can be obtained directly from the slope and

intercepts of data plotted as $\frac{n_f}{n_s}$ against n_f .

Such plots were constructed for the 1 hour isotherm data (Fig 5.7B) and the resulting data appear linear. The maximum number of surface sites estimated from a least-squares fit to the data is 4.9×10^4 sites/mg. If bacteriophage λ is assumed to occupy an area on the surface of approximately $0.04 \mu\text{m}^2$, there should be approximately 5×10^8 sites/mg, or a full 4 orders of magnitude more sites per unit mass of sand than is estimated from the Langmuir model. This result suggests that either the assumptions of the Langmuir model are not being satisfied in our system, or that viruses bind to specific sites on the sand surface that represent only $1/10^4$ of the total area available for adsorption. This last possibility seems unlikely since virus adsorption to oxide surfaces is thought to occur by a balance between electrostatic and van der Waal forces (Murray and Parks, 1980), both of which result in nonspecific interactions (Israelachvili, 1985). Further, Ottawa sand is mineralogically homogeneous. Thus,

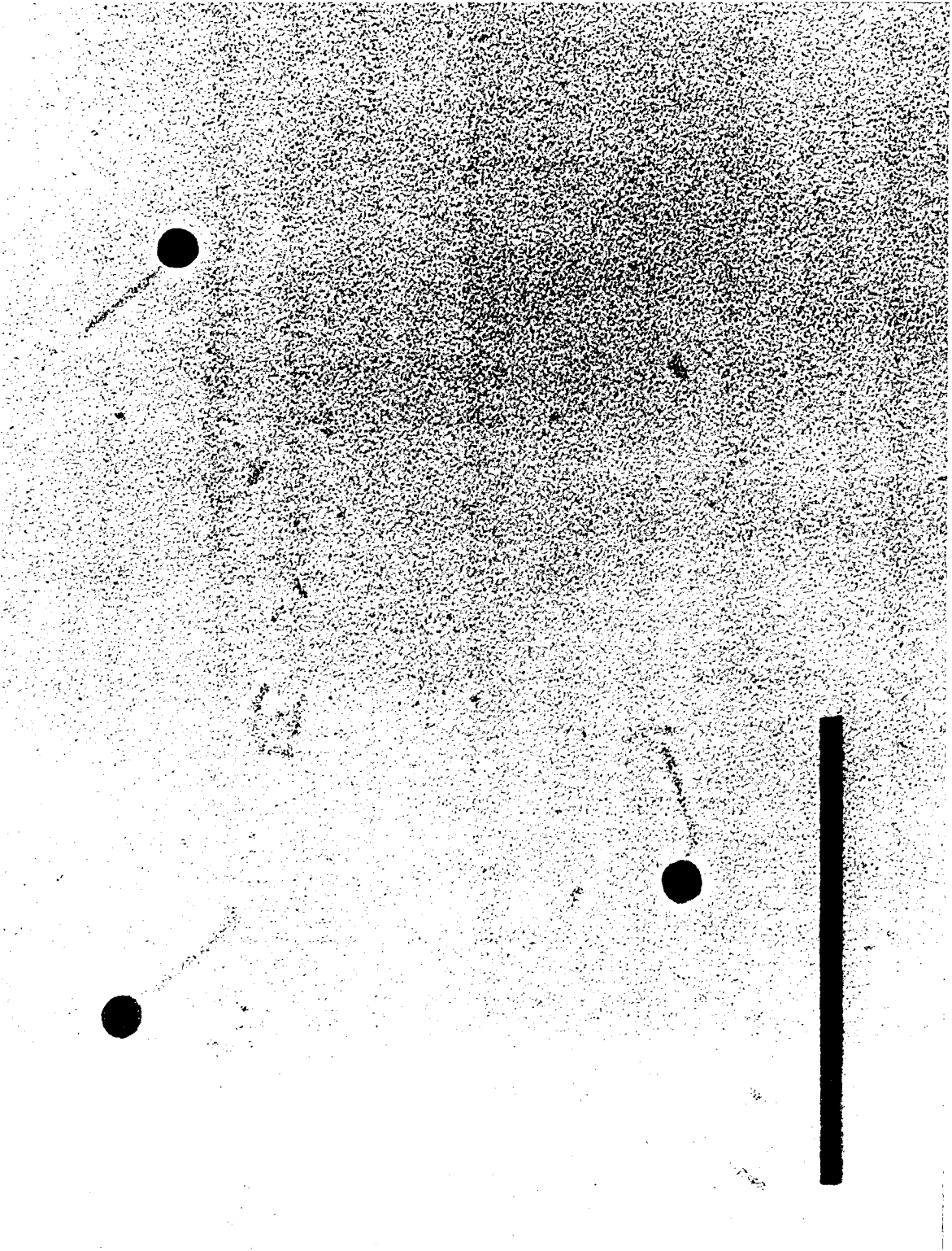
if sites for virus binding exist on the sand surface, they should be distributed over the full surface area of the sand.

The most likely explanation for the above discrepancy is that the underlying assumptions of the Langmuir model are not satisfied. This is supported by isotherm data from the 2 day incubation. When the distributions of adsorbed and suspended viruses are plotted for this second data set (Figure 5.7), the saturation profile seen in the 1 hour data is no longer present. These results suggest that after a 1 hour contact time, the distribution of viruses between adsorbed and suspended states is not at quasi-equilibrium.

5.4.5. Virus Aggregation and Biological Contamination

To determine if the results obtained above could be explained by either virus aggregation or biological contamination of the batch reactions, the particulates in the fluid phase of these experiments were observed directly with a transmission electron microscope (TEM). Particulates from fluid samples of sand-containing and sand-free batch reactions that had been incubated

Figure 5.8. Transmission electron micrograph of bacteriophage λ in the PIPES suspension. All of the phage we observed were present as monomers (such as these) for incubation times up to 2 weeks. Scale bar represents 500nm. Viruses shown in this figure were incubated for 1 week.



for periods up to 2 weeks were centrifuged onto a grid and inspected with a TEM. The viruses we observed on these grids all appeared as single particles (monomers), regardless of the length of time the phage were allowed to incubate for up to 2 weeks. A typical field of view from this experiment is shown in Figure 5.8. We found no evidence for biological contamination on any of the grids examined with the TEM.

5.5. Discussion

5.5.1 Summary of Results

The data above support the following set of conclusions:

(i) Bacteriophage λ adsorption to Ottawa sand proceeds in two steps. The initial step is first order with respect to n_f and rapid (rate constant 20/day). After this initial phase, the rate of virus adsorption decreases, and fluid infectivity declines slowly at a rate which is about twice as fast as can be accounted for by inactivation alone (rate constants 0.47/day and 0.25/day, respectively). The concentration of viruses on the surface at the time when virus adsorption changes from a fast to a slow process is estimated to be approximately 8.0×10^4 phage/mg. This coverage is approximately four orders of magnitude below estimated maximum surface coverage. Consequently, the decrease in adsorption rate is probably not due to virus/virus interactions at the surface, or "site" saturation. Either virus adsorption is occurring reversibly and 13 hours represents the onset of QEA, or virus adsorption is occurring

irreversibly and sub-populations of viruses exist with varying affinity for the sand surface.

(ii) Over longer time scales (>13 hours), the rate at which fluid infectivity decreases in the presence of sand is faster than can be explained by inactivation rates observed in the sand-free suspensions. This effect does not appear to be caused by sand-accelerated inactivation, since the number of viruses eluted with nutrient broth was higher than would be predicted if this was the operative mechanism. Again, the interpretation chosen depends on whether virus adsorption is assumed to occur reversibly or irreversibly in the adsorption experiment. If it is occurring reversibly, then long time scale decline in fluid infectivity probably represents a combination of normal inactivation (i.e. inactivation in the absence of sand) and a surface sink. If the viruses are adsorbing irreversibly, this second rate represents the intrinsic adsorption rate of a second sub-population of viruses.

(iii) When sand possessing surface-adsorbed viruses is resuspended in virus-free buffer, no desorption is observed, irrespective of whether the incubation step is allowed to take place over short (1 hour) or long (4 days) periods of time. This behavior cannot be explained by QEA theory, even if a surface sink for the viruses is included in the analysis. Since the adsorbed viruses can be eluted with nutrient broth, the viruses are clearly present on the surface, but unable to desorb on dilution.

(iv) Adsorption isotherm data obtained using incubation times of 1 hour and 2 days show different profiles. The saturation constant calculated from the 1 hour data is inconsistent with estimates of the surface area occupied by adsorbing phage. Isotherm data from the 2 day incubation do not show evidence of saturation.

(iv) Based on TEM observation of fluid particulates, under the conditions used in these experiments the virus suspensions are stable (i.e., do not aggregate with time) and no biological contamination was observed.

5.5.2 Alternative Adsorption Mechanisms

5.5.2.1. Reversible Adsorption

Despite the fact that virus adsorption appears irreversible when surface adsorbed viruses are diluted into clean buffer, it is theoretically possible that virus adsorption can still occur reversibly in the adsorption experiment (Figure 5.3). A potential adsorption mechanism that would give rise to this type of behavior is illustrated in Figure 5.9. Surface adsorbed viruses can desorb, but only when they are replaced by an identical virus present in solution. In the adsorption experiments, this exchange process can take place since fluid-borne viruses are present. When sand containing surface adsorbed viruses is diluted into clean buffer, this exchange process cannot take place and the adsorption appears irreversible. This type of mechanism has been well documented for specific systems involving protein adsorption to surfaces (Norde, 1986).

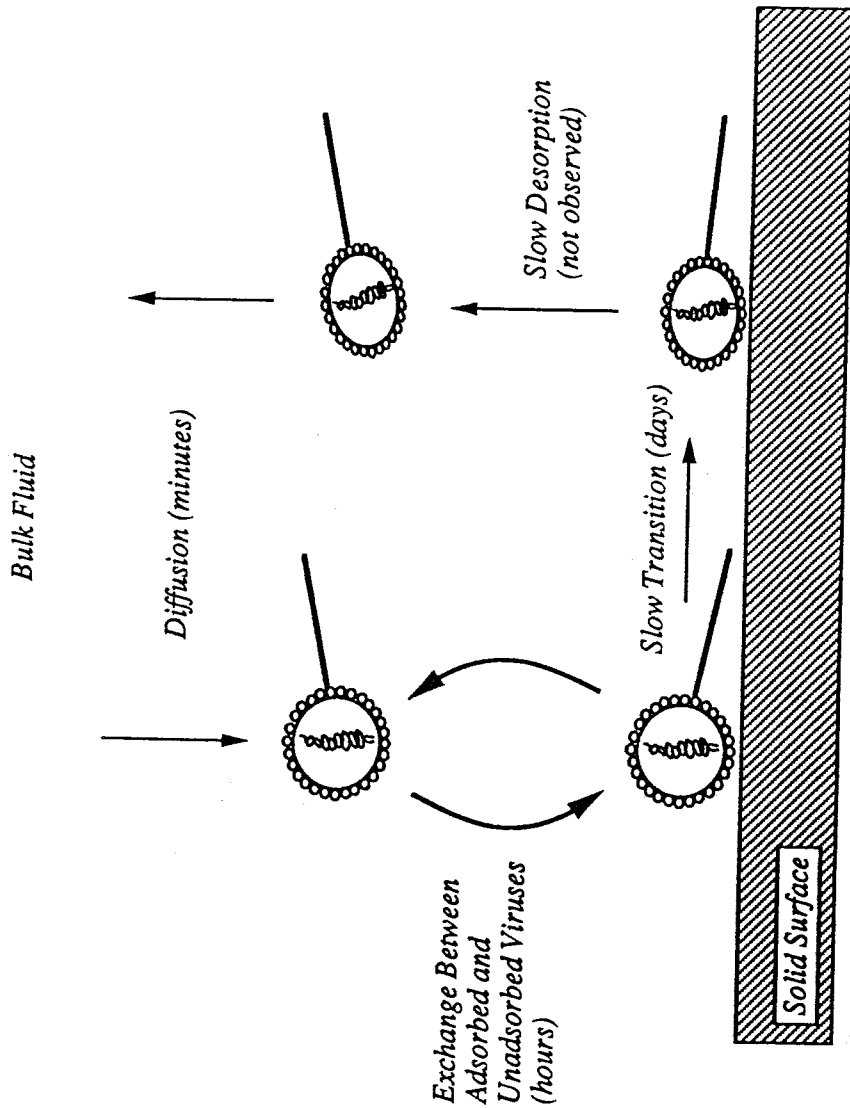


Figure 5.9. A kinetic model for virus adsorption in this system. Adsorption occurs in two steps. Initially, virus adsorption to the surface achieves quasi-equilibrium by direct exchange between adsorbed and suspended viruses. After this initial period, the viruses change their conformation with respect to the surface and become more tightly bound. This second process takes place more slowly and is a possible explanation for the surface sink observed in Figure 5.3.

The above argument can be extended to explain the infectivity decline observed after 13 hours. Nutrient broth elution data suggest that virus inactivation is not accelerated in the presence of sand, and thus this is not a likely explanation for the observed surface sink. A better explanation is that reversibly adsorbed viruses are slowly converted to an irreversibly (or more strongly adsorbed) state with time, possibly due to a change in the physical conformation of the virus at the surface. This type of mechanism also has precedents in the protein adsorption literature (Norde, 1986), but is difficult to justify for this system without further evidence.

5.5.2.2. Irreversible Adsorption

An alternative explanation for the adsorption data is that adsorption occurs irreversibly even in the adsorption experiment, but different sub-populations of viruses exhibit different degrees of affinity for the sand surface. In this context, the observed change in adsorption rates at 13 hours (Figure 5.3) may simply represent the complete removal from solution of a strongly binding virus sub-population. The slower rate that follows would simply represent a virus sub-population with overall weaker affinity for the sand surface.

In its favor, this model can be used to explain virtually all of the adsorption and elution data presented in this report, including the two-step adsorption rate in Figure 5.3 and the fact that viruses could not be desorbed when the sand was diluted into virus-free adsorption buffer. Since the surface of phage λ consists of interlocking protein molecules, it is theoretically possible that certain conformations of

these proteins could result in greater or lesser sand affinity (e.g. the exposure of hydrophobic groups on the surface could act to drive the virus out of solution). It is well documented that sub-populations of λ can exhibit different sensitivities to inactivation (see Chapters 3 and 6); presumably, the viruses differ in some physical way which makes them more or less sensitive to inactivation. In the case of inactivation, experimental procedures have been developed for isolating sub-populations (Sternberg and Weisberg, 1977). The same types of approaches could be used to isolate sub-populations of viruses for adsorption, as a means for testing the veracity of this particular mechanism. However, without further evidence, both of these proposed models for lambda adsorption to Ottawa sand should be viewed with skepticism.

5.5.3. Environmental Implications

5.5.3.1. Significance of Irreversible Adsorption

Virus adsorption in the model system presented here was found to exhibit at least some degree of irreversibility. Since most models of virus adsorption assume the adsorption process occurs reversibly, it is interesting to examine the possible environmental significance of irreversible adsorption. Figure 5.10 shows QEASS model estimates of fluid-borne, reversibly adsorbed and irreversibly adsorbed λ for the 4 day adsorption experiment conducted in this study. Despite the fact that the rate constant for converting adsorbed viruses from a reversible to an irreversible state is relatively slow in this model (0.22/day), the simulation predicts that the majority of

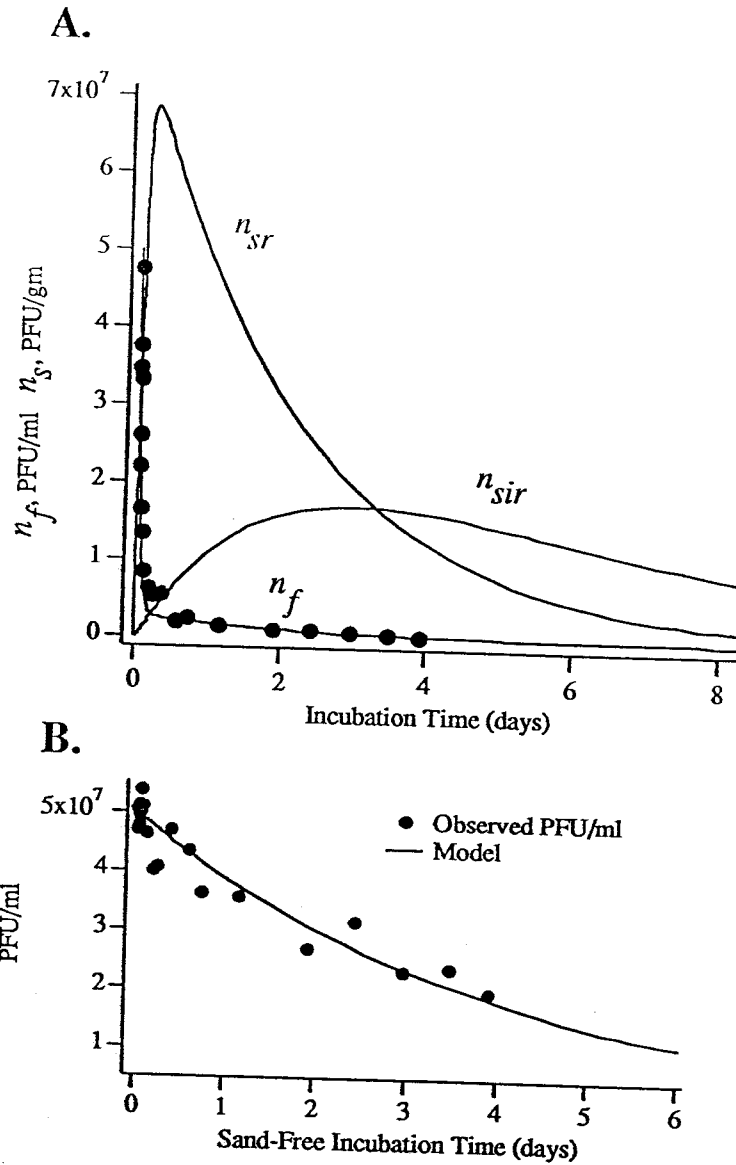


Figure 5.10. Numerical simulations of the adsorption experiment. (A) Time course of fluid borne viruses (n_f), reversibly adsorbed viruses (n_{sr}) and irreversibly adsorbed viruses (n_{sir}). Data (●) are fluid PFU measurements from the sand-containing batch reaction. (B) Observed fluid PFU (●) in the sand-free batch reaction. Line corresponds to the sum of all PFU in the system divided by the fluid volume. Parameters used for the model simulation included: $N_i=1.0$, $N_b=80.0$, $R=18.0$, and $N_s=1.87$.

viable viruses are irreversibly adsorbed within 3 days after the start of the experiment. Thus, even in the case where virus adsorption is assumed to occur as a fast reversible adsorption followed by a slow conversion of reversibly adsorbed viruses to an irreversible state (section 5.5.2.1), the irreversible adsorption step may be extremely important for environmental processes which operate over relatively long time scales. Examples of such systems are described below.

5.5.3.2. Environmental Transduction

Bacteriophage-mediated gene transfer between natural populations of bacteria by transduction may take place preferentially at surfaces (Stotzky, 1989). If irreversible adsorption involves a structural change in the virus, it is difficult to predict how gene transfer would be influenced by such a process. Irreversible adsorption would increase local phage concentrations near interfaces and thus make transduction more likely. On the other hand, structural changes in the virus might make host cell infection on surfaces more difficult, thereby reducing gene transfer activity.

5.5.3.3. Virus Mobility in Sandy Environments

Coarse sands (like the Ottawa sand used in this study) are considered relatively poor adsorbents for viruses (Gerba, 1984). While this may be true in cases where the adsorption occurs over relatively short time scales (e.g. packed beds used for filtration of wastewater effluent), these results suggest that virus adsorption to sand can be quite strong over time scales more relevant to many natural processes. In groundwater aquifers, for example, pore water

velocities range from 2m/day-2m/year (Todd, 1980). In systems like this, virus/surface interactions may take place over time scales ranging from days to months. These long surface residence times significantly increase the possibility that virus adsorption will occur irreversibly, suggesting that conclusions from short time scale experiments should be interpreted with caution when extended to natural systems.

5.5.3.4. Groundwater Transport Models

Geostatistical models developed for predicting safe septic tank setback distances (Yates, et al., 1986; Yates, 1990) assume that viruses in groundwater do not adsorb to the porous matrix. While this may lead to conservative estimates for setback distances, our results suggest that virus/surface interactions may be extremely important over transport time scales encountered in typical groundwater environments. Geostatistical models of this type may significantly underestimate the filtration potential of typical groundwater environments.

Deterministic models for virus transport in groundwater have been proposed and at least one of these considers the possibility for adsorption to occur irreversibly (Teutsch, et al., 1991). Models have also been developed assuming that adsorption occurs reversibly. In the last case, the distribution of viruses between the fluid and surface states has been modeled in two ways: by assuming that an instantaneous quasi-equilibrium is established between adsorbed and suspended viruses (Yates et al., 1987; Matthess and Pekdeger, 1981),

or by assuming that virus adsorption is rate limited by mass transfer across a stagnant boundary layer where quasi-equilibrium partitioning of viruses occurs (Vilker and Burge, 1984). The data presented in this report show that virus adsorption in a relatively simple batch experiment, using well-defined materials and buffer conditions, can result in data which is difficult to interpret within the context of traditional adsorption models. Such models should be viewed with skepticism, especially when they are applied to situations where both transport and adsorption processes are linked.

5.6. Conclusions

Experimental results presented in this report indicate that virus adsorption to natural surfaces can be relatively complex in nature, even when the model system is greatly simplified. In experiments where fluid suspensions of bacteriophage λ were mixed with Ottawa sand, fluid measurements of virus infectivity declined at a rate which was time scale dependent. Over the first 13 hours of the experiment, the decrease in infectivity followed first-order kinetics and was rapid. After 13 hours, infectivity declined more slowly, but at a rate which was faster than observed in sand-free batch experiments. Based on nutrient broth elution experiments, the loss of infectivity in the sand-containing batch experiments is not due to sand-enhanced inactivation, implying that observed infectivity declines were due to virus adsorption to the sand surface. The nature of this adsorption was investigated in a series of elution experiments using the adsorption buffer as the elutant. These experiments demonstrate that

virus adsorption to the sand surface occurs irreversibly, at least when the sand is diluted into virus-free buffer. A quasi-equilibrium adsorption model could be fit to the adsorption data. However, when this same model was used to predict the elution experiment, the model significantly overestimated virus desorption. These adsorption and elution data cannot be reconciled with widely assumed mechanisms for virus adsorption. Either virus desorption involves the direct exchange of fluid-borne and surface-adsorbed viruses, or virus adsorption occurs irreversibly. In the latter case, it is necessary to invoke the existence of sub-populations of viruses with different sand affinities in order to explain the observed adsorption data. The data do not support either Langmuir and Freundlich models of virus adsorption, despite the fact that our short time scale data can be made to fit a Langmuir adsorption isotherm model.

6. Effects of Solution pH and Electrolyte Composition on Long Time Scale Adsorption and Inactivation¹⁰

6.1 Summary

The effects of solution pH and electrolyte composition on virus/surface interactions are not well constrained, especially over time scales relevant to many natural processes. In this report, a series of batch experiments were performed using a range of pH values (5-10) and three different types of electrolytes (NaCl, MgCl₂, and humic acids). Fluid samples were collected from sand-containing and sand-free experiments over the course of 5-6 days and analyzed for PFU. When these data were plotted on semi-log graphs as normalized concentration against non-dimensional time, the data from sand-free experiments fell along a single line, while data from sand-containing experiments fell into three distinct categories. In the presence of humic acids and at pH=10, the sand strongly stabilized the phage. The sand stabilized the phage only weakly when NaCl and MgCl₂ were the electrolytes at pH=10. At lower pH values (5 and 7), the sand appeared to adsorb the phage, as evidenced by an accelerated decline in fluid PFU. This adsorption

¹⁰To be submitted as the third in a series of three papers to *Water Resources Research*.

adsorption appeared to be irreversible, based on the divergence of PFU data from the sand-containing experiments and the pure inactivation line. The time scales over which many of the processes occurred in this batch system were on the order of days, suggesting that batch experiments conducted over relatively short incubation times (e.g. hours) may not reflect processes occurring in nature. These results demonstrate the utility of a kinetic approach for investigating the effects of chemical factors on virus/surface interactions.

6.2. Introduction

The mobility, survival and ecology of viruses in nature is strongly influenced by the degree to which they partition to surfaces. Since different aquatic and groundwater environments can have widely varying chemistry, it is important to understand the effects of master variables like pH and electrolyte composition on the nature of virus/surface interactions. Previous batch studies of virus/surface interactions have been conducted over relatively short time scales (hours) using a conceptual framework which is difficult to justify in practice (see Chapters 4, 5). In this report, experimental data on virus/surface interactions were collected over the time course of 5-6 days and analyzed according to the kinetic approach proposed in Chapter 4. Results indicate that virus/surface interactions strongly depend on both the electrolyte composition and pH of the suspending fluid. The proposed kinetic approach proved extremely useful in evaluating the effects of solution pH and electrolyte composition on virus/surface interactions occurring over relatively long time scales.

6.3. Methods and Materials

6.3.1. Adsorption Experiments

Batch adsorption experiments were carried out using a range of pH values and electrolyte compositions. Stock preparations of bacteriophage λ (see Chapter 4) were diluted approximately 20,000 fold into two 50ml Sarstedt tubes, each containing 40ml of the appropriate buffer (described below). The final concentration of phage in these reactions was approximately 5×10^7 PFU/ml. To one of

these tubes, 25g of sand (treated to remove outer coatings or untreated) was added, and 0.04ml samples of both sand-containing and sand-free suspensions were taken at specified times over the course of 5 days, diluted in salt buffer (SM), and analyzed for plaque forming units (PFU).

Three different pH buffers were chosen for this study: pH5 buffer (5mM malic acid), pH7 buffer (5mM PIPES), and pH10 buffer (5mM NaHCO₃). All three buffers were adjusted to the appropriate pH by addition of strong base (5M NaOH) and filter sterilized prior to addition of phage. In separate experiments, three different electrolytes (at two different concentrations) were added to each of the three pH buffers described above. The electrolytes tested included NaCl (at 10 and 100mM), MgCl₂ (at 10 and 100mM) and Suwannee River humic acid (at 0.1 and 1.0mg/l). The humic acid was obtained from the International Humic Substance Society.

6.3.2. Plasma Emission Spectroscopy

The elemental content of pH10 buffer after contact with sand was determined using a plasma emission spectrometer (PES) (Spectra Span VB, Beckman). Three solutions of pH10 buffer were prepared as described above. NaCl was added to these buffers to a final concentration of 10mM. 25g of treated sand was added to one of the buffers and 25g of untreated sand to another. The third solution was treated as a blank. All three test solutions were incubated for 12 hours at room temperature. After the incubation period, the fluid fraction was isolated from each of the reactions

containing sand and reserved. The solution that was not exposed to sand was used to generate concentration standards of silica, iron, magnesium, calcium and aluminum ranging from 2-140ppm. PES measurements of the solutions exposed to treated and untreated sand were compared with the standards to obtain concentration estimates. Concentrations of the respective elements were reported as $\mu\text{moles/l}$ (μM).

6.3.3. Data Reduction

Data from the inactivation and adsorption experiments were non-dimensionalized as follows. PFU data from the sand-free batch experiments were plotted on a semi-log graph. Slopes were estimated from the data and used to calculate first-order inactivation constants (k_1). In cases where more than one sensitivity toward inactivation was observed (i.e. more than one slope was evident when the data were plotted semi-logarithmically), k_1 values were determined for the most dominant sub-population. Initial concentrations for the i th sub-population (n_{foi}) were determined by projecting the PFU data back to the y-axis, following the procedure outlined in Pollard and Solosko (1977). Values of k_1 and n_{foi} corresponding to a given electrolyte and pH condition were used to construct semi-log plots of normalized fluid PFU ($n_{fo}^* = \frac{n_f}{n_{foi}}$) against non-dimensional time ($\tau = k_1 t$), where t =time in days.

6.4. Results

Figures 6.1-6.3 show the results of the batch experiments prior to non-dimensionalization. Tables 6.1-6.4 list the raw data from these experiments. Below, the effects of buffer pH and electrolyte composition on both virus inactivation and adsorption are discussed.

6.4.1. Inactivation Data

6.4.1.1. NaCl as the Electrolyte

PFU data from the sand-free batch experiments are shown in Figure 6.4. The data were normalized relative to the concentration of fluid PFU at the start of each respective experiment. In the experiments conducted with NaCl (Figure 6.4A), phage λ appears to exhibit more than one sensitivity toward inactivation. The first sub-population is relatively sensitive and is fully inactivated by the second sample (<5 hours). This sensitive population accounts for approximately 40% of the initial PFU concentration (difference between the zero time sample and the second sample in Figure 6.4). The second sub-population is less sensitive (i.e. inactivates more slowly) and is indicated by the dashed lines in the Figure 6.4A. The rate at which this second sub-population inactivated was highly sensitive to both pH and the concentration of NaCl. At pH values of 7 and 10, the second sub-population inactivated relatively slowly, and persisted over the 5 day course of the experiment. In the pH5 buffer, the second sub-population inactivated more rapidly, exposing

Table 6.1. PFU/ml ($\times 10^{-6}$) in fluid samples from batch experiments with treated (Sand+) and untreated (Fe+) sand using NaCl at 10mM. Batch experiments conducted without sand are designated Sand- in the Table. Values are the average of two replicate titers.

Time (days)	pH 5.0			pH 7.0			pH 10.0		
	Sand-	Sand+	Fe+	Sand-	Sand+	Fe+	Sand-	Sand+	Fe+
0	13	12	11	22	12	14	13	12	14
0.17	0.25	0.025	0.0075	11	9.3	9.4	9.1	6.4	6.3
0.52	0.017	0.0013	0.0025	11	7.9	7.1	7.7	4.1	2.9
1.1	a	b	b	9.9	6.3	5.8	4.7	3.4	1.7
1.6	0.0015	b	b	8.3	5.1	4.25	3.3	2.6	1.2
2.1	0.0001	b	b	7.9	4.7	4.6	2.8	2.2	1.3
2.5	b	b	b	7.4	3.5	2.9	1.7	1.5	0.81
3.6	b	b	b	7.1	3.1	2.8	1.0	1.1	0.64
4.4	b	b	b	6.9	2.6	2.5	0.58	1.2	0.46
5.4	b	b	b	5.5	1.4	1.8	0.25	0.68	0.24

a. Values not determined.

b. Below lower limit of detection (< 0.00001).

Table 6.2. PFU/ml ($\times 10^{-6}$) in fluid samples from batch experiments with (Sand+) and without (Sand-) sand using NaCl at 100mM. Values are the average of two replicate samples.

Time (days)	pH 5.0		pH 7.0		pH 10.0	
	Sand-	Sand+	Sand-	Sand+	Sand-	Sand+
0	48	43	50	35	38	50
0.22	16	8.3	34	20	22	10
0.87	4.1	1.1	23	13	10	2.45
1.23	2	0.6	21	8.8	6.9	0.85
1.7	0.79	0.16	14	5.5	4.3	0.5
2.31	0.3	0.05	14	4.1	2.85	0.2
3.03	0.1	0.01	11	2.2	1.5	0.06
3.34	0.073	0.005	10	1.7	1	0.043
4.16	0.027	0.0015	a	1	0.5	0.019
5.27	0.0048	0.00027	5.4	0.55	0.162	0.0043

a. Values not determined.

Table 6.3. PFU/ml ($\times 10^{-6}$) in fluid samples from batch experiments with (Sand+) and without (Sand-) sand using $MgCl_2$ as the electrolyte. Values are the average of two replicate samples.

Time (days)	pH 5.0						pH 7.0						pH 10.0							
	$MgCl_2 = 10mM$		$MgCl_2 = 100mM$		$MgCl_2 = 10mM$		$MgCl_2 = 100mM$		$MgCl_2 = 10mM$		$MgCl_2 = 100mM$		$MgCl_2 = 10mM$		$MgCl_2 = 100mM$		$MgCl_2 = 10mM$		$MgCl_2 = 100mM$	
	Sand-	Sand+	Sand-	Sand+	Sand-	Sand+	Sand-	Sand+	Sand-	Sand+	Sand-	Sand+	Sand-	Sand+	Sand-	Sand+	Sand-	Sand+	Sand-	Sand+
0	16.3	16.9	14.4	12.5	14.4	12.5	14.4	12.2	9.53	22.5	15.0	16.9	19.4	14.4	16.9	21.9	7.23	9.83	7.23	9.83
0.25	13.8	10.4	15.2	10.9	12.2	10.9	12.2	9.53	6.25	9.53	14.7	11.2	7.5	7.13	7.13	9.83	6.35	6.35	5.15	5.15
0.9	11.9	5.75	10.0	5.55	12.9	5.55	12.9	6.25	4.13	4.13	9.1	4.18	7.23	3.68	4.2	3.6	3.6	3.6	2.05	2.05
1.52	7.8	3.73	9.03	3.33	9.3	3.33	9.3	4.13	2.08	2.08	7.38	2.18	2.68	0.58	3.1	2.68	1.2	1.2	1.2	1.2
1.94	6.23	2.03	11.6	1.6	7.3	1.6	7.3	2.08	1.5	1.5	7.08	1.59	2.18	1.5	2.68	1.2	1.2	1.2	1.2	1.2
2.4	5.8	1.5	6.68	1.18	6.7	1.18	6.7	1.5	0.71	0.71	4.6	0.75	a	1.06	1.68	2	2	2	2	2
2.9	3.25	0.70	4.1	0.51	4.6	0.51	4.6	0.71	3.88	3.88	0.5	1.2	0.60	1.2	0.60	1.2	0.91	0.91	0.91	0.91
3.56	3.18	0.51	3.63	0.35	4.0	0.35	4.0	0.51	3.4	3.4	0.38	0.38	1.2	0.66	a	a	a	a	a	a
4.63	2.7	0.36	2.98	0.18	2.98	0.18	2.98	0.42	2.4	2.4	0.16	0.16	1.1	0.68	a	a	a	a	a	a
5.6	2.2	0.15	2.0	0.073	1.9	0.073	1.9	0.18	0.18	0.18	0.16	0.16	1.1	0.68	a	a	a	a	a	a

a. Values not determined.

Table 6.4. PFU/ml ($\times 10^{-6}$) in fluid samples from batch experiments with (Sand+) and without (Sand-) sand using Humic Acids as the electrolyte. Values are the average of two replicate samples.

Time (days)	pH 5.0						pH 7.0						pH 10.0							
	Humics=0.1mg/l		Humics=1.0mg/l		Humics=0.1mg/l		Humics=1.0mg/l		Humics=0.1mg/l		Humics=1.0mg/l		Humics=0.1mg/l		Humics=1.0mg/l		Humics=0.1mg/l		Humics=1.0mg/l	
	Sand-	Sand+	Sand-	Sand+	Sand-	Sand+	Sand-	Sand+	Sand-	Sand+	Sand-	Sand+	Sand-	Sand+	Sand-	Sand+	Sand-	Sand+	Sand-	Sand+
0	20	13	20	23	25	23	25	24	22	22	23	24	25	25	22	25	22	25	22	22
0.08	0.0125	0.003	0.003	0.0075	0.0075	0.0075	0.0075	20	21	21	21	21	13	18	7.5	17.5	17.5	17.5	17.5	17.5
0.42	b	b	b	b	18	18	18	15	17	17	15	6.4	12	4	4	11.3	11.3	11.3	11.3	11.3
1	b	b	b	b	17	17	17	13	16	16	12	2.2	10	2.3	6.3	6.3	6.3	6.3	6.3	6.3
1.54	b	b	b	b	15	15	15	11	16	11	1.7	8.4	2.06	7.3	7.3	7.3	7.3	7.3	7.3	7.3
2	b	b	b	b	15	15	15	10	13	13	9.2	0.825	6.8	0.724	5.08	5.08	5.08	5.08	5.08	5.08
2.5	b	b	b	b	14	14	14	8.6	12	12	7.9	0.51	5.7	0.85	4.95	4.95	4.95	4.95	4.95	4.95
3	b	b	b	b	12	12	12	8.7	12	12	7.5	0.33	5.2	0.73	3.9	3.9	3.9	3.9	3.9	3.9
4	b	b	b	b	7.4	7.4	7.4	6.8	7	7	5	0.068	2.8	0.18	2.1	2.1	2.1	2.1	2.1	2.1
5.1	b	b	b	b	9.1	9.1	9.1	6.9	8.4	8.4	5.7	0.039	3.2	0.28	2.4	2.4	2.4	2.4	2.4	2.4

a. Values not determined.

b. Below lower limit of detection (<0.00001).

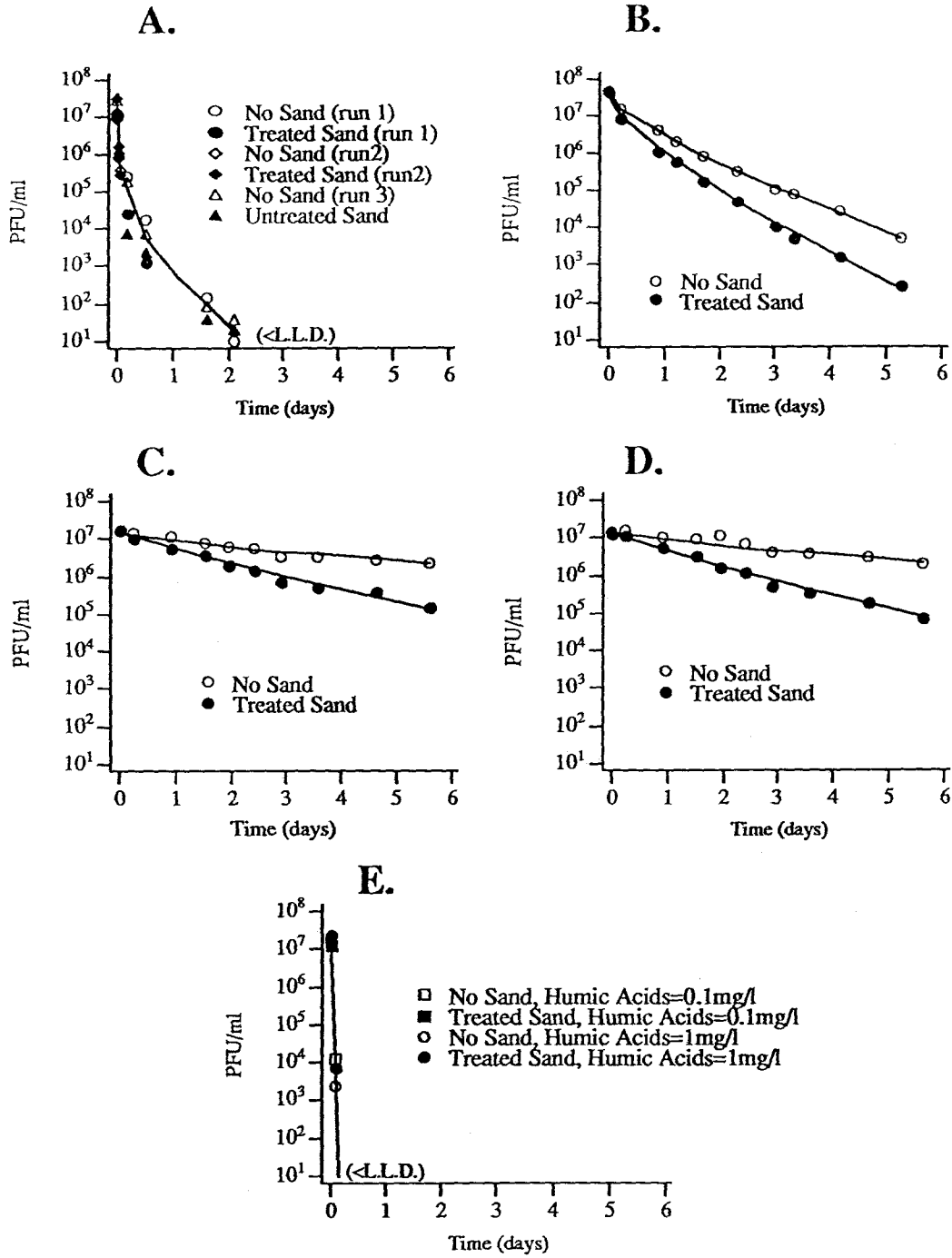


Figure 6.1. Results of batch experiments conducted with (●) and without (○) added sand using the pH5 buffer. Different graphs correspond to different electrolyte conditions: (A) NaCl=10mM, (B) NaCl=100mM, (C) MgCl₂=10mM, (D) MgCl₂=100mM, and (E) Humic acid = 0.1, 1.0 mg/l. L.L.D.=Lower Limit of Detection (approximately 10 PFU/ml).

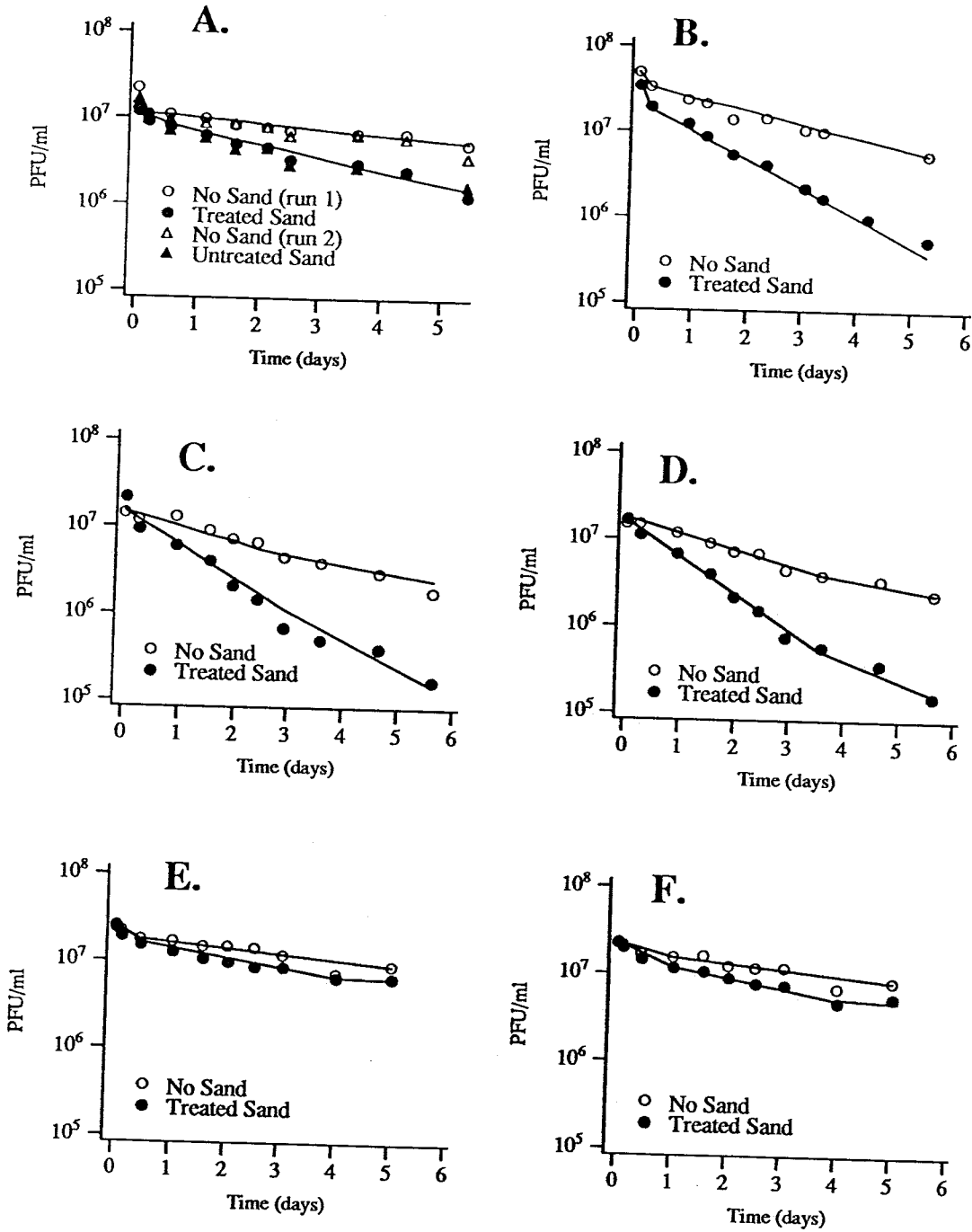


Figure 6.2. Results of batch experiments conducted with (●) and without (○) added sand using the pH7 buffer. Different graphs correspond to different electrolyte conditions: (A) NaCl=10mM, (B) NaCl=100mM, (C) MgCl₂=10mM, (D) MgCl₂=100mM, (E) Humic acid = 0.1 mg/l, and (F) Humic acid= 1.0 mg/l.

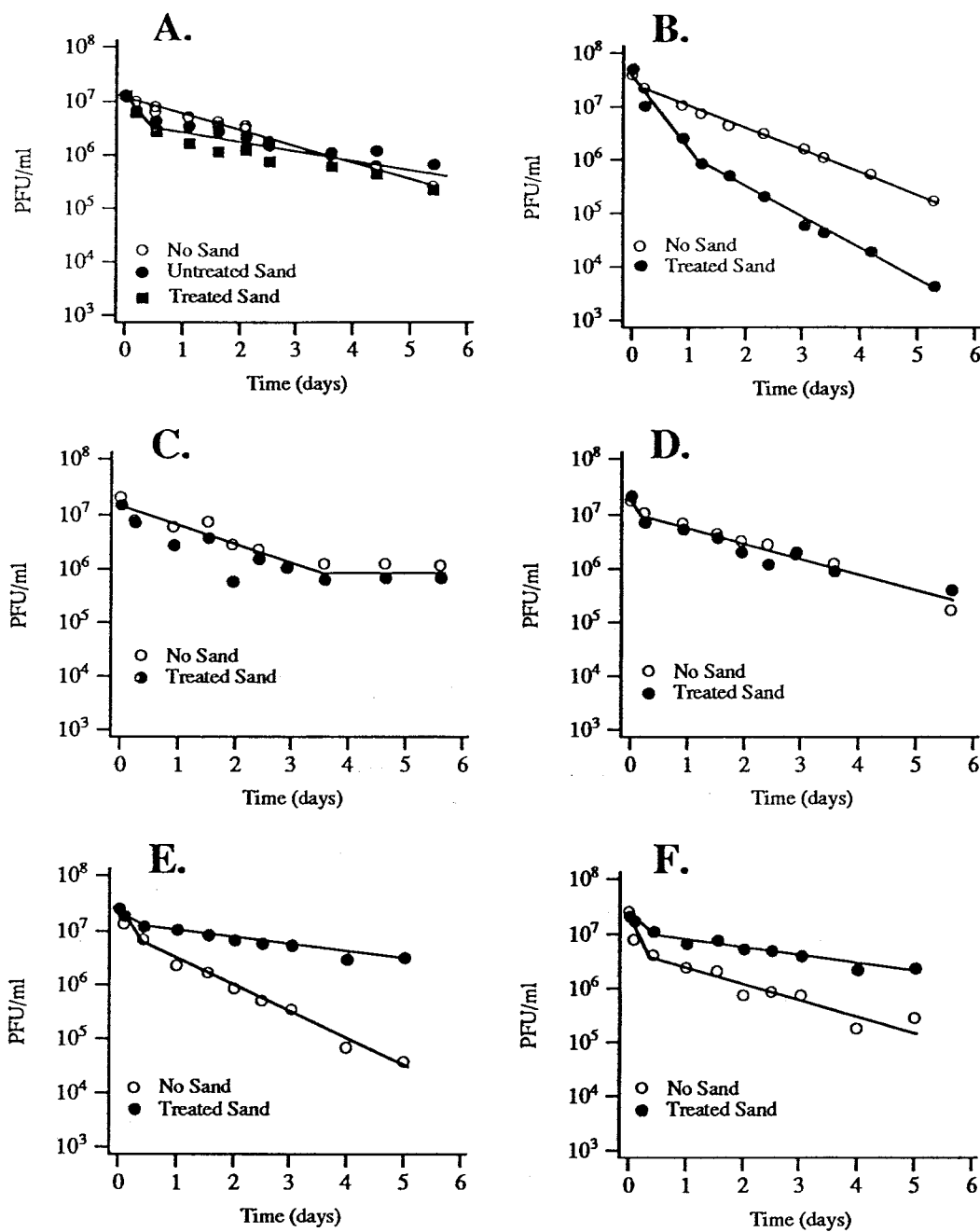


Figure 6.3. Results of batch experiments conducted with (●) and without (○) added sand using the pH10 buffer. Different graphs correspond to different electrolyte conditions: (A) NaCl=10mM, (B) NaCl=100mM, (C) MgCl₂=10mM, (D) MgCl₂=100mM, (E) Humic acid = 0.1 mg/l, and (F) Humic acid= 1.0 mg/l.

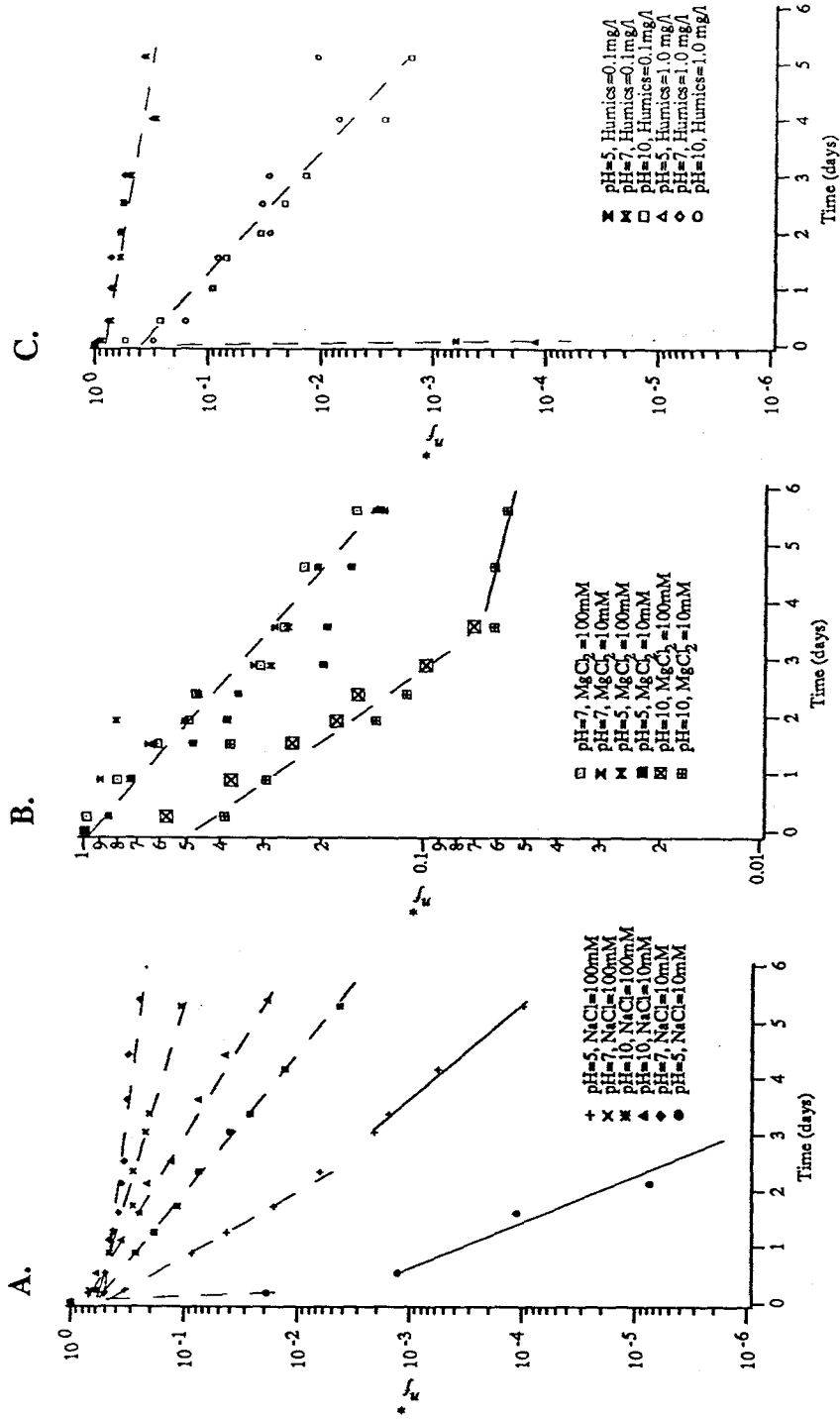


Figure 6.4. PFU data from batch experiments without added sand. PFU/ml data for each batch experiment were normalized by the initial concentration to give (η). The different graphs correspond to different choices of electrolyte: (A) NaCl, (B) MgCl₂, (C) Humic acid. The first sub-population drops rapidly and is not indicated by a line. Dashed lines correspond to the second sub-population. Solid lines correspond to the third sub-population.

a third sub-population of viruses below 1/300 of the initial PFU. This third population is indicated in Figure 6.4A by the solid line. In general, phage inactivated more slowly in the buffer with the higher NaCl concentration for a fixed value of pH.

6.4.1.2. MgCl₂ as the Electrolyte

Phage inactivation in the presence of MgCl₂ followed one of two trends as shown in Figure 6.4B. For experiments conducted at pH 10, approximately 50% of the viruses were inactivated by the second sample (<6 hours), after which time a second sub-population of viruses was present for up to four days. In the case where MgCl₂=10mM, a third sub-population may be present below 1/15 of the initial PFU. The data from experiments conducted at pH values of 5 and 7 followed a different trend. In experiments conducted at these lower pH values there appears to be only one phage sensitivity toward inactivation, and the rate of inactivation appears insensitive to both electrolyte composition (10 or 100mM) and pH (5 or 7).

6.4.1.3. Humic Acids as the Electrolyte

The rate at which viruses inactivated in the presence of humic acids (Figure 6.4C) was extremely sensitive to pH, but relatively insensitive to the different concentrations of humic acid tested (0.1 and 1.0mg/l). The phage were most stable at pH=7. Within experimental error, only one population of viruses was apparent at this pH. At pH 10, approximately 60% of the viruses were inactivated within 6 hours from the start of the experiment, after which time a second sub-population was observed for the duration of

the experiment (dashed line in the figure). At pH=5, virus inactivation was extremely rapid in the presence of humic acids, with complete inactivation of all the phage occurring within 6 hours of the start of the experiment.

Table 6.5. Parameters used to non-dimensionalize the adsorption and inactivation data. Fluid inactivation constants (k_1) were determined by measuring the slope of n_f in Figure 6.4 corresponding to the second sub-population of viruses. Initial virus concentrations (n_{fo}) also correspond to this second population. The column entitled "Range" refers to the range of experimental times for which the listed parameters apply.

Experimental Condition			Parameters		
Electrolyte	Concentration	pH	$n_{fo} (\times 10^7)$	k_1	Range (days)
NaCl	10mM	7	4.0	0.14	0-5.4
NaCl	10mM	10	1.6	0.68	0-5.4
NaCl	100mM	5	8.0	2.0	0-2.3
NaCl	100mM	7	8.1	0.33	0-5.3
NaCl	100mM	10	5.4	0.94	0-5.3
MgCl ₂	10mM	5	1.6	0.36	0-5.6
MgCl ₂	10mM	7	1.4	0.36	0-5.6
MgCl ₂	10mM	10	3.9	0.55	0-3.6
MgCl ₂	100mM	5	1.4	0.36	0-5.6
MgCl ₂	100mM	7	1.5	0.36	0-5.6
MgCl ₂	100mM	10	3.4	0.55	0-5.6
Humic Acid	0.1mg/l	7	3.0	0.12	0-5.1
Humic Acid	0.1mg/l	10	6.0	1.0	0-5.1
Humic Acid	1.0mg/l	7	2.6	0.12	0-5.1
Humic Acid	1.0mg/l	10	6.3	1.0	0-5.1

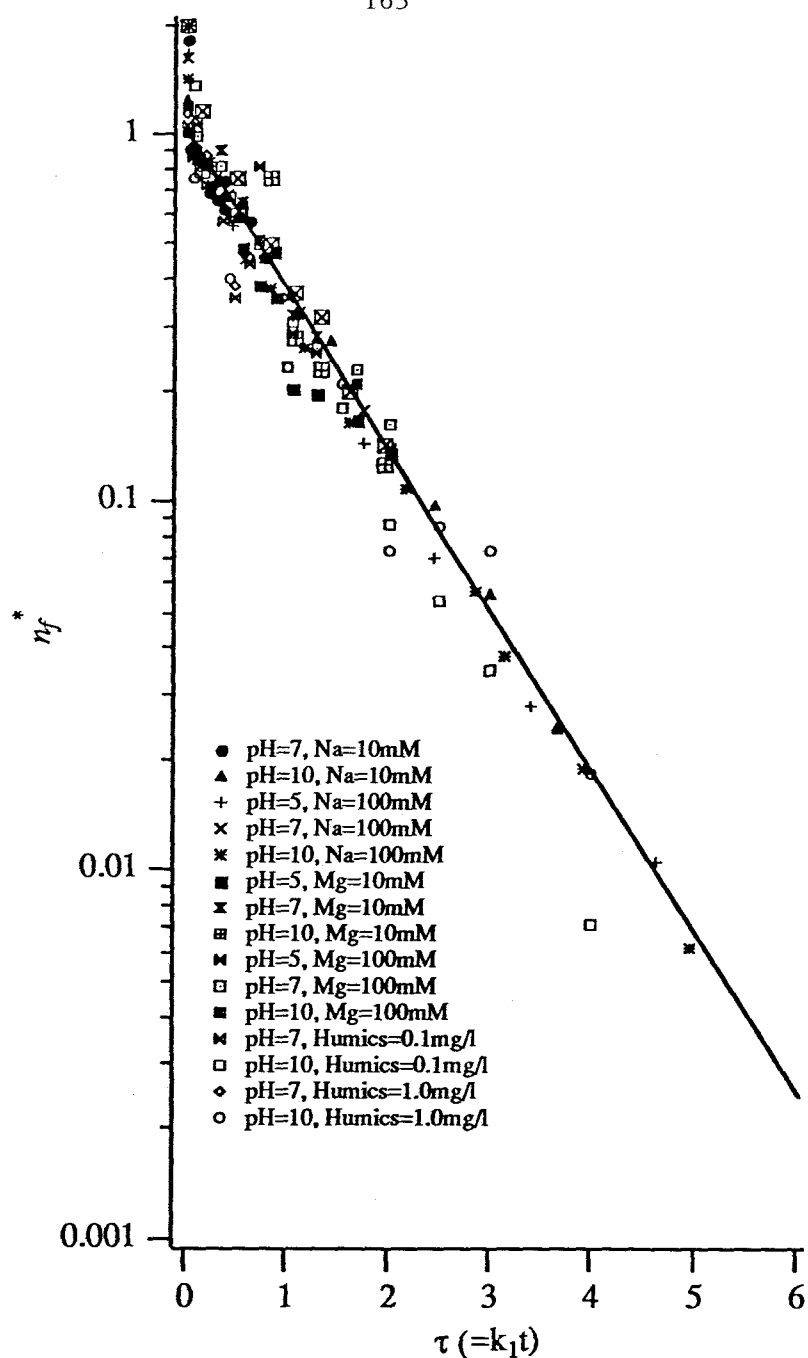


Figure 6.5. Normalized PFU data from batch experiments conducted without sand.

Data were normalized using the initial concentrations listed in Table 6.5. k_1 values are also listed in the table. The line represents the prediction for pure inactivation. The initial data above $n_f^* = 1$ represents the first sub-population of viruses (see text).

6.4.1.4. Normalization of Inactivation Data

First-order inactivation constants and initial fluid PFU were estimated for each of the data sets in Figure 6.4 using the procedures described in the methods section. In cases where more than one sub-population of viruses were present in the inactivating suspension, parameter values were estimated for the second sub-population since it was usually the dominant population under the conditions used in these experiments. Values of n_{fo} and k_I for most of the inactivation experiments are shown in Table 6.5. Certain data sets were excluded from this analysis (pH=5, NaCl=10mM and pH=5, humic acid=0.1,1.0mg/l) since virus inactivation in these experiments proceeded too rapidly to obtain useful information about virus adsorption. Using the parameter values in Table 6.5, the inactivation data in Figure 6.4 collapsed onto a single line when plotted as non-dimensional fluid PFU (n_{fo}^*) against non-dimensional time (τ) on a semi-log graph (Figure 6.5).

6.4.2. Adsorption Experiments

The decline in fluid PFU observed in the sand-containing experiments can be attributed to two factors: pure inactivation (i.e. inactivation that is not influenced by the presence of sand) and sand effects. Since both virus inactivation and adsorption to surfaces can be highly pH and electrolyte dependent, separating these two processes is difficult when the data are compared as is shown in Figures 6.1-6.3. As an alternative approach, the PFU data from sand-containing experiments was non-dimensionalized using the

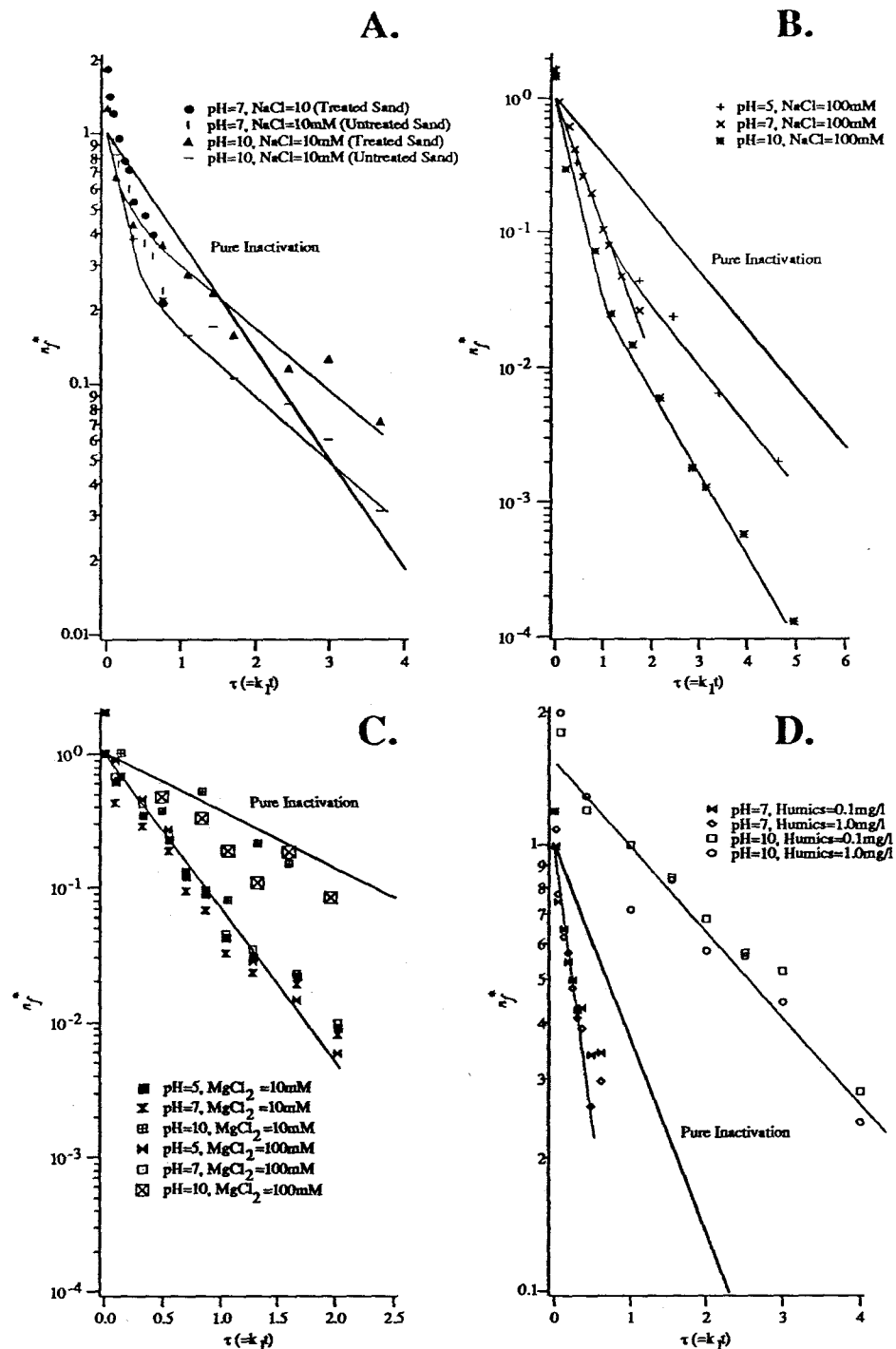


Figure 6.6. Normalized PFU data from batch experiments conducted with sand. Data were normalized using the initial concentrations listed in Table 6.5. First-order inactivation rates (k_1) used to develop nondimensional times are also listed in the table. The pure inactivation line is labelled for comparison to the Sand+ data. The different graphs correspond to different electrolyte conditions: (A) NaCl=10mM, (B) NaCl=100mM, (C) MgCl₂=10, 100mM, (D) Humic acid=0.1, 1.0mg/l.

parameters given in Table 6.5 and plotted semi-logarithmically in Figures 6.6 and 6.8. As demonstrated in the last section, when PFU data is plotted in this way, PFU decline due solely to pure inactivation will fall along a single line. Thus, the effects of sand on phage adsorption and stability can be determined for a range of electrolyte and pH conditions, irrespective of the intrinsic stability of the phage under these different solution conditions. The data shown in Figures 6.6 and 6.8 are discussed below.

6.4.2.1. NaCl at 10mM

Phage interaction with sand at NaCl=10mM appeared to be pH dependent. At pH=7, phage viability declined slightly faster than predicted based on pure inactivation. The rate of PFU decline was not significantly different when either untreated or treated sand was used. Phage viability in the pH 10 buffer declined slower in the presence of treated sand than in the sand-free experiments, suggesting that under these specific conditions the sand acts to stabilize the phage. In principle, this phage stabilization may result from two possible processes. Fluid-borne phage may be stabilized by the presence of chemical species desorbed from the surface of the sand and/or surface-adsorbed phage may be protected from inactivation by virtue of the adsorption process. It is not possible to discriminate between these two mechanisms for phage stabilization based on the data shown in Figure 6.6. At pH 10, there is a relatively significant difference in the temporal behavior of PFU data depending on whether the treated or untreated sand was used.

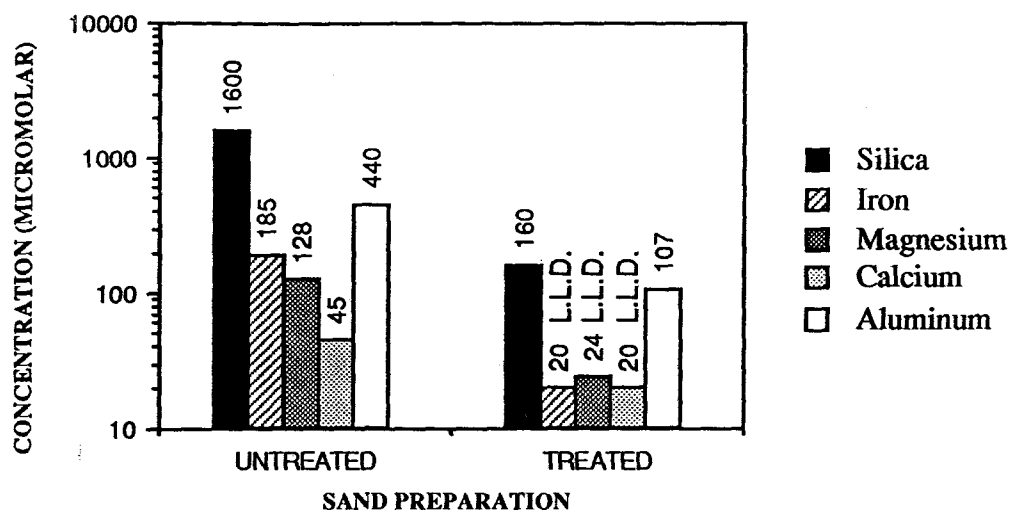


Figure 6.7. Elements released from the sand after exposure to the pH10 buffer. 25g of untreated sand (in one experiment) and sand treated for the removal of oxide coatings (in another experiment) were suspended in pH10 buffer and incubated at room temperature for 12 hours. After the incubation period, the fluid was analyzed for the elements shown above using a PES (see text). L.L.D.= Below the Lower Limit of Detection.

Like the treated sand, the untreated sand also appeared to increase phage stability, but the overall levels of PFU in the presence of untreated sand were lower.

To determine if this effect was due to the release of compounds from the sand surface, pH10 buffer with NaCl=10mM was exposed to treated and untreated sand. After a 12 hour exposure, the fluid fraction was isolated and analyzed for elemental content using a plasma emission spectrometer (PES) (Figure 6.7). Fluid exposed to the untreated sand had relatively high (100-

1000 μ M) concentrations of silica, iron, magnesium and aluminum. The concentrations of elements in the fluid exposed to the treated sand were approximately one log unit lower. However, even in this case the concentration of silica and aluminum were relatively high (>100 μ M). These results strongly suggest that virus stabilization in the presence of sand may be a consequence of metal equilibria that are established between the sand and suspending fluid.

6.4.2.2. NaCl at 100mM

At this electrolyte concentration, the presence of sand accelerated the decline in fluid PFU over that expected based on pure inactivation (Figure 6.6B). This accelerated decline was pH dependent, with an increasingly rapid loss of PFU for increasing values of pH. It is likely that this accelerated decline is due to virus adsorption (see Chapter 5), a trend of increasing adsorption with increasing pH is counter to that expected based on electrostatic arguments. Specifically, an increase in pH should increase the electrostatic repulsion between the virus and sand surfaces, resulting in a net decrease in the levels of adsorption (Gerba, 1984). The fact that the observed trend was opposite to this prediction may suggest that some other type of process (e.g. hydrophobic interaction) is responsible for virus adsorption under these conditions.

6.4.2.3. MgCl₂ at 10 & 100mM

Virus interactions with sand under these electrolyte conditions appeared to depend only on pH and not on the concentration of MgCl₂ used (Figure 6.6C). The presence of sand caused fluid PFU

at pH values of 5 and 7 to decline at a significantly faster rate than that observed in the sand-free experiments. The rate of this decline did not depend on the concentration of MgCl_2 used (10 or 100mM) or pH (5 or 7). PFU data from batch experiments conducted at pH 10 appeared to decline at a rate equal to that expected on the basis of pure inactivation. If adsorption is responsible for the accelerated decline in PFU observed at the lower pH values, then the observed trends are again difficult to reconcile with simple electrostatic models of adsorption. Although adsorption appears to decrease when the pH is increased to 10 (predicted), the amount of adsorption at the lower pH values does not appear to be significantly influenced by the electrolyte strength (not predicted).

6.4.2.4. Humic Acid at 0.1 & 1.0 mg/l

In the case where humic acids were used as the electrolyte, the effect of the sand on PFU decline was found to be strongly influenced by pH and not by the concentration of humic acid. At pH 10, the sand acted to strongly stabilize the viruses with respect to the inactivation rate observed in the sand-free batch experiments. However, when the pH7 buffer was used the viruses did not seem to be stabilized. Instead, PFU estimates declined more rapidly in the presence of the sand than they did in its absence. Interpreting these results is quite difficult since a number of different processes may be occurring. On the basis of the inactivation data presented in Figure 6.4C, it appears that humic acids themselves can actually destabilize phage λ under certain conditions. Since it is known that humic acids

can also adsorb to surfaces (Stumm and Morgan, 1981), the effect of sand in these experiments may be as an adsorptive surface for the viruses, as a stabilizer of the viruses, as an adsorptive surface removing the humic acids from solution, or some combination thereof. The fact that there is no observed difference in the response of virus/sand interactions to the two different concentrations of humic acids argues against surface adsorption of these compounds, since not 100% of the humic acids would be expected to adsorb. Without further experimentation, it is not possible to determine what factor, or combination of factors, are responsible for the observed results.

6.4.2.5. Comparison of Sand Data

Figure 6.8 is a composite plot of all the non-dimensionalized PFU data from the sand-containing experiments. Based on this figure, the effect of sand on phage stability and adsorption can be grouped into three categories discussed below.

(i) Strongly stabilizing. When the buffer contains humic acids at high pH (10), the sand strongly stabilizes the viruses with respect to inactivation.

(ii) Weakly stabilizing. When the buffer is at pH 10 and contains either NaCl (10mM) or MgCl₂ (10mM or 100mM), the phage are weakly stabilized in the presence of both treated and untreated sand.

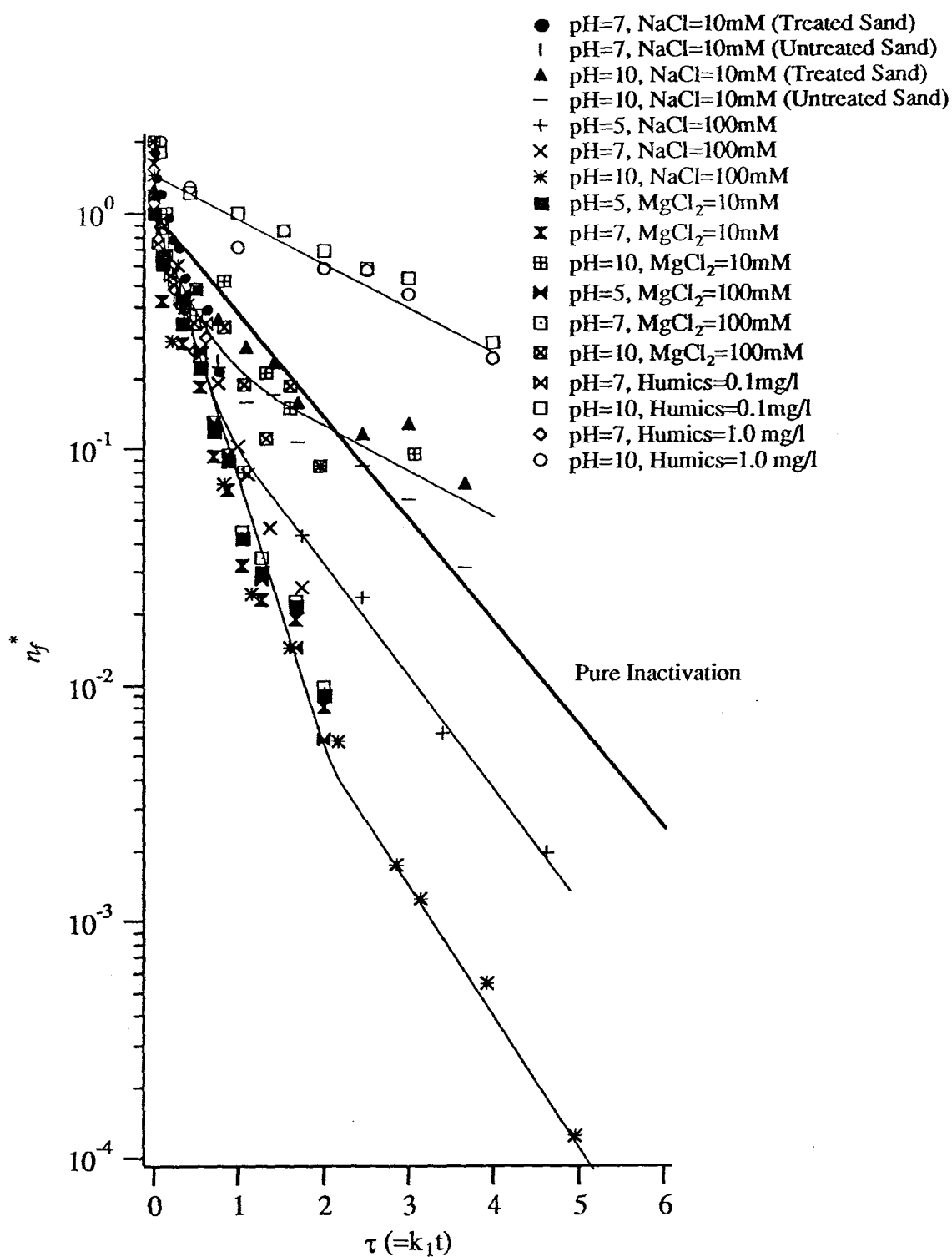


Figure 6.8. Comparison of all normalized PFU data from batch experiments conducted with sand.

(iii) Adsorbing. When the buffer is at low to intermediate pH values (5 or 7) and contains either MgCl_2 (10 or 100mM) or NaCl (10 or 100mM), the loss in fluid PFU is greater than can be explained by inactivation in the absence of sand. The most likely explanation for these data is that the sand is acting as an adsorbing surface which acts to remove PFU from the fluid phase. Strong adsorption was also observed with NaCl=100mM at pH 10.

6.5. Discussion

The above results demonstrate that virus/sand interactions can be quite varied, depending on the electrolyte composition and pH of the suspending fluid. In general, phage either did not adsorb or adsorbed only weakly in the pH10 buffer, irrespective of the electrolyte used or its concentration. The one exception to this rule was the pH10 buffer containing 100mM NaCl. In this last case, the loss of fluid PFU was considerably accelerated in the presence of sand, suggesting that virus adsorption may have been occurring. The pH10 buffers appeared to weakly stabilize the phage (compared to companion experiments in which no sand was added). PES analysis of the buffer after exposure to sand indicated that the fluid contained relatively high concentrations of several elements that might have been responsible for the observed stabilization.

PFU declines in the presence of sand at lower pH values (5 and 7) were significantly faster than can be explained by pure inactivation alone. One possible explanation for these data is that the phage inactivate faster in the presence of sand. However, this seems

unlikely since in the one case where this possibility was examined in detail (pH=7 and $\text{MgCl}_2=10\text{mM}$, see Chapter 5), surface accelerated inactivation could not be demonstrated. The most likely explanation for these observations is that the sand surface adsorbed viruses from solution. If this is the case, the adsorption process appeared to be irreversible for most of the electrolyte conditions tested, since data from the sand-containing experiments consistently diverged from the pure inactivation line. The exceptions to this rule were data from pH5 and 10 buffers in which NaCl was the electrolyte (100mM). In these last two cases, the decline in PFU eventually paralleled the pure inactivation line, possibly indicating a state of quasi-equilibrium adsorption (QEA). However, as detailed in Chapter 4, such observations should not be taken as definitive evidence of QEA since other adsorption mechanisms can be envisioned (e.g. different sub-populations of viruses which have different affinities for the sand surface).

Humic acids strongly destabilized the phage at low and high pH. This effect was reduced at high pH if sand was added. Since virus adsorption appeared weak at this pH (Figure 6.6D), the effect of the sand may be to act as a surface for the adsorption of humic acids. If a sufficient quantity of humics are removed from solution by adsorption to the sand surface, inactivation of fluid-borne viruses could be reduced. However, as discussed earlier, this interpretation is difficult to reconcile with the fact that varying the concentration of

humic acids by a full order of magnitude had virtually no effect on the resulting PFU data.

Perhaps the most significant contribution of this work is that it demonstrates the importance of conducting these types of experiments over relatively long time scales. For example, in most of the experiments conducted at pH 10 using NaCl and MgCl₂ as the buffer, addition of sand resulted in a net stabilization of the phage particles. As is shown in Figure 6.7, this stabilization was not evident until a non-dimensional time of approximately 3. Depending on the specific experiment, this non-dimensional time corresponds to between 3-6 days of incubation time, or a full order of magnitude longer than typical incubation times (see Table 5.1).

6.6. Conclusions

Both the pH and electrolyte composition of the suspending fluid exert strong influences on the rate at which viruses inactivate and the nature of virus/surface interactions. Although virus inactivation rates varied by a full order of magnitude, all of the data collapsed onto a single line by plotting them non-dimensionally on a semi-log graph. By non-dimensionalizing PFU data from sand-containing experiments and plotting it in the same way, virus/sand interactions were compared for widely varying conditions of pH and electrolyte composition. Results indicate that the effect of sand on virus viability in batch systems can be grouped into three categories: strongly stabilizing, weakly stabilizing, or adsorbing. The time scale over which these processes occur is relatively long (days), suggesting that

data from batch experiments which are conducted over relatively short time scales should be interpreted with caution. These results are important because they validate the proposed approach for studying virus/surface interactions, and they suggest that even in a relatively idealized system, significant changes in the dominant virus/surface interactions can result from relatively small changes in the chemistry of the system.

7. Conclusions and Future Research

7.1 Conclusions

This research has made significant progress in developing new methodologies for detecting viruses and for studying their adsorption to surfaces. The following conclusions are supported by this work.

(i) DNA/DNA Hybridization assays of filtered bacteriophage DNA can be used to obtain quantitative estimates of the concentration of DNA present in fluid samples, provided the concentration of MgSO_4 (and possibly other divalent salts) is the same in all of the samples, and the possibility of signal variations across a given membrane is considered.

(ii) Hybridization signals depend strongly on the concentrations and relative ratios of NaOH, EDTA, and MgSO_4 . In addition, the following factors were also found to influence hybridization intensities: the presence of precipitate in the samples, the presence of even small quantities (1%) SDS, and the buffer used in the pre-filtration treatment of the sample. Hybridization intensities were found to depend weakly (or not at all) on the concentration of NaCl in the sample, and the length of time samples were heated prior to filtration.

(iii) A new hybridization assay has been developed which discriminates between soluble and virus-encapsulated nucleic acids.

This assay was used to monitor the concentration and state of bacteriophage λ DNA during an inactivation experiment. Measurements of encapsulated DNA declined in parallel with estimates of phage viability, indicating that the assay can be used to obtain upper-limit estimates of infective bacteriophage. Transmission electron microscope observations confirmed that bacteriophage inactivation in this system occurred by head rupture and nucleic acid release.

(iv) A kinetic theory for virus adsorption and inactivation in batch experiments was developed. Four classes of virus/surface interactions can be identified, based on comparisons between PFU decline in the presence and absence of added solids. This theory suggests a new experimental approach for conducting batch experiments which allows virus adsorption to be investigated over relatively long time scales.

(v) Experiments were performed to elucidate the mechanisms involved in virus adsorption to natural surfaces over the time scale of days using bacteriophage lambda and Ottawa sand as a model system. Results indicate that Ottawa sand has significant adsorptive capacity for bacteriophage lambda when the adsorption is allowed to occur over the time scale of days. Surface adsorbed viruses did not desorb when diluted into clean buffer, suggesting that the adsorption of lambda onto the sand surface was at least partially irreversible. Quasi-equilibrium adsorption models could not be reconciled with both adsorption and elution data, and it is not presently clear what

mechanism is responsible for lambda adsorption under these conditions. Several alternative mechanisms are proposed, but no direct evidence for any of these models is presented in this report. These results have important implications both for the ecology of natural virus populations and the dispersal of viruses in the environment.

(vi) A series of batch experiments were performed using a range of pH values (5-10) and three different types of electrolytes (NaCl, MgCl₂, and humic acids). Fluid samples were collected from sand-containing and sand-free experiments over the course of 5-6 days and analyzed for PFU. When these data were plotted on semi-log graphs as normalized concentration against non-dimensional time, the data from sand-free experiments fell along a single line, while data from sand-containing experiments fell into three distinct categories. In the presence of humic acids and at pH=10, the sand strongly stabilized the phage. The sand stabilized the phage only weakly when NaCl and MgCl₂ were the electrolytes at pH=10. At lower pH values (5 and 7), the sand appeared to adsorb the phage, as evidenced by an accelerated decline in fluid PFU. This adsorption appeared to be primarily irreversible, based on the divergence of PFU data from the sand-containing experiments and the pure inactivation line. The time scales over which many of the processes occurred in this batch system were on the order of days, suggesting that batch experiments conducted over relatively short incubation times (e.g. hours) may not reflect processes occurring in nature.

These results demonstrate the utility of a kinetic approach for investigating the effects of chemical factors on virus/surface interactions.

7.2 Implications for Future Research

The new techniques developed in this thesis may find application in a number of important areas of environmental research. One of the most important unresolved issues in microbial ecology is why bacteriophage are present in marine environments at extremely high levels. Before this issue can be addressed, it is imperative to enumerate and classify natural populations of bacteriophage. The optimization data presented in Chapter 2 can be used to construct sampling programs for hybridization assays of natural bacteriophage populations, once specific probes that can detect classes of bacteriophage are developed. The modified hybridization techniques developed in Chapter 3 could be expanded to answer a number of specific questions, including:

-What fraction of the total reservoir of viral nucleic acids in aquatic environments are associated with viable viruses?

-How diverse are the bacteriophage communities in these environments? Do the bacteriophage observed with TEM represent large numbers of closely related viruses, or large assemblages of distantly related viruses?

-What are the temporal and seasonal fluctuations in bacteriophage populations? Can these fluctuations be correlated with ecosystem biogeochemical cycling and activities?

-What is the role of bacteriophage in the exchange of genetic material between natural populations of bacteria? To what extent are natural populations of bacteria lysogenized? Are specific phage implicated in this lysogeny?

Another important potential application for the hybridization techniques presented in Chapter 3 is the detection of disease-causing viruses in the environment. Although the procedures presented in this thesis were developed for bacteriophage, in principle similar protocols could be developed for mammalian viruses.

The proposed experimental procedure for examining virus/surface interactions also has many potential applications. Long time scale adsorption studies could be conducted to answer a number of important questions, including:

-What is the role of surfaces in phage ecology? Does irreversible adsorption increase interactions between bacteriophage and bacteria by increasing effective concentrations? Or does it affect bacteriophage structure so that infection of bacteria is no longer possible?

-What is the effect of long-time scale adsorption phenomena on the mobility of disease-causing viruses in the environment? Are extant studies of mammalian virus mobility conducted over short time scales relevant to dispersal processes operating in soil and groundwater systems? What effect does adsorption have on the possibility of bacteriophage as vectors for the dispersal of recombinant DNA from genetically engineered viruses?

The research presented here should provide a foundation for future investigations into the role of viruses in the environment.

References

Anilionis, A., & Riley, M., Conservation and Variation of Nucleotide Sequences Within Related Bacterial Genomes: *E. coli* strains, *J. Bacteriol.*, *143*, 355-365, 1980.

Arber, W., Enquist, L., Hohn, B., Murray, M., & Murray, K., Experimental Methods for use with Lambda. In *Lambda II*, eds. Hendrix, R.W., Roberts, J., Stahl, F., and Weisberg, R., Cold Spring Harbor Laboratory Press, 1983.

Atlas, R.M., & Bartha, R., *Microbial Ecology: Fundamentals and Applications*, Addison-Wesley Publishing Company, Inc.: Massachusetts, 1981.

Babich, H. & Stotzky, G., Reductions in Inactivation Rates of Bacteriophage by Clay Minerals in Lake Water, *Water Res.*, *14*, 185-187, 1980.

Bales, R.C., Gerba, C.P., Grondin, G.H., & Jensen, S.L., Bacteriophage Transport in Sandy Soil and Fractured Tuff, *Appl. Environ. Microbiol.*, *55*, 2061-2067, 1989.

Bej, A.K., Steffan, R.J., DiCesare, J., Haff, L., Atlas, R.S., Detection of Coliform Bacteria in Water by Polymerase Chain Reaction (PCR) and Gene Probes, *Appl. Environ. Microbiol.*, **56**, 307-314, 1990.

Bergh, O., Borsheim, K.Y., Bratbak, G., & Heldal, M., High Abundance of Viruses Found in Aquatic Environments, *Nature*, **340**, 467-468, 1989.

Bitton, G., Adsorption of Viruses Onto Surfaces in Soil and Water, *Water Res.*, **9**, 473-484, 1974.

Bitton, G. & Mitchell, R., *Water Res.*, **8**, 227-229, 1974.

Bitton, G, Pancorbo, O, & Gifford, G.E., Factors Affecting the Adsorption of Polioviruses to Magnetite in Water and Wastewater, *Water Res.*, **10**, 978-980, 1976.

Black, C.A. *Methods of Soil Analysis*, American Society of Agronomy: Madison, Wis., 1965.

Bolt, G.H., & Bruggenwert, M.G.M. *Soil Chemistry A. Basic Elements*, Chapter 1, Elsevier: New York, 1978.

Borsheim, K.Y., Bratbak, G., and Heldal, M., Enumeration and Biomass Estimation of Planktonic Bacteria and Viruses by

Transmission Electron Microscopy, *Appl. Environ. Microbiol.*, **56**, 352-356, 1990.

Breindl, M., The Structure of Heated Poliovirus Particles, *J. Gen. Virol.*, **11**, 147-156, 1971.

Brock, T.D. and Madigan, M.T., *Biology of Microorganisms*, Prentice Hall:New Jersey, 1988.

Carlson, G.F., Woodward, F.E., Wentworth, D.K., & Sproul, O.J., Virus Inactivation on Clay Particles in Natural Waters, *J. Water Poll. Control Fed.*, R89-R106, 1968.

Cookson, J.T., Kinetics and Mechanisms of Adsorption of E.Coli bacteriophage T4 to Activated Carbon, Ph.D. dissertation, Caltech, Pasadena, CA., 1965.

Cookson, J.T., & North, W.J., Adsorption of Viruses on Activated Carbon, Equilibria and Kinetics of the Attachment of *E. coli* Bacteriophage T4 on Activated Carbon, *Environ. Sci. & Tech.*, **1**, 46-52, 1967.

Dabros, T. & Adamczyk, Z., Noninertial Particle Transfer to the Rotating Disk Under an External Force Field (Laminar Flow), *Chem. Eng. Sci.*, **34**, 1041-1049, 1978.

De Leon, R. & Gerba, C.P. Detection of Rotaviruses in Water by Gene Probes, *Wat. Sci. Tech.*, **24**, 281-284, 1991.

Dizar, H., Nasser, A., and Lopex, J.M., Penetration of Different Human Pathogenic Viruses into Sand Columns Percolated with Distilled Water, Groundwater, or Wastewater, *Appl. Environ. Microbiol.*, **47**, 409-415, 1984.

Drewry, W.A., & Eliassen, R., Virus Movement in Groundwater, *J. Water Poll. Control Fed.*, **40**, R257-R271, 1968.

Duboise, S.M., Moore, B.E., and Sagik, B.P., Poliovirus Survival and Movement in a Sandy Forest Soil, *Appl. Environ. Microbiol.*, **31**, 536-543, 1976.

Dubrou, S., Kopecka, J., Lopez Pila, J. M., Marechal, J., & Prevot, J. Detection of Hepatitis A Virus and Other Enteroviruses in Wastewater and Surface Water Samples by Gene Probe Assay, *Wat. Sci. Tech.*, **24**, 267-272, 1991.

Elimelech, M., Effect of Particle-Size on Collision Efficiency in the Deposition of Brownian Particles with DElectrostatic Energy Barriers, *Langmuir*, **6**, 1153-1163, 1990.

Elimelech, M. & O'Melia, C.R., Kinetics of Deposition of Colloidal Particles in Porous Media, *Environ. Sci. & Tech.*, **24**, 1528-1541, 1990.

Farrah, S.R., Chemical Factors Influencing Adsorption of Bacteriophage MS2 to Membrane Filters, *Appl. Environ. Microbiol.*, **43**, 659-663, 1982.

Fitzpatrick, J.A., & Spielman, L.A., Filtration of Aqueous Latex Suspensions Through Beds of glass Spheres, *J. Colloid and Interface Science*, **43**, 350-369, 1973.

Fraenkel-Conrat, H., *The Viruses, Catalogue, Characterization, and Classification*, p. 209, Plenum Press:New York, 1985

Gebhard, K., Influence of Assay Conditions on Infectivity of Heated Poliovirus, *Virology*, **12**, 601-603, 1960.

Gerba, C.P., Applied and Theoretical Aspects of Virus Adsorption to Surfaces, in *Adv. in Appl. Microbiol.*, v30, pp. 133-168, Academic Press, Inc., 1984.

Gerba, C.P. & Bitton, G., Microbial Pollutants: Their Survival and Transport Pattern to Groundwater, in *Groundwater Pollution Microbiology*, p. 83, John Wiley & Sons, New York, 1984.

Gerba, C.P., Farrah, S.R., Goyal, S.M., Wallis, C.P., & Melnick, J.L., Concentration of Enteroviruses from Large Volumes of Tap Water, Treated Sewage and Water, *Appl. Environ. Microbiol.*, 35, 540-548, 1978.

Gerba, C.P., Goyal, S.M., Cech, I., & Bogdan, G.F., Quantitative Assessment of the Adsorptive Behavior of Viruses to Soil, *Environ. Sci. & Tech.*, 15, 940-944, 1981.

Gerba, C.P. & Lance, J.C., Poliovirus Removal from Sewage Effluent by Soil Filtration, *Appl. Environ. Microbiol.*, 36, 247-251, 1978.

Gerba, C.P. and Schaiberger, G.E., Effect of particulates on Virus Survival in Sea Water, *J. Wat. Poll. Control Fed.*, 47, 93-103, 1975.

Gerba, C.P., Sobsey, M.D., Wallis, C., & Melnick, J.L., Adsorption of Poliovirus onto Activated Carbon in Wastewater, *Environ. Sci. & Tech.*, 9, 727-731, 1975.

Gerba, C.P., Wallis, C., & Melnick, J.L., Fate of Wastewater Bacteria and Viruses in Soil, *J. of the Irrig. & Drain. Div.*, **101**, 157-174, 1975.

Goyal, S.M., & Gerba, C.P., Comparative Adsorption of Human Enteroviruses, Simian Rotaviruses and Selected Bacteriophage to Soils, *Appl. Environ. Microbiol.*, 38, 241-247, 1979.

Hejkal, T.W., Wellings, F.M., Lewis, A.L. & LaRock, P.A., Distribution of Viruses Associated with Particles in Wastewater, *Appl. Environ. Microbiol.*, 41, 628-634, 1981.

Herbold-Paschke, K., Straub, U., Hahn, T., Teutsch, G., & Botzenhart, K., Behavior of Pathogenic Bacteria, Phages and Viruses in Groundwater During Transport and Adsorption, *Water Sci. Tech.*, 24, 301-304, 1991.

Hernandez, L., Characterization of Virus Transport Through Porous Media, Summer Under Graduate Research Fellowship (SURF) Report, Caltech, Pasadena, CA., 1989.

Hershey, A.D., & Dove, W., Introduction to Lambda in *Lambda II*, eds. Hendrix, R.W., Roberts, J., Stahl, F., and Weisberg, R., Cold Spring Harbor Laboratory Press, p. 8, 1983.

Hill, G.H. Jr., An Introduction to Chemical Engineering Kinetics and Reactor Design, p. 3, John Wiley & Sons, New York, 1977.

Hurst, C.J., Gerba, C.P., & Cech, I., Effects of Environmental Variables and Soil Characteristics on Virus Survival in Soil, *Appl. Environ. Microbiol.*, 40, 1067-1079, 1980.

Hurst, C.J., Schaub, S.A., Sobsey, M.D., Farrah, S.R., Gerba, C.P., Rose, J.B., Goyal, S.M., Larkin, E.P., Sullivan, R., Tierney, J.T., O'Brien, R.T., Safferman, R.S., Morris, & M.E., Wellings, F.M., Evaluation of Methods for Detecting Enteric Viruses in Soils, *Appl. Environ. Microbiol.*, 57, 395-401, 1991.

IAWRC Study Group, Bacteriophages as Model Viruses in Water Quality Control, *Wat. Res.*, 25, 529-545, 1991.

Israelachvili, J.N., *Intermolecular and Surface Forces*, Academic Press:Wisconsin, 1985.

Jaques, R.P. The Potential of Pathogens for Pest Control, *Agriculture, Ecosystems and the Environment*, 10, 101-126, 1983.

Kallay, N., Barouch, E., & Matijevic, E., Diffusional Detachment of Colloidal Particles from Solid/Solution Interfaces, *Adv. in Colloid & Interface Sci.*, 27, 1-42, 1987.

Katsura, I., Structure and Function of the Major Tail Protein of Bacteriophage λ , *J. Mol. Biol.*, 146, 493-512, 1981.

Katsura, I. and Kobayashi, H., Structure and Inherent Properties of the Bacteriophage λ Head Shell, VII. Molecular Design of the Form-determining Major Capsid Protein, *J. Mol. Biol.*, **213**, 503-511, 1990.

Keswick, B.H., Chapter 3 in *Groundwater Pollution Microbiology*", eds. Bitton, G. & Gerba, C.P., John Wiley & Sons:New York, 1984.

Keswick, B.H. & Gerba, C.P., Viruses in Groundwater, *Environ. Sci. & Tech.*, **14**, 1290-1300, 1980.

Ketratanakul, A., Ohgaki, S., & Yano, K., Comparative Study on Adsorption Mechanisms of RNA-F-Specific Coliphages and Polioviruses in Activated Sludge Process, *Water Sci. Tech.*, **24**, 407-412, 1991.

Kokjohn, T.A., Transduction: Mechanism and Potential for Gene Transfer in the Environment, in *Gene Transfer in the Environment*, Levy, S.B. & Miller, R.V., eds., McGraw Hill, 1989.

LaBelle, R.L., & Gerba, C.P., Influence of pH, Salinity, and Organic Matter on the Adsorption of Enteric Viruses to Estuarine Sediment, *Appl. Environ. Microbiol.*, **38**, 93-101, 1979.

- Lance, J.C., Gerba, C.P., and Melnick, J.L., Virus Movement in Soil columns Flooded with Secondary Sewage Effluent, *Appl. Environ. Microbiol.*, **32**, 520-526, 1976.
- Landry, E.F., Vaughn, J.M., Thomas, M.Z., and Beckwith, C.A., Adsorption of Enteroviruses to Soil Cores and their Subsequent Elution by Artificial Rainwater, *Appl. Environ. Microbiol.*, **38**, 680-687.
- Liew, Pei-Fung & Gerba, C.P., Thermostabilization of Enteroviruses by Estuarine Sediment, *Appl. Environ. Microbiol.*, **40**, 305-308, 1980.
- Lin, E.C., Goldstein, R., and Syvang, M., *Bacteria, Plasmids and Phages: An Introduction to Molecular Biology*, 1984.
- Lo, S.H., & Sproul, D.J., Poliovirus Adsorption from Water onto Silicate Minerals, *Water Res.*, **11**, 653-658, 1977.
- Margolin, A.B., Hewlett, M.J., & Gerba, C.P., The Application of a Poliovirus cDNA Probe for the Detection of Enteroviruses in Water, *Wat. Sci. Tech.* **24**, 277-280, 1991.
- Marsily, G. de., *Quantitative Hydrogeology, Groundwater Hydrology for Engineers*, p. 256, Academic Press, Inc., Orlando, 1986.

Matthess, G. & Pekdeger, A.S.A.F., Concepts of a Survival and Transport Model of Pathogenic Bacteria and Viruses in Groundwater, *The Science of the Total Environ.*, **21**, 1981.

Matthess, G., Pekdeger, A., & Schroeter, J., Persistence and Transport of Bacteria and Viruses in Groundwater - A Conceptual Evaluation, *J. Cont. Hydrol.*, **2**, 171-188, 1988.

McDowell-Boyer L.M., Hunt, J.R., & Sitar, N., *Water Resources Research*, **22**, 1901, 1986.

Miller, H. in *Guide to Molecular Cloning Techniques*, eds. Berger, S. L. & Kimmel, A.R. , Academic Press, Inc.: San Diego, California, p. 161, 1987.

Mix, T.W., *Dev. Ind. Microbiol.*, **15**, 136-142.

Moore, R.S., Taylor, D.H., Reddy, M.M., & Sturman, L.S., Adsorption of Reovirus by Minerals and Soils, *Appl. Environ. Microbiol.*, **44**, 852-859, 1982.

Moore, R.S., Taylor, D.H., Sturman , L.S., Reddy, M.M., & Fuhs, G.W., Poliovirus Adsorption by 34 Minerals and Soils, *Appl. Environ. Microbiol.*, **42**, 963-975, 1981.

Morel, F., *Principles of Aquatic Chemistry*, J. Wiley, New York, 1983.

Murray, J.P., & Parks, G.A., Poliovirus Adsorption on Oxide Surfaces: Correspondence with the DLVO-Lifshitz Theory of Colloid Stability, in *Particulates in Water*, Kavanaugh, M.C., & Leckie, J.O., eds., Adv. in Chem. Ser. 189, pp. 97-133, American Chemical Society, Washington, D.C., 1980.

Norde, W., Adsorption of Proteins from Solution at the Solid-Liquid Interface, *Adv. in Colloid & Interface Sci.*, 25, 267-340, 1986.

Norde W., & Lyklema, J., The Adsorption of Human Plasma Albumin and Bovine Pancrease Ribonuclease at Negatively Charged Polystyrene Surfaces: V. Microcalorimetry, *J. Colloid and Interface Science*, 66, 295-300, 1978.

Ogunseitan, O. A., Sayler, G.S., Miller, R.V., Dynamic Interactions of *Pseudomonas aeruginosa* and bacteriophages in Lake Water, *FEMS Microb. Ecol.*, in press.

Olson, B.H., Tracking and Using Genes in the Environment, *Environ. Sci. & Tech.* 25, 604-611, 1991.

Pollard, E.C. & Solosko, W., The Thermal Inactivation of T4 and λ Bacteriophage, *Biophysical Journal*, **11**, 66-74, 1971.

Press, W.H., Flannery, B.P., Teukolsky, S.A., & Vetterling, W.T., *Numerical Recipes*, p. 550, Cambridge University Press, Cambridge, 1986.

Preston, D.R., Chaudhry, G.R., & Farrah, S.R. *Can. J. Microbiol.* **36**, 664-669, 1990.

Preston, D.R., & Farrah, S.R., Activation Thermodynamic of Virus Adsorption to Solids, *Appl. Environ. Microbiol.*, **54**, 2650-2654, 1988.

Proctor, L.M., & Fuhrman, J.A., Viral Mortality of Marine Bacteria and Cyanobacteria, *Nature*, **343**, 60-62, 1989.

Richardson, K.J., Margolin, A.B., & Gerba, C.P. A Novel Method for Liberating Viral Nucleic Acid for Assay of Water Samples with cDNA Probes, *J. Virol. Methods*. **22**, 13-21, 1988.

Riley, M., & Anilionis, A., Conservation and Variation of Nucleotide Sequences within Related Bacterial Genomes: Enterobacteria, *J. Bacteriol.*, **143**, 365-376, 1980.

Romanowski, G., Lorenz, M.G. & Wackernagel, W., Adsorption of Plasmid DNA to Mineral Surfaces and Protection against DNase I, *Appl. Environ. Microbiol.*, **57**, 1057-1061, 1991.

Sabatino, C.M. & Maier, S., Differential Inactivation of Three Bacteriophage by Acid and Alkaline pH used in the Membrane Adsorption-elution Method of Virus Recovery, *Can. J. Microbiol.*, **26**, 1403-1407, 1980.

Sambrook, J., Fritsch, E.F., & Maniatis, T., *Molecular Cloning*, Cold Spring Harbor Laboratory Press, pp.260-276, 1989.

Saye, D.J. and Miller, R.V., The Aquatic Environment: Consideration of Horizontal Gene Transmission in a Diversified Habitat, in *Gene Transfer in the Environment*, Levy, S.B. & Miller, R.V., eds., McGraw Hill, 1989.

Sayler, G.S. & Layton, A.C., Environmental Application of Nucleic Acid Hybridization, *Annu. Rev. Microbiol.*, **44**:625-648, 1990.

Shields, P.A. & Farrah, S.R., Influence of Salts on Electrostatic Interactions Between Poliovirus and Membrane Filters, *Appl. Environ. Microbiol.*, **45**, 526-531, 1982.

Shields , P.A., Ling, T.F., Tjatha, V., Shah, D.O., and Farrah, S.R.,
Comparison of Positively Charged Membrane Filters and their Use in
Concentrating Bacteriophages in Water, *Water Res.*, **20**, 145-151,
1986.

Smith, E.M., Gerba, C.P. & Melnick, J.L., Role of Sediment in the
Persistence of Enteroviruses in the Esturine Environment, *Appl.*
Environ. Microb., **35**, 1978.

Sobsey, M.D., Dean, C.H., Knuckles, M.E., & Wagner, R.A.,
Interactions and Survival of Enteric Viruses in Soil Materials, *Appl.*
Environ. Microbiol., **40**, 92-101, 1980.

Sobsey M.D. & Jones, B.L., *Appl. Environ. Microbiol.*, **37**, 588-595,
1979.

Stagg, C.H., Wallis, C., & Ward, C.H., Inactivation of Clay
Associated Bacteriophage MS-2 by Chlorine, *Appl. Environ.*
Microbiol., **33**, 385-391, 1977.

Steffan, R.J., & Atlas, R.M., DNA Amplification to Enhance
Detection of Genetically Engineered Bacteria in Environmental
Samples, *Appl. Environ. Microbiol.*, **54**, 2185-2191, 1988.

Sternberg, N. & Weisberg, R. Packaging of Coliphage Lambda DNA II. The Role of the Gene D Protein, *J. Mol. Biol.*, **117**, 717-731, 1977.

Stotzky, G., Gene Transfer Among Bacteria in the Soil, in *Gene Transfer in the Environment*, McGraw Hill, 1989.

Stumm, W. & Morgan, J.J., *An Introduction to Aquatic Chemistry*, Chapter 10, John Wiley and Sons:New York, 1981.

Taylor, D.H., Bellamy, A.R., & Wilson, A.T., Interactions of Bacteriophage R17 and Reovirus Type III with the Clay Mineral Allophane, *Water Res.*, **14**, 339-346, 1980.

Taylor, D.H., Moore, R.S., & Sturman, L.S., Influence of pH and Electrolyte Composition on Adsorption of Poliovirus by Soils and Minerals, *Appl. Environ. Microbiol.*, **42**, 976-984, 1981.

Teutsch, G., Herbold-Paschke, K., Tougianidou, D., Hahn, T., & Botzenhart, Transport of Microorganisms in the Underground - Processes, Experiments and Simulation Models, *Water Sci. & Tech.*, **24**, 309-314, 1991.

Todd, D.K., *Groundwater Hydrology*, 2nd Edition., p. 82., John Wiley and Sons: New York, 1980.

- Touganidou, D. & Botzenhart, K., Detection of Poliovirus in Water by Direct Isolation of the RNA and Hybridization with Gene Probes, *Wat. Sci. Tech.* **24**, 273-276, 1991.
- U.S. Environmental Protection Agency, Office of Water, EPA 440/4-87-008, Washington, November, 1987.
- Vilker, V.L., & Burge, W.D., Adsorption Mass Transfer Model for Virus Transport in Soils, *Water Res.*, **14**, 783-790, 1980.
- Vilker, V.L., Meronek, G.C., & Butler, P.C., Interactions of Poliovirus with Montmorillonite Clay in Phosphate-Buffered Saline, *Environ. Sci. & Tech.*, **17**, 631-634, 1983.
- Ward, R.L., Mechanism of Poliovirus Inactivation by Ammonia, *J. of Virology* **26**, 299-305, 1977.
- Weber, W.J., McGinley, P.M., & Katz, L.E., Sorption Phenomenon in Subsurface Systems: Concepts, Models and Effects on Contaminant Fate and Transport, *Wat. Res.*, **25**, 499-528, 1991.
- Yamagishi, H., Eguchi, G., Matsuo, H., & Ozeki, H., Visualization of Thermal Inactivation in Phages Lambda and $\phi 80$, *Virology*, **53**, 277-282, 1973.

Yamagishi, H. & Ozeki, H., Comparative Study of Thermal Inactivation of Phage ϕ 80 and Lambda, *Virology*, **48**, 316-322, 1972.

Yates, M.V., The Use of Models for Creating Variances from Mandatory Disinfection of Groundwater used as a Public Water Supply, *EPA Report /600/2-90/010*, March, 1990.

Yates, M.B., Gerba, C.P. and Kelley, L.M., Virus Persistence in Groundwater, *Appl. Environ. Microbiol.*, **49**, 778-781, 1984.

Yates, M.V., Yates, S.R., Wagner, J., & Gerba, C.P., Modeling Virus Survival and Transport in the Subsurface, *J. Cont. Hydrol.*, **1**, 329-345, 1987.

Yates, M.V., Yates, S.R., Warrick, A.W., & Gerba, C.P., Use of Geostatistics to Predict Virus Decay Rates for Determination of Septic Tank Setback Distances, *Appl. Environ. Microbiol.*, **52**, 479-483, 1986.

Yeager, J.G. & O'Brien, R.T., Structural Changes Associated with Poliovirus Inactivation in Soil, *Appl. Env. Microbiol.*, **38**, 702-709, 1979.

Young, D.C., & Sharp, D.G., Poliovirus Aggregates and Their Survival in Water, *Appl. Environ. Microbiol.*, **33**, 168-177, 1977.

Zarybnicky, B., Reich, M., and Wolf, G., A Mathematical Model for the Reversible Two-step Interaction Between T5 phage and its Receptor in vitro, *FEMS Microbiological Letters*, 7, 29-33.

Zawadzki, M.E., Harel, Y. & Adamson, A.W., Irreversible Adsorption from Solution 2. Barium Dinonylnaphthalene sulfonate on Anatase, *Langmuir*, 3, 363-368, 1987.

Zeph, L.R. & Stotzky, G., Use of a Biotinylated DNA Probe to Detect Bacteria Transduced by Bacteriophage P1 in Soil, *Appl. Environ. Microbiol.*, 55, 661-665, 1989.

Appendix A

In this appendix, a closed form solution is developed for the limiting case where binding and resuspension are assumed to reach an instantaneous quasi-equilibrium. Applying the quasi-equilibrium adsorption (QEA) assumption, $\frac{d\xi_2}{d\tau} = 0$, (4.9a) can be used to solve for ξ_2^* :

$$\xi_2^* = \frac{R-1}{R}(1-\xi_1^*) + \frac{N_s \xi_3^*}{R}. \quad (\text{A1})$$

Using this expression for ξ_2^* , the first rate equation (4.6a) becomes,

$$\frac{d\xi_1^*}{d\tau} = \frac{1}{R}(1-\xi_1^* - N_s \xi_3^*). \quad (\text{A2})$$

Substituting (A1) into the third rate expression (4.9b),

$$\frac{d\xi_3^*}{d\tau} = \frac{R-1}{R} N_i (1-\xi_1^* - N_s \xi_3^*). \quad (\text{A3})$$

Taking the ratio of these last two rate expressions,

$$\frac{d\xi_1^*/d\tau}{d\xi_3^*/d\tau} = \frac{1}{(R-1)N_i}. \quad (\text{A4})$$

Integrating the above result and solving for the third extent of reaction,

$$\xi_3^* = (R-1)N_i \xi_1^*. \quad (\text{A5})$$

Substituting this expression into (A2),

$$\frac{d\xi_1^*}{d\tau} = \frac{1}{R} - \xi_1^* \frac{[1+(R-1)N_s N_i]}{R}. \quad (\text{A6})$$

This last equation is a first order linear differential equation for ξ_1^* . Applying the initial condition that $\xi_1^* = 0$ at $\tau=0$, the above equation can be integrated to yield:

$$\xi_1^* = \frac{1}{R} \left(1 - e^{-\frac{R'}{R}\tau} \right) \quad (\text{A7})$$

where $R' = [1 + (R-1)N_i N_s]$.

From the definition of n_f^* (assuming that all of the viruses present initially are in the fluid phase),

$$n_f^* = 1 - \xi_1^* - \xi_2^* \quad (\text{A8})$$

Combining equations (A1), (A5), (A7) and (A8), the following expression for fluid phase PFU is derived,

$$n_f^* = \frac{e^{-\left(\frac{R'}{R}\right)\tau}}{R}. \quad (\text{A9})$$

Appendix B

Here a closed form solution for the limiting case where virus binding occurs irreversibly on the solid surface is developed. By dividing rate expressions for ξ_1^* and ξ_6^* (4.14a and b),

$$\frac{d\xi_1^*/d\tau}{d\xi_6^*/d\tau} = \frac{1}{N_{bir}}. \quad (\text{B1})$$

Integrate this expression and solve for ξ_1^* :

$$\xi_1^* = \frac{\xi_6^*}{N_{bir}}. \quad (\text{B2})$$

Substitute this expression for ξ_1^* into (4.14b):

$$\frac{d\xi_6^*}{d\tau} = N_{bir} - \xi_6^*(1 + N_{bir}). \quad (\text{B3})$$

Integrating this differential equation using the initial conditions $\xi_6^*=0$ at $\tau=0$, the following expression emerges for ξ_6^* :

$$\xi_6^* = \frac{N_{bir}}{1 + N_{bir}} (1 - e^{-(1+N_{bir})\tau}). \quad (\text{B4})$$

Combining (B4), (B2), and (4.5a), the following expression for the fluid concentration of viruses as a function of nondimensional time (τ) is derived:

$$n_j^* = e^{-(1+N_{bir})\tau}. \quad (\text{B5})$$

Appendix C

The following is a computer listing of the FORTRAN program used to perform the numerical simulations presented in Chapter 4. The program was compiled using the Microsoft Fortran Compiler (v. 4.1) implemented on an IBM/AT personal computer.

```

$DEBUG
PROGRAM INTEGRATE
C
C -----
C  USES VARIABLE STEP R-K METHOD TO INTEGRATE SET OF 3 LINEAR
C  O.D.E.s FOR VIRUS INACTIVATION AND ADSORPTION
C
C  CREATED BY S. GRANT, 7/16/91
C  -----
C
REAL*8 NS,NB,R,NL,TSTART,TEND
COMMON /PATH/ NS,NB,R,NI
PARAMETER (NVAR=3, EPS=1.E-5, NSTEP=100)
DIMENSION VSTART(NVAR), V(NVAR), DV(NVAR), XX(200), Y(NVAR,200),
+ CA(200)
INTEGER I, K, NSTEP, TSTEP, NVAR
C
C  OPEN FILE
C
OPEN (2, FILE='A:\OUTPUT\INTEG.OUT', FORM='FORMATTED')
WRITE (2,*) 'DATA FILE GENERATED BY PROGRAM INTEGRATE'
WRITE (2,*) 'WRITTEN BY S. GRANT, 7/15/91'
C
C  GET INPUT DATA
C
PRINT *,TSTART, TEND, NI, NS, NB, & R'
READ (*,*) TSTART,TEND,NI,NS,NB,R
PRINT *,'DATA RECORDED AS FOLLOWS:'
PRINT *,'TSTART= ',TSTART,' TEND= ',TEND
PRINT *,' NI= ',NI,' NB= ',NB
PRINT *,' R= ',R,' NS= ',NS
PAUSE 'IF THIS DATA IS NOT O.K., HIT CTRL C; OTHERWISE HIT RETURN'
C
C -----
C  VARIABLE INITIALIZATION
C  -----
C
C  1. APPLY INITIAL CONDITIONS
C
DO 10 I=1,NVAR
  V(I)=0.
  Y(I,1)=0.

```

```

10 CONTINUE
C
C 3. INITIALIZE INDEPENDENT VARIABLE
C
  XX(1)=TSTART
  X=TSTART
C
C 4. TAKE A GUESS AT STEPPING INTERVAL
C
  HTRY=(TEND-TSTART)/NSTEP
C
C -----
C BEGIN R-K INTEGRATION
C -----
C
  K=1
  TSTEP=1
25  K=K+1
    CALL DERIVS(X,V,DV)
    CALL RKQC(V,DV,X,HTRY,EPS,V,H,HNEXT,DERIVS)
    XX(K)=X
    DO 30 I=1,NVAR
      Y(I,K)=V(I)
30  CONTINUE
    HTRY=HNEXT
    TSTEP=TSTEP+1
    PRINT *,TSTEP= ',TSTEP
    IF (TSTEP.GT. 190) PAUSE 'TOO MANY STEPS'
    IF (X.LT. TEND) GOTO 25
C
C -----
C CALCULATE ANSWER
C -----
C
  DO 40 I=1, TSTEP
    CA(I)=(1.-Y(1,I)-Y(2,I))
40  CONTINUE
C
C -----
C OUTPUT ANSWER
C -----
C
  WRITE (2,*) 'INPUT PARAMETERS:'
  WRITE (2,*) ' TSTART  TEND'
  WRITE (2,45) TSTART,TEND
  WRITE (2,*) ' NI    NB    R    NS'
  WRITE (2,47) NI,NB,R,NS
45  FORMAT (F7.1, 8X, F7.1)
47  FORMAT (5X, F6.3, 6X, F6.3, 5X, F10.1,5X, F10.1)
  WRITE (2,*) '-----CALCULATED CONCENTRATIONS-----'
  WRITE (2,*) ' TAO    (CA/CAO)    Ln(CA/CAO)'
  DO 50 I=1,TSTEP
    IF (CA(I).GT. 1.E-10) THEN
      X=LOG(CA(I))
    ELSE
      X=666
    ENDIF
    WRITE (2,60) XX(I),CA(I),X
50  CONTINUE
60  FORMAT (4X,F10.4,6X,F10.8,8X,F10.6)
  STOP
  END

```

```

C
C
SUBROUTINE RKQC(Y,DYDX,X,HTRY,EPS,YSICAL,HDID,HNEXT,DERIVS)
C
C DRIVER FOR VARIABLE STEP R-K METHOD
C COPIED FROM NUMERICAL RECIPES PG. 558, 1986.
C
PARAMETER (N=3,PGROW=-0.20, PSHRNK=-0.25,FCOR=1./15.,
+ ONE=1.,SAFETY=0.9,ERRCON=6.E-4)
EXTERNAL DERIVS
DIMENSION Y(N),DYDX(N),YSICAL(N),YTEMP(N),YSAV(N),DYSAV(N)
XSAV=X
DO 11 I=1,N
  YSAV(I)=Y(I)
  DYSAV(I)=DYDX(I)
11 CONTINUE
H=HTRY
1 HH=0.5*H
CALL RK4(YSAV,DYSAV,XSAV,HH,YTEMP,DERIVS)
X=XSAV+HH
CALL DERIVS(X,YTEMP,DYDX)
CALL RK4(YTEMP,DYDX,X,HH,Y,DERIVS)
X=XSAV+H
IF(X.EQ.XSAV)PAUSE 'STEP SIZE NOT SIGNIFICANT IN RKQC'
CALL RK4(YSAV,DYSAV,XSAV,H,YTEMP,DERIVS)
ERRMAX=0.
DO 12 I=1,N
  YTEMP(I)=Y(I)-YTEMP(I)
  ERRMAX=MAX(ERRMAX,ABS(YTEMP(I)/YSICAL(I)))
12 CONTINUE
ERRMAX=ERRMAX/EPS
IF (ERRMAX.GT.ONE) THEN
  H=SAFETY*H*(ERRMAX**PSHRNK)
  GOTO 1
ELSE
  HDID=H
  IF(ERRMAX.GT.ERRCON) THEN
    HNEXT=SAFETY*H*(ERRMAX**PGROW)
  ELSE
    HNEXT=4.*H
  ENDIF
ENDIF
DO 13 I=1,N
  Y(I)=Y(I)+YTEMP(I)*FCOR
13 CONTINUE
RETURN
END
C
C
SUBROUTINE RK4(Y,DYDX,X,H,YOUT,DERIVS)
C
C ADVANCES ODE SOLUTION BY H USING FOURTH ORDER R-K
C COPIED FROM NUMERICAL RECIPES, PG 553, 1986
C
PARAMETER (N=3)
DIMENSION Y(N),DYDX(N),YOUT(N),YT(N),DYT(N),DYM(N)
HH=H*0.5
H6=H/6.
XH=X+HH
DO 11 I=1,N
  YT(I)=Y(I)+HH*DYDX(I)
11 CONTINUE

```



```

CALL DERIVS (XH,YT,DYT)
DO 12 I=1,N
  YT(I)=Y(I)+HH*DYT(I)
12 CONTINUE
CALL DERIVS(XH,YT,DYM)
DO 13 I=1,N
  YT(I)=Y(I)+H*DYM(I)
  DYM(I)=DYT(I)+DYM(I)
13 CONTINUE
CALL DERIVS(X+H,YT,DYT)
DO 14 I=1,N
  YOUT(I)=Y(I)+H6*(DYDX(I)+DYT(I)+2.*DYM(I))
14 CONTINUE
RETURN
END
C
C
SUBROUTINE DERIVS(T,X,DXDT)
C
C CALCULATES THE RHS OF ODE SET, DXDT (ASSUMING CBO=0)
C
DIMENSION X(3),DXDT(3)
REAL*8 NB,NS,R,NI
COMMON /PATH/ NS,NB,R,NI
DXDT(1)=-X(1)-X(2)+1
DXDT(2)=-NB*X(1)-NB*R*X(2)/(R-1)+NB*X(3)*NS/(R-1)+NB
DXDT(3)=-NI*X(2)-NI*NS*X(3)
RETURN
END

```

Appendix D

In this appendix, the methods used to estimate the initial conditions for the elution experiment simulations are described. Initial conditions were needed for the concentration of viruses in the resuspension buffer (n_{fo}), the concentration of viruses reversibly adsorbed to the sand surface (n_{so}) and, in the case of the QEASS model, the concentration of irreversibly adsorbed viruses (n_{sirro}) at the time of resuspension.

Values of n_{fo} were estimated in two ways. (i) The amount of phage-containing fluid transferred with the sand into the elution buffer was determined. This value was then used to calculate the initial virus concentration in the elution buffer by simple dilution. (ii) Samples of the resuspension buffer were taken immediately after addition of sand, before phage adsorption or desorption could occur.

For sand that had been incubated for 4 days, estimates of n_{fo} using the two techniques were in relatively close agreement (2.3×10^5 PFU/ml from dilution calculations versus 1.7×10^5 PFU/ml from the initial sampling). The values were not close, however, for the 1 hour incubation time (1.1×10^6 and 2.8×10^5 from dilution and initial sample, respectively). After the sand is removed from the incubation buffer, some time is required before it can be drained, weighed and resuspended. During this period, the retained fluid undoubtedly became depleted in viruses, resulting in a lower initial fluid PFU

concentration than if the retained fluid had been diluted into the elutant directly. Therefore, we decided that it was best to estimate n_{fo} from the PFU in the initial sample.

Estimates of total adsorbed phage were made from (5.1). This value was then broken into a reversibly and irreversibly adsorbed fraction by running computer simulations of the (forward) adsorption experiment which were stopped at incubation times of 1 hour and 4 days.

Appendix E

The following is a computer listing of the FORTRAN program used to perform the numerical simulations of suspended, reversibly adsorbed and irreversibly adsorbed viruses described in Chapter 5. The program was compiled using the Microsoft Fortran Compiler (v. 4.1) implemented on an IBM/AT personal computer.

```

$DEBUG
PROGRAM INTEGRATE
C
C -----
C USES VARIABLE STEP R-K METHOD TO INTEGRATE SET OF 4 LINEAR
C O.D.E.s FOR VIRUS INACTIVATION AND ADSORPTION. THIS VERSION
C OUTPUTS DIMENSIONAL QUANTITIES.
C
C CREATED BY S. GRANT, 7/16/91
C MODIFIED BY S. GRANT, 8/3/91
C -----
C
REAL*8 VOL,WT,KONE,NS,XF(200),NB,R,NI,TSTART,TEND,
+ XSR(200),XSIR(200),TIME,NSIR,INR,INIR,INF
COMMON /PATH/ NS,NB,R,NI,NSIR,INF,INR,INIR,WT,VOL
PARAMETER (NVAR=4, EPS=1.E-5, NSTEP=100)
DIMENSION VSTART(NVAR), V(NVAR), DV(NVAR), XX(200), Y(NVAR,200)
INTEGER I, K, NSTEP, TSTEP, NVAR
C
C OPEN FILE
C
OPEN (2, FILE='A:\OUTPUT\NTEG.OUT', FORM='FORMATTED')
WRITE (2,*) 'DATA FILE GENERATED BY PROGRAM INTEGRATE'
WRITE (2,*) 'WRITTEN BY S. GRANT, 7/15/91'
C
C GET INPUT DATA
C
PRINT *, TSTART, TEND, NI, NS, NB, R, & NSIR'
READ (*,*) TSTART,TEND,NI,NS,NB,R,NSIR
PRINT *, 'DATA RECORDED AS FOLLOWS:'
PRINT *, 'TSTART= ',TSTART,' TEND= ',TEND
PRINT *, 'NI= ',NI,' NB= ',NB
PRINT *, 'R= ',R,' NS= ',NS,' NSIR= ',NSIR
PAUSE IF THIS DATA IS NOT O.K., HIT CTRL C; OTHERWISE HIT RETURN'
C
PRINT *, 'VOL, WT, KONE, & INITIAL NF'
READ (*,*) VOL,WT,KONE,INF
PRINT *, 'DATA RECORDED AS FOLLOWS:'
PRINT *, 'VOL= ',VOL,' WT= ',WT

```

```

PRINT *, KONE= 'KONE,' INF= 'INF'
PAUSE 'IF THIS DATA IS NOT O.K., HIT CTRL C; OTHERWISE HIT RETURN'
C
PRINT *, 'INITIAL NSR & NSIR'
READ (*,*) INR,INIR
PRINT *, 'DATA RECORDED AS FOLLOWS:'
PRINT *, 'INITIAL NSR= 'INR,' INITIAL NSIR= 'INIR
PAUSE 'IF THIS DATA IS NOT O.K., HIT CTRL C; OTHERWISE HIT RETURN'
C
-----
C VARIABLE INITIALIZATION
C -----
C
C 1. APPLY INITIAL CONDITIONS
C
DO 10 I=1,NVAR
  V(I)=0.
  Y(I,1)=0.
10 CONTINUE
C
C 3. INITIALIZE INDEPENDENT VARIABLE
C
XX(1)=TSTART
X=TSTART
C
C 4. TAKE A GUESS AT STEPPING INTERVAL
C
HTRY=(TEND-TSTART)/NSTEP
C
-----
C BEGIN R-K INTEGRATION
C -----
C
K=1
TSTEP=1
25 K=K+1
CALL DERIVS(X,V,DV)
CALL RKQC(V,DV,X,HTRY,EPS,V,H,HNEXT,DERIVS)
XX(K)=X
DO 30 I=1,NVAR
  Y(I,K)=V(I)
30 CONTINUE
HTRY=HNEXT
TSTEP=TSTEP+1
PRINT *, 'TSTEP= ',TSTEP
IF (TSTEP .GT. 190) PAUSE 'TOO MANY STEPS'
IF (X .LT. TEND) GOTO 25
C
-----
C CALCULATE ANSWER
C -----
C
DO 40 I=1, TSTEP
  XF(I)=INF-INF*(Y(1,I)+Y(2,I))
  XSR(I)=INR+VOL*INF*(Y(2,I)-Y(3,I)*NS)/WT
  XSIR(I)=INIR+VOL*INF*(Y(3,I)*(NS-1)-Y(4,I))/WT
40 CONTINUE
C
-----
C OUTPUT ANSWER
C -----
C
WRITE (2,*) 'INPUT PARAMETERS:'

```

```

WRITE (2,*) ' TSTART  TEND'
WRITE (2,45) TSTART,TEND
WRITE (2,*) ' NI  NB  R  NS'
WRITE (2,47) NI,NB,R,NS
45  FORMAT (F7.1, 8X, F7.1)
47  FORMAT (5X, F6.3, 6X, F6.3, 5X, F10.1,5X, F10.1)
WRITE (2,*) ' VOL  WT  KONE  INF'
WRITE (2,48) VOL,WT,KONE,INF
48  FORMAT (5X, F6.3, 6X, F6.3, 5X, F10.1,5X, F10.1)
WRITE (2,*) '-----CALCULATED CONCENTRATIONS-----'
WRITE (2,*) 'TIME  FL  REV ADS  IRR ADS'
DO 50 I=1, TSTEP
  TIME=XX(I)/KONE
  WRITE (2,60) TIME,XF(I),XSR(I),XSIR(I)
50  CONTINUE
60  FORMAT (2X,F10.4,2X,F11.1,4X,F11.1,4X,F11.1)
STOP
END
C
C
SUBROUTINE RKQC(Y,DYDX,X,HTRY,EPS,YSCAL,HDID,HNEXT,DERIVS)
C
C DRIVER FOR VARIABLE STEP R-K METHOD
C COPIED FROM NUMERICAL RECIPES PG. 558, 1986.
C
PARAMETER (N=4,PGROW=.20, PSHRNK=.25,FCOR=1./15.,
+ ONE=1.,SAFETY=.9,ERRCON=6.E-4)
EXTERNAL DERIVS
DIMENSION Y(N),DYDX(N),YSCAL(N),YTEMP(N),YSAV(N),DYSAV(N)
XSAV=X
DO 11 I=1,N
  YSAV(I)=Y(I)
  DYSAV(I)=DYDX(I)
11 CONTINUE
H=HTRY
1  HH=0.5*H
  CALL RK4(YSAV,DYSAV,XSAV,HH,YTEMP,DERIVS)
  X=XSAV+HH
  CALL DERIVS(X,YTEMP,DYDX)
  CALL RK4(YTEMP,DYDX,X,HH,Y,DERIVS)
  X=XSAV+H
  IF(X.EQ.XSAV)PAUSE 'STEPSIZE NOT SIGNIFICANT IN RKQC'
  CALL RK4(YSAV,DYSAV,XSAV,H,YTEMP,DERIVS)
  ERRMAX=0.
  DO 12 I=1,N
    YTEMP(I)=Y(I)-YTEMP(I)
    ERRMAX=MAX(ERRMAX,ABS(YTEMP(I)/YSCAL(I)))
12 CONTINUE
  ERRMAX=ERRMAX/EPS
  IF (ERRMAX.GT.ONE) THEN
    H=SAFETY*H*(ERRMAX**PSHRNK)
    GOTO 1
  ELSE
    HDID=H
    IF(ERRMAX.GT.ERRCON) THEN
      HNEXT=SAFETY*H*(ERRMAX**PGROW)
    ELSE
      HNEXT=.4.*H
    ENDIF
  ENDIF
DO 13 I=1,N
  Y(I)=Y(I)+YTEMP(I)*FCOR

```

```

13 CONTINUE
RETURN
END
C
C
SUBROUTINE RK4(Y,DYDX,X,H,YOUT,DERIVS)
C
C ADVANCES ODE SOLUTION BY H USING FOURTH ORDER R-K
C COPIED FROM NUMERICAL RECIPES, PG 553, 1986
C
PARAMETER (N=4)
DIMENSION Y(N),DYDX(N),YOUT(N),YT(N),DYT(N),DYM(N)
HH=H*0.5
H6=H/6.
XH=X+HH
DO 11 I=1,N
  YT(I)=Y(I)+HH*DYDX(I)
11 CONTINUE
CALL DERIVS(XH,YT,DYT)
DO 12 I=1,N
  YT(I)=Y(I)+HH*DYT(I)
12 CONTINUE
CALL DERIVS(XH,YT,DYM)
DO 13 I=1,N
  YT(I)=Y(I)+H*DYM(I)
  DYM(I)=DYT(I)+DYM(I)
13 CONTINUE
CALL DERIVS(X+H,YT,DYT)
DO 14 I=1,N
  YOUT(I)=Y(I)+H6*(DYDX(I)+DYT(I)+2.*DYM(I))
14 CONTINUE
RETURN
END
C
C
SUBROUTINE DERIVS(T,X,DXDT)
C
C CALCULATES THE RHS OF ODE SET, DXDT (ASSUMING CBO=0)
C
DIMENSION X(4),DXDT(4)
REAL*8 NB,NS,R,NL,NSIR,INF,INR,INIR,WT,VOL
COMMON /PATH/ NS,NB,R,NL,NSIR,INF,INR,INIR,WT,VOL
DXDT(1)=-X(1)-X(2)+1
DXDT(2)=-NB*(1-WT*INR/((R-1)*VOL*INF)-X(1)-R*X(2)/(R-1)+
* X(3)*NS/(R-1))
DXDT(3)=-NI*(WT*INR/(VOL*INF)+X(2)-NS*X(3))
DXDT(4)=-NSIR*(INIR*WT/(INF*VOL)+X(3)*(NS-1)-X(4))
RETURN
END

```